ACQUISITION RESEARCH SPONSORED REPORT SERIES

The Evaluation of HOMER as a Marine Corps Expeditionary Energy Pre-deployment Tool

21 November 2010

by

Capt. Brandon H. Newell, USMC

Advisors: Dr. Sherif Michael, Professor, and

Dr. Daniel Nussbaum, Professor

Graduate School of Engineering and Applied Sciences

Naval Postgraduate School

Prepared for: Naval Postgraduate School, Monterey, California 93943

ACQUISITION RESEARCH PROGRAM
GRADUATE SCHOOL OF BUSINESS & PUBLIC POLICY
NAVAL POSTGRADUATE SCHOOL

ABSTRACT

In this thesis, the author evaluates whether HOMER Micropower Optimization should be used by the Marine Corps as a pre-deployment tool for meeting expeditionary energy demands. The author created two unique experiments to facilitate the evaluation of HOMER's modeling capability. First, a grid-tied-photovoltaic (PV) system at the Naval Postgraduate School was monitored for a one-month period. During this experiment, a HOMER model of the system was created. The actual energy production from the system was compared to the model. Then, the model was calibrated to the particular system to ensure that the model's energy estimate matched that of the actual system. The second experiment involved the use of two different types of PV panels and a small wind turbine. Each system was monitored over a one-month period, and the results were compared to a HOMER model of the systems. The difficulty of modeling wind turbines and the related limitations of HOMER's modeling strategy is discussed in this thesis. The calibration method established in the grid-tied-PV experiment was used to ensure the HOMER models were accurate. Following the calibration, the concept of expeditionary energy density as it pertains to power production was defined and utilized to evaluate each of the systems. The final portion of this thesis shows the advantage of using HOMER as part of the Experimental Forward Operating Base (ExFOB). The ExFOB was conducted by the Marine Corps to evaluate alternative power solutions currently on the market for expeditionary energy purposes. Four distinct power production solutions were chosen by the Marine Corps following the ExFOB. These solutions were then field tested in Morocco and scheduled to be deployed to Afghanistan. This thesis details how the use of HOMER would have benefited the ExFOB process had it been utilized.

THIS PAGE INTENTIONALLY LEFT BLANK

ACQUISITION RESEARCH SPONSORED REPORT SERIES

The Evaluation of HOMER as a Marine Corps Expeditionary Energy Pre-deployment Tool

21 November 2010

by

Capt. Brandon H. Newell, USMC

Advisors: Dr. Sherif Michael, Professor, and

Dr. Daniel Nussbaum, Professor

Graduate School of Engineering and Applied Sciences Naval Postgraduate School

Naval Postgraduate School

THIS PAGE INTENTIONALLY LEFT BLANK

TABLE OF CONTENTS

LIST OF FIGURES

THIS PAGE INTENTIONALLY LEFT BLANK

LIST OF TABLES

LIST OF ACRONYMS AND ABBREVIATIONS

AC	Alternating Current
AOR	Area of Responsibility
CMC	Commandant of the Marine Corps
COE	Cost of Energy
DC	Direct Current
DESC	Defense Energy Support Center
DoD	Department of Defense
ExFOB	Experimental Forward Operating Base
E2O	Expeditionary Energy Office
FBCF	Fully Burdened Cost of Fuel
FOB	Forward Operating Base
FUE	Field User Evaluation
GMT	Greenwich Mean Time
HFN	Hastily Formed Networks
I-V	Current-Voltage
IED	Improvised Explosive Device
JP	Jet Propellant
kW	Kilowatt
kWh	Kilowatt-hour
LD	Load
MARCORSYSCOM	Marine Corps Systems Command
MEAT	Marine Energy Assessment Team
MEB–A	Marine Expeditionary Brigade–Afghanistan
MEP	Mobile Electric Power
MPP	Maximum Power Point
MPPT	Maximum Power Point Tracker
NASA	National Aeronautics and Space Administration
NOTC	Nominal Operating Cell Temperature
NPC	Net Present Cost
NPS	Naval Postgraduate School

NREL	National Renewable Energy Laboratory
NYSERDA	New York State Energy Research & Development Agency
PG&E	Pacific Gas & Electric
PM	Program Manager
PST	Pacific Standard Time
PV	Photovoltaic
RFI	Request for Information
USMC	United States Marine Corps
UTC	Coordinated Universal Time
Wh	Watt-hour

EXECUTIVE SUMMARY

August 13, 2009, marked a dramatic shift in the United States Marine Corps' (USMC) view of alternative energy. On this day, General James T. Conway, 34th Commandant of the Marine Corps (CMC), held the first ever USMC Energy Summit in Washington, DC. Speaking about energy use within the Marine Corps, he stated, "I am unsettled by what I now know about where we are, particularly with regard to our expeditionary capabilities and energy efficiencies. … [T]he alarm was set for 5:00 this morning; at 4:00, I was staring at the ceiling thinking about what we're going to do about this problem [1]." He showed obvious concern about how the Marine Corps viewed energy and about the lack of priority given to doing things efficiently. He went on to discuss how the Marine Corps' great thirst for and reliance on fossil fuels comes at an unacceptable price in national treasure and risk to human life.

Since that day, the CMC has gone to great lengths to change the way the USMC looks at expeditionary energy. Reducing the amount of fuel and water that is transported around the battlefield has become one of his top priorities. This thesis was designed to generate ideas that will help the Marine Corps reduce that demand for fuel. The evaluation of HOMER Micropower Optimization modeling software as a pre-deployment tool has only one objective: to determine whether or not the use of this tool will ultimately lead to a reduced demand for fuel in combat.

The HOMER Micropower Optimization modeling software, developed by the National Renewable Energy Laboratory (NREL), was designed to compare multiple power production capabilities in order to meet a particular load. The software models power systems based on the physical behavior of the systems as well as on economic ramifications. HOMER allows a user to compare many different design options based on the inherent technical and economic estimates. The details of each comparison are derived from the performance characteristics of the equipment and the unique availability of the required resources for a particular location, such as the solar radiation profile, the wind patterns, and the price of fuel.

The following process was used to analyze HOMER's modeling capability:

- Conduct photovoltaic (PV) experiment,
- Develop a calibration process to match the HOMER model to measured energy,
- Conduct wind turbine and PV experiment,
- Refine calibration process for PV,
- Develop calibration process for wind,
- Develop expeditionary energy density concept, and
- Integrate HOMER into the Experimental Forward Operating Base (ExFOB).

To evaluate HOMER's potential as a pre-deployment tool, the modeling accuracy first had to be scrutinized. This was accomplished by creating an experiment in which the unknown variables were kept to a minimum. For example, the exact azimuth and orientation of solar panels had to be known; the exact solar and wind resource at the location of the PV and wind turbines, respectively, had to be tracked; and the temperature at these locations had to be monitored. Then, and only then, could a HOMER simulation input with these known variables be effectively evaluated against the actual measured production from the utilized equipment. A positive evaluation was not necessarily the result of a perfect match between HOMER's model and the actual measured energy production. Rather, it was the determination of whether a specific HOMER model could be calibrated to a unique setup and still achieve comparable results.

Therefore, two unique experiments were designed to properly evaluate HOMER's modeling capability. The first experiment involved a PV system installed in 2006 on the campus of the Naval Postgraduate School. The system is tied to the Pacific Gas & Electric grid, which supports the school's electricity requirements. It includes 56 Kyocera panels, rated at 205 watts apiece, forming three separate PV arrays.

The initial HOMER model estimated an energy production level that was over 25% higher than the actual measured energy. However, the following calibration method was developed to improve HOMER's accuracy. The calibration method included these three steps:

1. Include temperature effects in the model,

2. Add the true solar irradiance levels from the experiment, which replace estimates derived from monthly averages, and

Vary the derating factor to account for system inefficiencies.

The second experiment was also on the Naval Postgraduate School campus and consisted of two non-fixed solar panels and one mobile wind turbine. Each of these components was set up for the purpose of this experiment and was not tied to the grid. The two solar panels were a 50-watt-rated hard panel from Kyocera and a 60-watt-rated flexible panel from PowerFilm. The wind turbine was a 400-watt-rated Air X from Southwest Wind.

This experiment was an opportunity to evaluate HOMER's modeling of small PV and wind systems. The objective was to compare the measured energy output of these systems to a HOMER model of each configuration. Both the experimental setup and the HOMER model were conducted one system at a time, rather than all together. The PV portion of this experiment showed the effectiveness of HOMER's modeling capability. However, the same cannot be said for HOMER's wind turbine modeling. Wind as an energy resource is much more variable than solar irradiance. Therefore, HOMER's modeling strategy of hourly simulations was insufficient in the context of this experiment and perhaps insufficient in the context of expeditionary energy all together.

The PV calibration method detailed in the first experiment was used to effectively calibrate both PV models in this experiment. A similar calibration was then developed for the wind turbine model. It included the following two steps:

1. Add the true anemometer measured wind speeds, which replace estimates derived from monthly averages, and

2. Use HOMER's sensitivity analysis capability to vary the hub height and surface roughness length to account for turbulence.

While the result of this wind model calibration was successful for this experiment, it is unclear if it would be successful in a pre-deployment context.

The concept of expeditionary energy density was developed to provide a metric to evaluate how a system would perform in the context of how much valuable space it consumed within a Forward Operating Base (FOB). HOMER is used to estimate the energy production capability of a system in a specific location over a defined time frame. Then, that energy estimate is divided by the area of the system in squared meters and by the number of days. The result is an energy density in a kilowatt-hour per meter squared per day (kWh/m²/d) value. An expeditionary energy density was calculated for each of the three systems used in the second experiment: the Kyocera KC50T solar panel, the PowerFilm FM-15 3600 flexible solar panel, and the Southwest Windpower Air X wind turbine. The results are shown in Table 1, revealing that the Kyocera KC50T will provide a higher energy density per day at NPS.

Table 1.   Expeditionary Energy Density Calculations from Wind-PV Experiment

	Energy Total (kWh)	System Length and Width (m x m)	Consumed Area (m²)	Exp. Energy Density (kWh/m^2)	No. of days in period	Exp. Energy Density per day (kWh/m/d)
Kyocera KC50T	5.367	0.639 x 0.652	0.417	12.881	30	0.429
PowerFilm FM-15 3600	4.781	1.499 x 1.092	1.637	2.921	30	0.097
Air X	1.538	11.5 x 3.45	39.675	0.039	30	0.001

The Experimental Forward Operating Base (ExFOB) concept was first established by the USMC in September 2009. It involved the following three major components, described in the context of power production:

- Evaluation and selection of commercial off-the-shelf power production systems; March in Quantico, Virginia;

- Testing of selected power production systems; May in Morocco; and

- Fielding of selected power production systems; October in Afghanistan.

Four PV power systems were selected by the ExFOB process. These four systems were used to illustrate HOMER's potential as a tool for evaluating alternative power systems. Each system was modeled in the three locations and months listed above. Two different modeling strategies were utilized. The first involved modeling all four systems

as a single system. The PV inputs were intentionally chosen to underestimate the collective energy production capability of the systems. This established a low bound estimate for the systems, which would benefit those responsible for meeting the energy demands of a forward operating base (FOB).

The second modeling strategy involved the creation of a model for each of the PV systems, and it involved evaluating them individually at each location and date. This refined the energy production estimates, which could be used to better inform those responsible for power planning. The results of the two modeling strategies, along with the percentage of the energy load (8,650 kWh) they represent, are shown in Table 2.

Table 2.   HOMER Modeling Results for the ExFOB Selected PV Systems, Using Both the Collective and Individual Modeling Methods

	Quantico (kWh)	Morocco (kWh)	Afghanistan (kWh)
PV Combined	**1645**	**2074**	**1984**
Percent of Load	19%	24%	23%
Individual			
PowerShade	191	223	240
GREENS	583	606	675
ZeroBase	430	449	501
NEST	822	839	940
Cumulative	**2026**	**2117**	**2356**
Percent of Load	23%	24%	27%

Overall, HOMER proved to be a very capable tool, which could benefit the Marine Corps in many ways. The Marine Corps should further explore the HOMER calibration processes discussed in this thesis and the role they might play in the pre-deployment process. The idea of wind turbine modeling should also be researched further to determine whether the hourly simulation strategy is compatible with the use of small wind turbines used for expeditionary energy. Finally, the use of HOMER in evaluating systems according to their expeditionary energy density should also be explored further.

THIS PAGE INTENTIONALLY LEFT BLANK

ACKNOWLEDGMENTS

I want to thank my wife, Sara, for all of the support she gave me through this process. Recognizing my passion for alternative energy, she encouraged me in my efforts and tolerated my many absences. The fact that she is a great wife and mother blesses me every day. I also want to thank my three-year-old daughter, Sierra, and one-year-old son, Kai. Their smiles greeted me every day, helping me to release the stresses of writing a thesis.

I have been incredibly blessed during my time at Naval Postgraduate School. I view this thesis as the culminating product of the Lord's favor over these two years. I arrived at the school in the summer of 2008 with the expectation that I would find a way to focus my efforts on alternative power. I quickly realized that, at the time, the opportunities were very limited. Alternative energy had not yet become the hot topic, in our society or the military, that it is today. My original thesis topic was focused on designing a plan to meet the 25% renewable energy mandate at Camp Pendleton, utilizing solar, wind, and ocean energy. To acquire the necessary knowledge required to research this, I scoured the internet. I emailed or called anyone I could find contact information for, to seek advice. My networking diagram grew well beyond my expectations as I discovered so many experts gracious enough to advise me and connect me to others in their respective fields. To each of these individuals, I am grateful.

Eventually, my networking led me to Dr. John Barnett of the National Renewable Energy Laboratory (NREL). He facilitated the great experience I had of assisting Dr. Andy Walker, also of NREL, in doing solar assessments on rooftops in the San Francisco area in January 2009, for the Department of Energy's Solar City program. I want to thank Andy for his mentoring. John also facilitated my internship at NREL, which provided me with an unparalleled learning experience and gave me the honor of becoming the first active duty serviceman to work at the laboratory. John has become a great friend since that time, and I am grateful for his counsel.

During the last week of my internship, I attended the USMC Energy Summit, hosted by the Commandant of the Marine Corps, General James T. Conway. I was greatly inspired to see his passion, dedication, and leadership for changing the way the Marine Corps views energy. This event was the launching point for my work in expeditionary energy.

A few weeks later, the Commandant selected me as one of six members of the Afghanistan Marine Energy Assessment Team (MEAT). I was humbled and honored by this selection. In September 2009, I joined MEAT on a three-week mission to Helmand Province, Afghanistan. I am grateful to Colonel T. C. Moore for his leadership during this trip. Following this trip, I decided to change my research focus from installation energy to expeditionary energy.

The list of individuals at the Naval Postgraduate School who have assisted me in this process is extensive, and I am grateful for this opportunity to recognize them. I would like to thank the following individuals: my thesis advisors, Dr. Sherif Michael and Dr. Daniel Nussbaum, for their guidance, patience, and encouragement; Dr. Paul Shebalin, director of the Meyer Institute, for his encouragement and research funding support; Professor Tim Stanton and James Stockel, of the Oceanography Department, for his assistance in my wind power experiment; Dick Lynd, of the Meteorology Department, and Jeff Knight, of the Electrical and Computer Engineering Department, for their assistance in my solar power experiment; Stephen Dootson, of NPS Facilities, for his assistance in my grid-tied-PV experiment; Sue Higgins and Alison Kerr, of the Cebrowksi Institute, for their encouragement and guidance; the Acquisition Research Program, for their funding and thesis-writing support; LtCol Vaughn Pangelinan, Senior Marine Corps Representative, for his encouragement and guidance; Brian Steckler, of the Hastily Formed Networks Research Group, for inviting me to take part in the humanitarian aid/disaster relief efforts in Haiti; and Dr. Giovanna Oriti, my thesis advisor for my initial thesis topic, for her patience and guidance.

I. INTRODUCTION

In January 2010, Hastily Formed Networks (HFN) deployed to Haiti in support of the Humanitarian Aid/Disaster Relief (HADR) efforts following the country's devastating earthquake. HFN is a Naval Postgraduate School (NPS) organization that specializes in providing small, self-sufficient communications packages in support of civil-military HADR efforts. To be self-sufficient in a disaster area requires that HFN bring their own power sources. Simply having small generators is not adequate because fuel is usually in short supply and high demand following natural disasters, such as the earthquake in Haiti. Therefore, HFN maintains solar panels and wind turbines in their inventory.

The author was a member of the six-person HFN team that deployed to Haiti. The team held the general assumption that solar and wind power would be very useful during the deployment due to Haiti's location near the equator and to the presence of strong trade winds on islands in that region. Recognizing the critical role power plays in HFN missions, the author conducted HOMER analysis, before deploying, to truly determine if solar and wind power would meet the HFN's needs. This HOMER analysis detailed the specific characteristics of the HFN's PowerFilm Solar Field Shelter solar panels and the Southwest Windpower Air X wind turbines, in combination with the 12-volt deep cycle batteries. Utilizing the specifics of Port-au-Prince's solar and wind resource, the HOMER analysis was completed. The author discovered that there was great potential for solar power, but wind power could not be relied on due to marginal wind speeds at best. With this knowledge, the HFN team ensured that the solar panels received the highest priority as the team set up in different locations around Port-au-Prince. In Figure 1, the author can be seen setting up a wind turbine and solar panels on the grounds of the destroyed Haitian National Palace.

Figure 1. **Photos of the Author Setting Up a Wind Turbine and Solar Panels Outside the Destroyed Haitian National Palace, January 2010**

Just as HOMER facilitated the HFN's needs for the HADR mission in Haiti, there is potential that it could play a substantial role in the Marine Corps. In Chapter II, a discussion of why alternative energy capabilities are important to the Marine Corps is presented. Actions taken by the Command of the Marine Corps in 2009 and 2010, which speak to the high priority of expeditionary energy throughout the Service, are detailed. The role HOMER could play in Marine Corps expeditionary energy is highlighted.

This is followed by an explanation of HOMER's capabilities in Chapter III. The reader is provided the critical information needed to use HOMER themselves. The focus of this chapter is centered on the details of HOMER's capabilities as they pertain to this thesis.

In Chapters IV and V, the two controlled experiments created for this thesis are discussed. Both experiments provided an opportunity to measure actual alternative power production as a comparison to HOMER's modeled power production. As detailed in Chapter IV, the first experiment is a grid-tied-PV system, which is installed at Naval

Postgraduate School. The system was monitored for a one-month period, the results of which were then compared to a HOMER model of the same system. Through this analysis, a method for calibrating HOMER to the particulars of the system was developed.

In Chapter V, the second experiment is covered. This experiment focused on two mobile solar panels and one small-scale wind turbine installed specifically for this thesis. These systems were installed separately and were also monitored over a one-month period. Again, these results were compared to HOMER models created to match the systems. The calibration unique to each model is detailed. Additionally, the concept of expeditionary energy density is developed as a metric for expeditionary energy analysis.

In Chapter VI, this thesis concludes with a discussion of the benefits that using HOMER could have brought to the Marine Corps' alternative power evaluation process. This process, known as the Experiment Forward Operating Base (ExFOB), is detailed. HOMER analysis is then integrated into the ExFOB to provide examples of the tool's potential.

THIS PAGE INTENTIONALLY LEFT BLANK

II. THE MARINE CORPS AND ALTERNATIVE ENERGY

August 13, 2009, marked a dramatic shift in the United States Marine Corps' (USMC) view of alternative energy. On this day, General James T. Conway, 34th Commandant of the Marine Corps (CMC), held the first ever USMC Energy Summit in Washington, DC. Speaking about energy use within the Marine Corps, he stated, "I am unsettled by what I now know about where we are, particularly with regard to our expeditionary capabilities and energy efficiencies. … [T]he alarm was set for 5:00 this morning; at 4:00, I was staring at the ceiling thinking about what we're going to do about this problem [1]." He showed obvious concern about how the Marine Corps viewed energy and about the lack of priority given to doing things efficiently. He went on to discuss how the Marine Corps' great thirst for and reliance on fossil fuels comes at an unacceptable price in national treasure and risk to human life.

For example, in Helmand Province, Afghanistan, Marine Expeditionary Brigade–Alpha (MEB–A) receives fuel via a Defense Energy Support Center (DESC) contract with Supreme Fuels. Supreme delivers jet propellant 8 (JP-8) to three locations within the MEB's area of responsibility (AOR). Marine units are responsible for transporting required fuel from these three distribution points to each of the additional Marine locations within Helmand Province. Although the cost of fuel delivered by Supreme is concrete ($6.39/gallon, as of September 2010), when Marines are required to transport fuel around the battlefield, the Fully Burdened Cost of Fuel (FBCF) increases. The FBCF is a metric to incorporate all of the hidden costs behind providing fuel to certain areas of the battlefield. Many documents have been published within the Department of Defense (DoD) concerning the FBCF and what should be incorporated in its calculation. In November 2009, the Marine Corps calculated the FBCF to be $11.70 per gallon for fuel delivered to various MEB–A forward operating bases (FOBs). In August 2009, MEB–A used over 88,000 gallons of fuel. At Supreme's contracted price, this fuel cost the DoD more than $560,000, but by taking the FBCF into account, one could see that, in fact, fuel actually costs the Marine Corps much more [2], [3].

The "threat to human life," taken from the CMC's quote in the first paragraph of this chapter, is based on the fact that the number-one danger for Marines in Afghanistan is Improvised Explosive Devices (IEDs). Every convoy on the road is in danger of being targeted with an IED. A large number of these convoys are logistics convoys supplying FOBs. The high demand for fuel on the various FOBs necessitates a higher number of Marines and vehicles on the roads to supply that fuel. What concerned the Commandant was the knowledge that unless the Marine Corps was doing all in its power to reduce that demand for fuel, Marines would be put in harm's way more than was necessary [3].

To address these concerns, the Commandant made the following remarks:

> We have got to look at reorganization at the headquarters. We have got to start with people that are going to manage this for us. And, by the end of the month, I want an evaluation team in Afghanistan to look at what we're doing and how we're not doing. … We have got to make sure that we are operating at max efficiency and effectiveness with regard to the energy that we are providing on a daily basis. [1]

Basically, the Commandant initiated a two-pronged effort to address the energy issue: sending a team to Afghanistan and creating a permanent energy office. Both efforts contributed to this thesis. First, the author was selected as a member of the six-man team sent to Afghanistan to investigate the details of fuel and water usage within MEB–A. The details of the investigation are used as part of the evaluation criteria within this thesis. Second, the author will be transferring to the newly formed Expeditionary Energy Office (E2O) following his graduation from the Naval Postgraduate School.

The Afghanistan Marine Energy Assessment Team deployed to Helmand Province in September 2009. The team, led by Colonel T. C. Moore, USMC, was focused on uncovering all details concerning how fuel and water were delivered to and utilized by MEB–A. The team researched how power was produced in various locations and noted the efficiency of that production. Following the trip, the team briefed the Commandant on these findings and presented recommendations for reducing the demand for fuel. One of those recommendations was to strive for self-sufficient FOBs, which would include increasing energy efficiency and incorporating alternative power sources.

This thesis is an effort to make this incorporation of alternative power sources more effective by providing HOMER as a tool to accurately predict the power production of power systems for unique locations around the world.

Following the briefing of the assessment team's recommendations, the Commandant created the Expeditionary Energy Office. This office was commissioned to "analyze, develop, and direct the Marine Corps' energy strategy in order to optimize expeditionary capabilities across all warfighting functions [4]." One of the first efforts undertaken by E2O was the Experimental Forward Operating Base (ExFOB). The ExFOB was created to simulate the energy and water demands of forward deployed forces and to facilitate the evaluation of renewable energy and energy efficiency solutions to meet these needs. Phase I of ExFOB was completed in March 2010, resulting in commercial off-the-shelf (COTS) equipment selected by the Marine Corps for deployment to MEB–A in the fall of 2010. This thesis made use of the power demand criteria and the resulting renewable energy equipment selected during the ExFOB [5].

In summary, this newfound focus within the Marine Corps on reducing the fuel demand for forward deployed forces directly led to the need for this thesis. It is not enough for the Marine Corps to purchase alternative energy systems such as solar panels and wind turbines. The Marine Corps must provide commanders with the tools necessary to maximize the potential of these resources. If alternative power sources are used incorrectly or inefficiently—such as by employing them in locations where the solar and/or wind resources are poor—Marines will lose confidence in the capability of these power sources and will return to the fossil fuel–driven generators because of their consistent production.

THIS PAGE INTENTIONALLY LEFT BLANK

III. HOMER

The HOMER Micropower Optimization modeling software, developed by the National Renewable Energy Laboratory (NREL), was designed to compare multiple power production capabilities in order to meet a particular load. The software models power systems based on the physical behavior of a system as well as on economic ramifications. HOMER allows a user to compare many different design options based on the inherent technical and economic estimates. The details of each comparison are derived from the performance characteristics of the equipment and the unique availability of the required resources for a particular location, such as the solar radiation profile, wind patterns, and price of fuel.

To fully understand what HOMER is capable of, one must understand what a micropower system is. As the creators of the software, Tom Lambert, Paul Gilman, and Peter Lilienthal defined a micropower system in the book *Integration of Alternative Sources of Energy*, as "a system that generates electricity, and possibly heat, to serve a nearby load. Such a system may employ a combination of electrical generation and storage technologies and may be grid-connected or autonomous, meaning separate from any transmission grid [6]." There are many uses of micorpower systems within the DoD. For example, solar panels mounted to the roof of barracks aboard Marine Corps Base Camp Pendleton supplement the grid in meeting the power demands of the barracks. Another example is the use of wind turbines at the Naval Auxiliary Landing Field, San Clemente Island, which combine with diesel generators on the island to meet the entire demands of the base [7]. Micropower systems are diverse throughout the DoD's installations, but they are generally one dimensional in forward deployed locations. Most FOB energy demands are met by a micropower system consisting of only diesel generators. As discussed previously, the CMC is not content with this. During the USMC Energy Summit, he stated, "The next opportunity [to change expeditionary energy], we believe, is going to need to be with industry so we can start to partner on what is the art of the possible [1]." HOMER, if used effectively, can show what the "art of the possible" is for the use of diverse micropower systems in deployed locations.

A.   OVERVIEW

HOMER was developed in the 1990s by the National Renewable Energy Laboratory (NREL). At the time, NREL had a program, called the Village Power Program, that focused on "helping developing countries incorporate renewable power into their rural electrification program [8]". To facilitate the program's mission, HOMER was created to evaluate design trade-offs and alternative system configurations. HOMER's capabilities have evolved through the years to meet NREL's and the public's need to optimize on-grid and off-grid micropower configurations. In 2009, NREL executed a commercial license for HOMER. This gave HOMER Energy, LLC, exclusive rights to enhance and distribute the modeling software. As a result, the software is now available for download from the HOMER Energy website (www.homerenergy.com) [8].

The programmers summed up HOMER's modeling capability by stating, "HOMER can model grid-connected and off-grid micropower systems serving electric and thermal loads, and comprising any combination of photovoltaic (PV) modules, wind turbines, small hydro, biomass power, reciprocating engine generators, microturbines, fuel cells, batteries, and hydrogen storage [6]." They elaborated with the following description of the three the principal tasks:

> HOMER performs three principal tasks: simulation, optimization, and sensitivity analysis. In the simulation process, HOMER models the performance of a particular micropower system configuration each hour of the year to determine its technical feasibility and life-cycle cost. In the optimization process, HOMER simulates many different system configurations in search of the one that satisfies the technical constraints at the lowest life-cycle cost. In the sensitivity analysis process, HOMER performs multiple optimizations under a range of input assumptions to gauge the optimal value of the variables over which the system designer has control such as the mix of components that make up the system and the size or quantity of each. Sensitivity analysis helps assess the effects of uncertainty or changes in the variables over which the designer has no control, such as the average wind speed or the future fuel price. [6]

Figure 2 is a graphic representation of the relationship between simulation, optimization, and sensitivity analysis in HOMER. It shows that a single optimization

requires multiple simulations. Similarly, sensitivity analysis requires multiple optimizations.
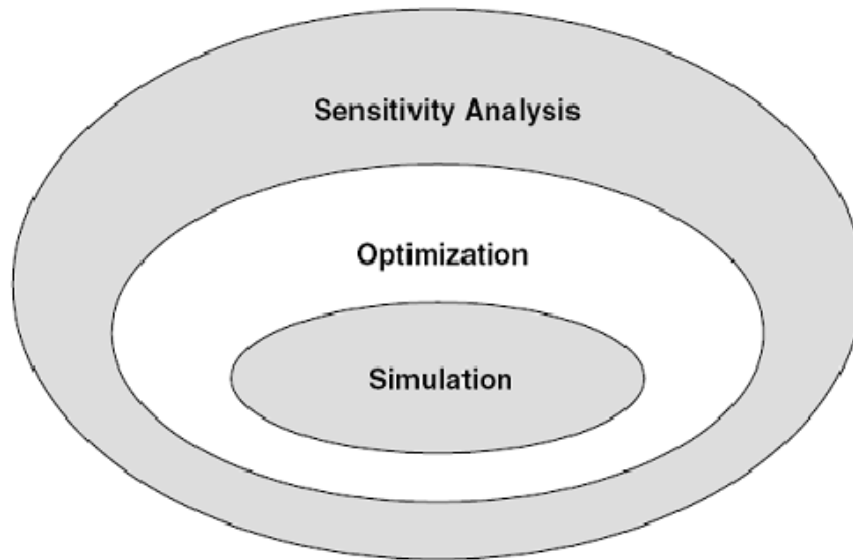
Figure 2.   Relationship Between Simulation, Optimization, and Sensitivity Analysis, From [6]

B.   SIMULATION

The programmers stated, "HOMER's fundamental capability is simulating the long-term operation of a micropower system [6]." The optimization and sensitivity rely on the simulation building block. To simulate, HOMER "determines how a particular system configuration, a combination of system components of specific sizes, and an operating strategy that defines how those components work together, would behave in a given setting over a long period of time [6]." As shown in Figure 3, HOMER is capable of simulating a wide variety of system configurations with diverse system components. The user can chose from any of these options when creating a micropower system. These options, especially those utilized within this thesis, will be discussed in greater detail later in this chapter.
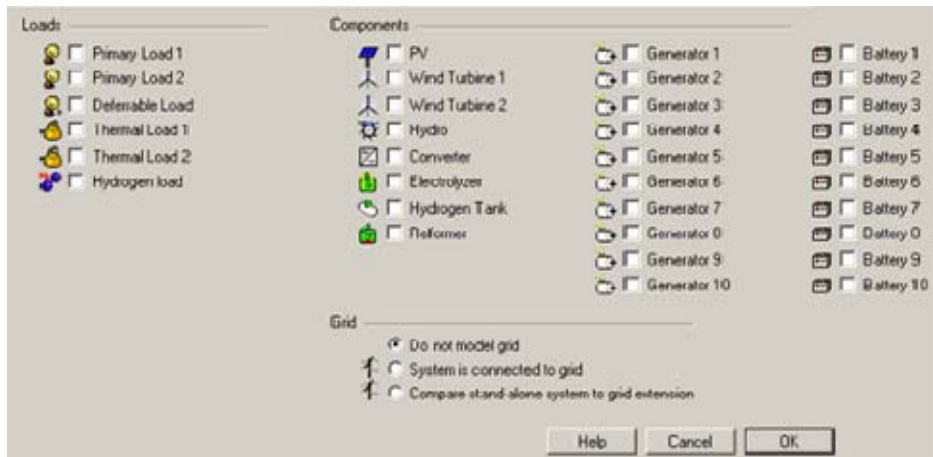
Figure 3.   HOMER Component Options for the Micropower System

Once the user chooses the equipment to be modeled, HOMER displays this equipment in a schematic diagram on the main page. In Figure 4, two diagrams of the distinct systems being evaluated are shown. Represented in the first diagram of Figure 4 is a grid-connected PV system serving an alternating current (AC) electric load. The second diagram is a generator-PV-wind system serving an AC electric load. The values of the load in these diagrams can be disregarded because they are simply examples. Loads will be discussed in greater detail later.
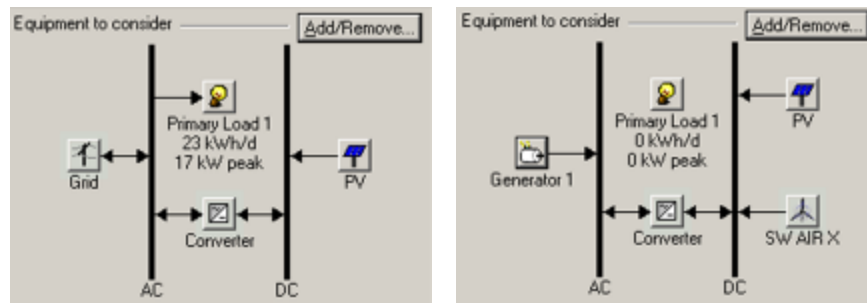
Figure 4.   Schematic Diagrams of Two Micropower System Types that HOMER Models

How HOMER undergoes the simulation process is best summarized by the programmers:

> The simulation process serves two purposes. First, it determines whether the system is feasible. HOMER considers the system to be feasible if it can adequately serve the electric and thermal loads and satisfy any other

constraints imposed by the user. Second, it estimates the life-cycle cost of the system, which is the total cost of installing and operating the system over its lifetime. The life-cycle cost is a convenient metric for comparing the economics of various system configurations. [6]

HOMER simulates each hour of the year to ensure the micropower system options dictated by the user can feasibly meet the dictated load. The programmers explained this process in the following excerpt:

> HOMER models a particular system configuration by performing an hourly time series simulation of its operation over one year. HOMER steps through the year one hour at a time, calculating the available renewable power, comparing it to the electric load, and deciding what to do with surplus renewable power in times of excess, or how best to generate (or purchase from the grid) additional power in times of deficit. When it has completed one year's worth of calculations, HOMER determines whether the system satisfies the constraints imposed by the user on such quantities as the fraction of the total electrical demand served, the proportion of power generated by renewable sources, or the emissions of certain pollutants. HOMER also computes the quantities required to calculate the system's life-cycle cost, such as the annual fuel consumption, annual generator operating hours, expected battery life, or the quantity of power purchased annually from the grid. [6]

While the economics and the life cycle cost of the systems are not a central focus of this thesis, it is important for a user to understand how HOMER utilizes them in the simulation process. This will ensure that the user is not limiting the number of simulated systems unknowingly. Additionally, the life cycle cost aspect of HOMER could be of great benefit to program managers (PMs) and acquisition professionals when evaluating the purchase of renewable power production equipment to augment traditional generators.

C. OPTIMIZATION

HOMER's optimization process is focused on finding the best possible system configuration from the successfully simulated configurations. The optimization process hinges on finding the lowest net present cost (NPC), which is best described in the following excerpt from the programmers:

In HOMER, the best possible, or optimal, system configuration is the one that satisfies the user-specified constraints at the lowest total net present cost. The goal of the optimization process is to determine the optimal value of each decision variable that interests the modeler. A decision variable is a variable over which the system designer has control and for which HOMER can consider multiple possible values in its optimization process. Possible decision variables in HOMER include:

- The size of the PV array

- The number of wind turbines

- The size of each generator

- The number of batteries

- The size of the AC-DC converter

- The dispatch strategy (the set of rules governing how the system operates). [6]

There are several other decision variables within HOMER, but the ones above are most relevant to this thesis. The user is capable of entering multiple values for each decision variable. In Figure 5, an example of a HOMER search space is displayed. The search space includes the set of all variables a generator-PV-wind system. In this example, the user has specified that HOMER should consider using one of the following PV options: 3 kilowatt (kW), 6 kW, or no array at all. Similarly, the quantities of batteries given to HOMER vary from eight to 56. Within this search space, there are 242 possible systems configurations.
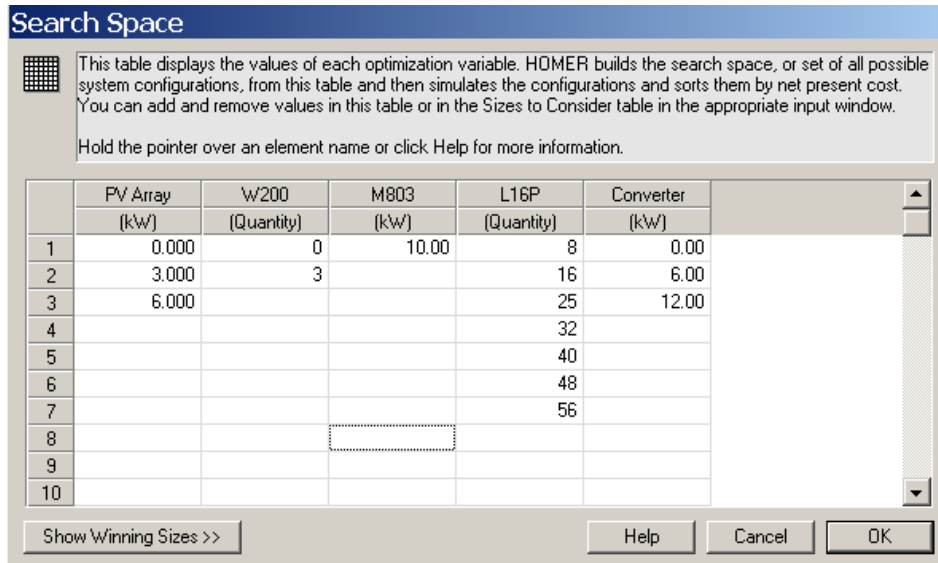
Figure 5. Search Space of a Unique Generator-PV-Wind System, with 242 Possible System Configurations (3 x 4 x 1 x 7 x 3 = 242)

The user has the freedom to input as many values in each decision variable as he desires. HOMER then simulates every system configuration in the search space and displays the feasible ones. Of the 242 possible system configurations in the example above, only four were determined to be feasible by HOMER. These four are displayed in Figure 6. Based on the values entered by the user for variables such as price of fuel, wind speed, solar strength, and the NPC of each piece of equipment, HOMER determined one solution of the four to be the optimal. This optimal solution is displayed in the first row of Figure 6. The optimal solution is comprised of a 6-kW PV array, 3 SW Whisper 200 wind turbines, a 10-kW generator, 40 batteries, and a 6-kW AC-DC converter.

Also displayed in the top row of Figure 6 are HOMER's calculation for the initial capital required to install the system, the operating cost per year, the total NPC covering some user-specified system lifetime, the cost of energy (COE), the fraction of renewable produced energy versus total energy, the fuel consumption throughout the lifetime, and the hours the generator is required. While the four feasible solutions are ranked according to their total NPC, HOMER displays this additional data to assist the user if NPC is not the critical factor in selecting a system. For example, if the user must meet a mandate of a specified percentage of renewable generation, the column labeled *Ren.*

Frac, which displays the fraction of the overall load met by renewables, would receive greatest attention. Although, in this example, the result is the same as valuing total NPC, this is rarely the case. However, if the user has determined that a low startup capital is the number one criteria for selecting a system, then the system configuration in the third row would be selected by the user.

	PV (kW)	W200	M803 (kW)	L16P	Conv. (kW)	Initial Capital	Operating Cost ($/yr)	Total NPC	COE ($/kWh)	Ren. Frac.	JP-8 (L)	M803 (hrs)
	6	3	10	40	6	$ 47,600	14,037	$ 227,037	0.572	0.43	7,367	2,784
	6		10	40	6	$ 38,600	14,878	$ 228,785	0.577	0.29	9,015	3,222
			10	25	6	$ 22,100	17,754	$ 249,061	0.628	0.00	12,786	4,764
		3	10	25	6	$ 31,100	17,423	$ 253,824	0.640	0.14	11,346	4,656

Figure 6.   Optimization Results from the Example Displayed in Figure 5

D.   SENSITIVITY ANALYSIS

HOMER's third principal task is sensitivity analysis, which calculates how sensitive the outputs are to changes in the inputs. HOMER does this by slightly varying each input and performing multiple optimizations. The process is described in greater detail by the programmers in the following excerpt:

> In a sensitivity analysis, the HOMER user enters a range of values for a single input variable. A variable for which the user has entered multiple values is called a sensitivity variable. Almost every numerical input variable in HOMER that is not a decision variable can be a sensitivity variable. [6]

Examples include the price of fuel, the average wind speed, even the magnitude of the load. Sensitivity analysis is of great value to the Marine Corps as a way to determine whether power production equipment for deployable units will perform adequately in the diverse environments that Marines tend to deploy to. For example, if a 2-kW wind turbine is given to a unit prior to deploying to Afghanistan, what power production should the unit expect considering that they are unsure of their final destination? A HOMER user would determine the range of average wind speeds from the list of possible locations. This range of wind speeds would be input as a sensitivity variable, and HOMER would display the system performance at these varying speeds.

Dealing with uncertainty, like the scenario just described, is not the only use for sensitivity analysis. The following excerpt from the programmers effectively shows the diversity of sensitivity analysis:

> A system designer can use sensitivity analysis to evaluate trade-offs and answer such questions as: How much additional capital investment is required to achieve 50% or 100% renewable energy production? An energy planner can determine which technologies, or combinations of technologies, are optimal under different conditions. A market analyst can determine at what price, or under what conditions, a product (e.g., a fuel cell or a wind turbine) competes with alternatives. A policy analyst can determine what level of incentive is needed to stimulate the market for a particular technology, or what level of emissions penalty would tilt the economics toward cleaner technologies. [6]

It is easy to see that there are a number of utilities for this capability throughout the Marine Corps [6].

E.   PHYSICAL MODELING

This section will discuss how HOMER models the physical operation of systems. For detailed descriptions of physical modeling, the reader should turn to *Integration of Alternative Sources of Energy*. A micropower system in HOMER must have at least one energy source and at least one load. The energy source can be any of the options shown in Figure 3, such as a wind turbine, PV, or a generator. Similarly, there are different types of loads. HOMER micropower systems can also include conversion devices, such as AC-DC converters, and energy storage devices [6].

1. 1. Loads

The term *load* is used within HOMER to identify a demand for electrical or thermal energy. When modeling a micropower system, HOMER models the load first. Although HOMER allows the user to dictate three types of loads—primary, deferrable, and thermal—this thesis is focused on meeting primary loads only. As a result, deferrable and thermal loads will not be discussed in further detail.

The HOMER user is responsible for inputting the primary load. Two options are available. The first option allows the user to import a file containing hourly data. The other option allows the user to input a daily load profile from which HOMER then synthesizes hourly data.

Within HOMER, primary loads require an operating reserve specified by the user. Operating reserve refers to additional power production capability in order to accommodate a sudden increase in the electric demand. For example, utility Marines are taught not to exceed 80% of a generator's capability when meeting a particular load [9]. This means that a 10-kW generator should only be used for loads that generally do not exceed 8 kW. The additional 20% is meant to serve as an operating reserve, which will accommodate any sudden increases in the load without any negative side effects. Likewise, HOMER ensures that there is an operating reserve within the entire array of energy sources selected in a user's particular micropower system.

2. 2. Resources

HOMER uses the term *resource* to include "anything coming from outside the system that is used by the system to generate electric or thermal power [6]." This refers to the renewable resource (i.e., solar, wind, hydro, and biomass) and to traditional fuel. All resources vary wildly depending upon location. Solar radiation is affected by the latitude (the closer to the equator, the stronger the kW/m2) and by cloud cover. Wind is much more arbitrary and can show substantial differences in two locations in close proximity. While hydro and biomass are not considered in this thesis, it is important to note that both are highly variable based on location. As for fuel, it varies much more for Marine Corps pre-deployment purposes than for more traditional micropower scenarios. This variation depends on the particulars of a DESC contract and on the use of the FBCF. The following subsections elaborate on HOMER's use of solar and wind resources.

3. *a. Solar Resource*

Within this thesis, two methods for loading the solar resource were used. One method was to input the latitude and longitude and allow HOMER to generate a

monthly average global solar radiation, which it then applied to a predetermined variability. HOMER retrieves this monthly average from the National Aeronautics and Space Administration's (NASA) Surface Meteorology and Solar Energy website (http://eosweb.larc.nasa.gov/sse/). The other method is to insert actual metered solar radiation data, measured by a pyranometer.

b. Wind Resource

The same NASA website referred to in the Solar Resource subsection was used to find the average monthly wind speeds. Additionally, other methods to capture appropriate wind resource data were used. These methods will be discussed throughout this thesis, when applicable.

c. Fuel

HOMER provides a library of fuels for users to select from. Understandably, JP-8 is not one of the fuels predefined in HOMER. Therefore, the physical properties were input by the author of this thesis. For expeditionary energy purposes, the user must decide whether to input the actual DESC-contracted fuel price or the FBCF. This should depend on what type of analysis HOMER is being used for. If it is simply a fiscal analysis for actual costs, then the contracted fuel price would suffice. If the user is focused on evaluating the long-term comparison of future procurements of generators versus renewable sources, then he should use the FBCF.

4. 3. Components

In HOMER, the term *component* refers to any piece of equipment that generates, delivers, converts, or stores energy [6]. The following components are applicable to this thesis: photovoltaic modules, wind turbines, generators, the grid, converters, and batteries. To fully understand how HOMER models these components, the reader should consult *Integration of Alternative Sources of Energy*. The following subsections elaborate on each component as it relates to this thesis.

a. PV Array

PV array is the component most utilized in this thesis. It is applicable to both test cases and every HOMER scenario. The size of a PV array is very important to forward deployed Marines, but because of limited space secured within a FOB perimeter, HOMER's apathy towards size is not a limitation. It simply means that Marines must assess space and the corresponding PV-array size restrictions elsewhere in the planning process. Separately, the derating factor is critical for Marines using HOMER. Due to the nature of the harsh climates the Marine Corps is prone to deploy to, the effects of dust and temperature cannot be disregarded. For example, in Afghanistan, gusting winds coat everything with sand and dust. Dust atop a PV array limits the solar radiance reaching the photovoltaic cells, seriously hindering their performance. Similarly, the extreme heat of Afghanistan summers will degrade the performance of the system. As mentioned previously, a user must incorporate this into the derating factor to properly model the PV-array output.

b. *Wind Turbine*

HOMER utilizes power curves to model the performance of wind turbines. Power curves are a graphic representation of a particular turbine's power output versus its wind speed. Every different model of turbine performs differently as the wind speed varies, even those that are rated at the same power output. This is due to the different designs and to how those designs respond to a variable input, such as wind. Figure 7 is the power curve of Southwest Windpower's Air X model, which is used within this thesis. The graph shows how the power output varies at different wind speeds. For safety reasons, the turbine controller begins to shut down the turbine when wind speeds exceed 14 m/s, as seen in the graph. Obviously, this information is critical to HOMER's model because it utilizes the wind resource.
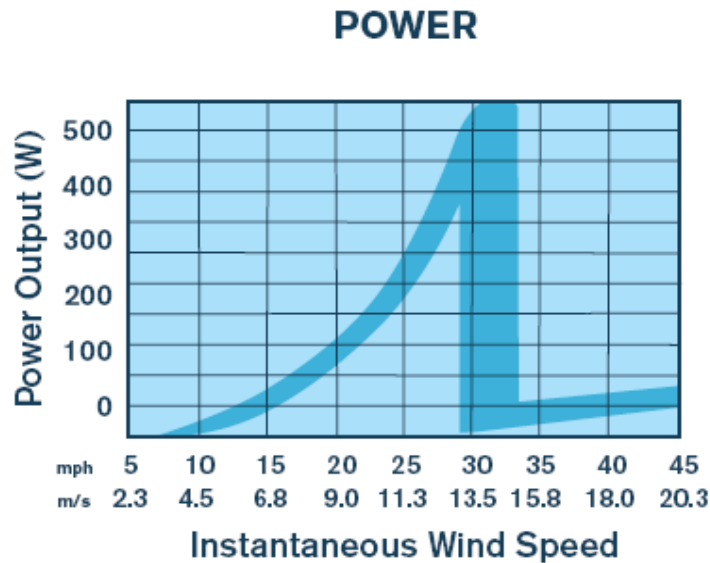
POWER

Figure 7.   Southwest Windpower Air X Power Curve, From [10]

HOMER already has built into its software the power curve of many common wind turbines. If a user wants to model a different turbine, HOMER provides the opportunity for a user to input a power curve.

c.   *Grid*

HOMER's grid modeling capability was used only once within this thesis during a controlled experiment to assist in verifying HOMER's modeled output for the PV array in the experiment. The details of how HOMER models a grid are unnecessary for this thesis. However, if HOMER were used by the DoD to optimize micropower systems for actual installations, the grid component would be critical. Additionally, it is the desire of the author that one day the Marine Corps will have the capacity to tap into local grids, if the opportunity presents itself at a forward deployed location. In this case, HOMER's grid modeling capability would be of great value as well.

F.   SUMMARY

HOMER is a highly advanced and thorough optimization package. A high level of expertise was required to create this tool, but, thankfully, end users are not required to have this level of expertise. Some understanding of power and the different systems is called for, but this thesis will show that advanced expertise is not required.

IV. CONTROLLED EXPERIMENT: GRID-TIED-PV

A. INTRODUCTION

To evaluate HOMER's potential as a pre-deployment tool, its modeling accuracy first had to be scrutinized. This was accomplished by creating an experiment in which the unknown variables were kept to a minimum. For example, the exact azimuth and orientation of solar panels had to be known; the exact solar and wind resource at the location of the photovoltaic panels and wind turbines, respectively, had to be tracked; and the temperature at those locations had to be monitored. Then, and only then, could a HOMER simulation input with these known variables be effectively evaluated against the actual measured production from the utilized equipment. A positive evaluation was not necessarily the result of a perfect match between HOMER's model and the actual measured energy production. Rather, it was the determination of whether a specific HOMER model could be calibrated to a unique setup to achieve comparable results.

Therefore, two unique experiments were designed to properly evaluate HOMER's modeling capability. The first experiment involved a photovoltaic system installed in 2006 on the campus of Naval Postgraduate School. The system is tied to the Pacific Gas & Electric (PG&E) grid, which supports the school's electricity requirements. It includes 56 Kyocera panels, rated at 205 watts apiece, forming three separate PV arrays.

The second experiment, which is discussed fully in Chapter V, was also conducted aboard the Naval Postgraduate School campus and consisted of two non-fixed solar panels and one mobile wind turbine. Each of these components was set up for the purpose of this experiment and was not tied to the grid. The two solar panels were a 50-watt-rated hard panel from Kyocera and a 60-watt-rated flexible panel from PowerFilm. The wind turbine was a 400-watt-rated Air X from Southwest Windpower. Both experiments were conducted over a period of 30 days. The data collection periods for the experiments overlapped, but the timelines were not identical. The grid-tied-PV experiment was monitored April 2–May 1, 2010. The wind-PV experiment was monitored April 24–May 23, 2010.

B.   GRID-TIED-PV

The grid-tied-PV experiment consisted of 56 Kyocera KD205GX panels, each rated at 205 watts. At the NPS campus, the panels are positioned on an azimuth of 231° and have a slope of 15%. As seen in Figure 8, the building characteristics led to this configuration—they are not ideal.   Ideally, solar panels in the northern hemisphere face due south, or 180°. For optimal performance, fixed-position solar panels should have a slope that matches the latitude of their location. This would ensure that the panels received the most direct sunlight throughout the year. The Naval Postgraduate School is at a latitude of 36.58° north. Therefore, optimal performance would be achieved by a slope of 37°.
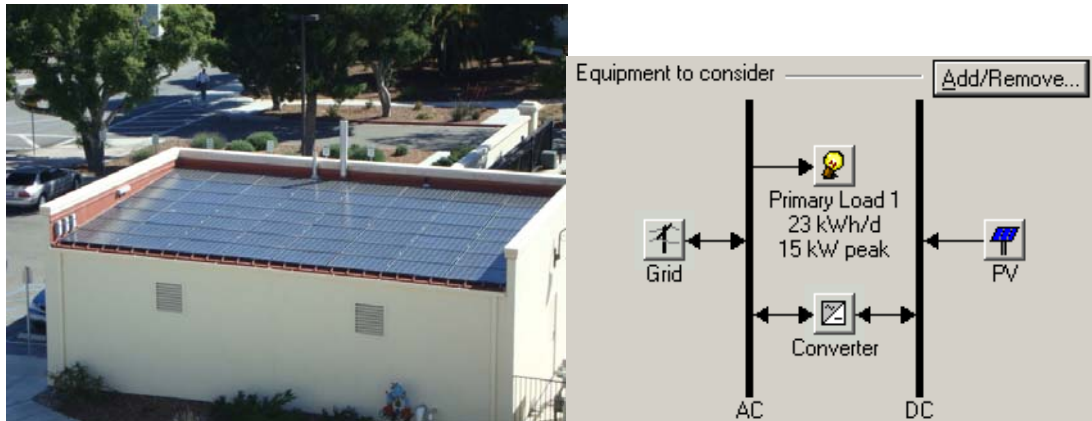
Figure 8.   Photo of the Grid-Tied-PV System, HOMER System Model

The panels are configured to form three separate arrays, each tied to a SunnyBoy SB300U inverter. Two of the arrays consist of 17 panels apiece, and the third has 22 panels. Each array-inverter system is tied to the PG&E grid to displace some of the power draw from the grid. The system was installed in 2006. Table 3 displays the rated capacity of each array and the cumulative 11.48-kW capacity.

Table 3.   Grid-Tied-PV Details

	No. of Panels	Power Rating/ Array (kW)
Inverter 1	17	3.485
Inverter 2	22	4.510
Inverter 3	17	3.485
Total	56	11.48

5. 1. System Details

The Kyocera 205-watt panels used are high-efficiency multicrystal photovoltaic modules. They consist of 54 cells and have a conversion efficiency of over 16% in standard test conditions. The maximum power voltage and current are 26.6V and 7.71A, respectively [11]. The electrical characteristics can be seen in the I-V curve shown in Figure 9.
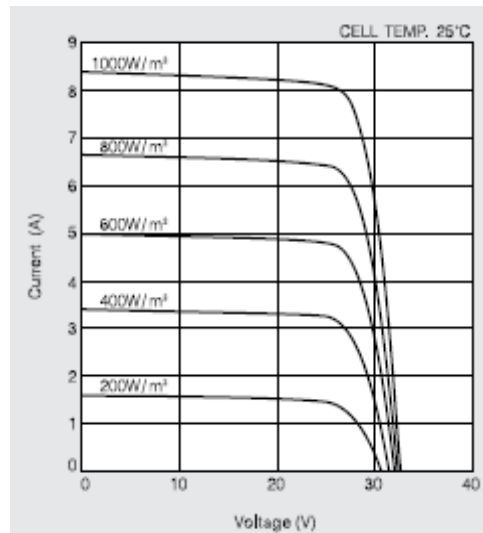
Figure 9.   Current-Voltage Characteristics of KD205GX at Various Irradiance Levels, From [11]

The SunnyBoy SB3800U inverters have a weighted efficiency of 94.5% [12]. Each inverter has a display that is the only metering device on the system. It does not store or transmit the data; as a result, during the experiment, someone had to visit the display each day to collect the relevant data. The inverters display the kWh produced

that day, the kWh produced in the system's lifetime, and the real-time voltage and wattage.

6. 2. Measured Data

To collect the energy data from the PV system, a visual reading was conducted each day. The most important data collected was the *E-Total (kWh)* and *E-Today (kWh)* readings from each inverter. E-Total is the current amount of energy fed into the grid from the inverter, while E-Today reflects the current energy fed into the grid that day. It is important to note that both numbers reflect the energy after the inverter's inefficiency losses, rather than what is actually being generated from the solar panels. Displayed in Figure 10 is the energy fed to the grid from each inverter for each day of the experiment.
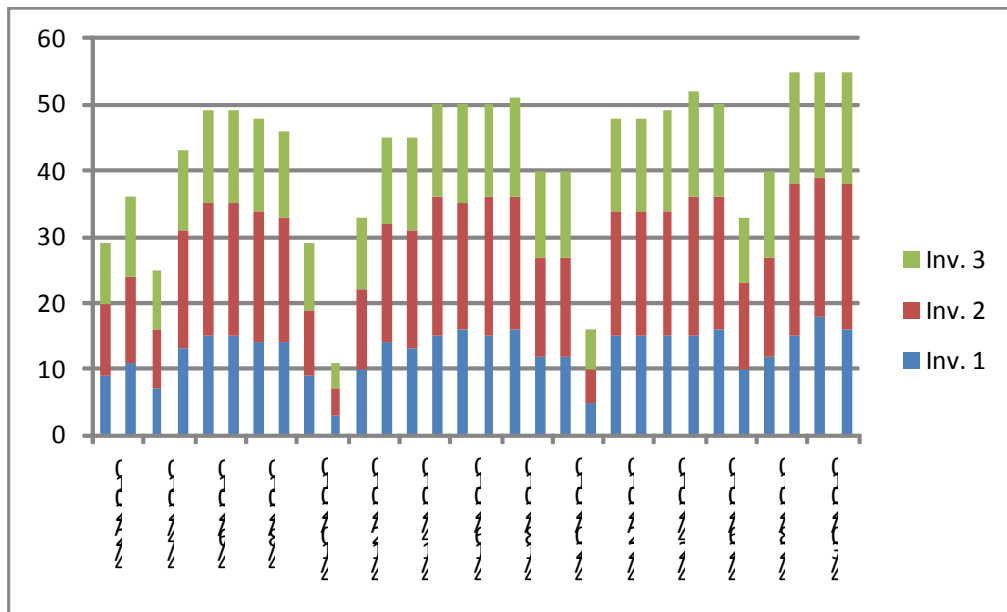
Figure 10. Graph Displaying the Energy Output of Each Inverter in kWh Throughout the Experiment Period

The total production is displayed in Figure 11. The total energy fed to the grid from the three inverters was 1,270 kWh.
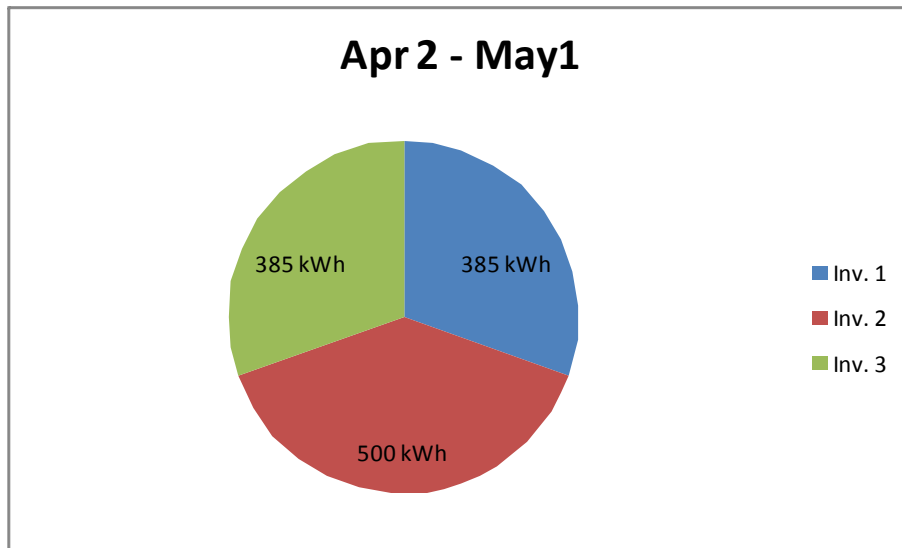
Figure 11.   Graph Displaying the Total Energy Fed to the Grid by Each Inverter During the Period

7. 3. HOMER Simulation

a.   *Load*

To conduct a HOMER evaluation, a user must insert a specific load to be met. Since the PV system is actually meeting a minor portion of the very large load of NPS, there are never instances in which the PV production exceeds the load, which would require the system to shut off. Therefore, any load that exceeds the PV power production at any given time can be inserted into HOMER.

For this experiment, the chosen load was taken from the ExFOB, discussed in Chapter II: The Marine Corps and Alternative Energy. For the purposes of the ExFOB, the Marine Corps established an hourly load profile for a company-sized FOB. The load ranges from about 9–15 kW throughout the day. The load displayed in Figure 12 is the load used for evaluations throughout the ExFOB process.
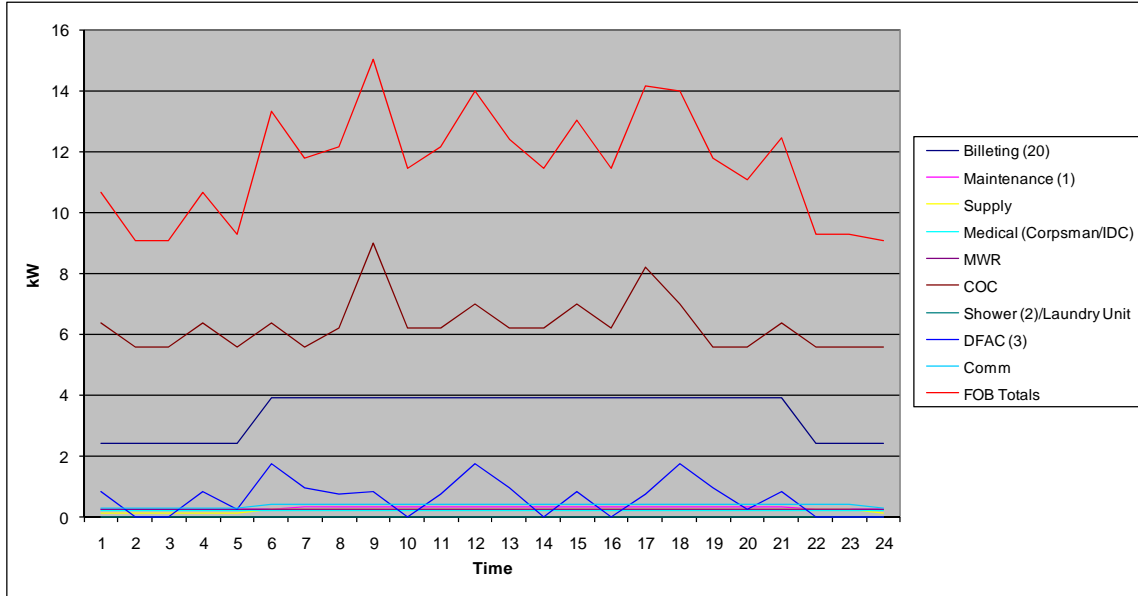
Figure 12.   ExFOB Load Profile for a Company-Sized FOB, From [13]

For the purposes of this thesis, the ExFOB load profile displayed in Figure 12 was rounded to the closest kW for each hour. The result is displayed in Figure 13 in one of HOMER's exported graphs. While HOMER allows the user to insert a degree of variability to a load, that option was not used within this paper. It added no inherit benefit to the evaluation. However, this option should be utilized in most scenarios because loads are rarely consistent.
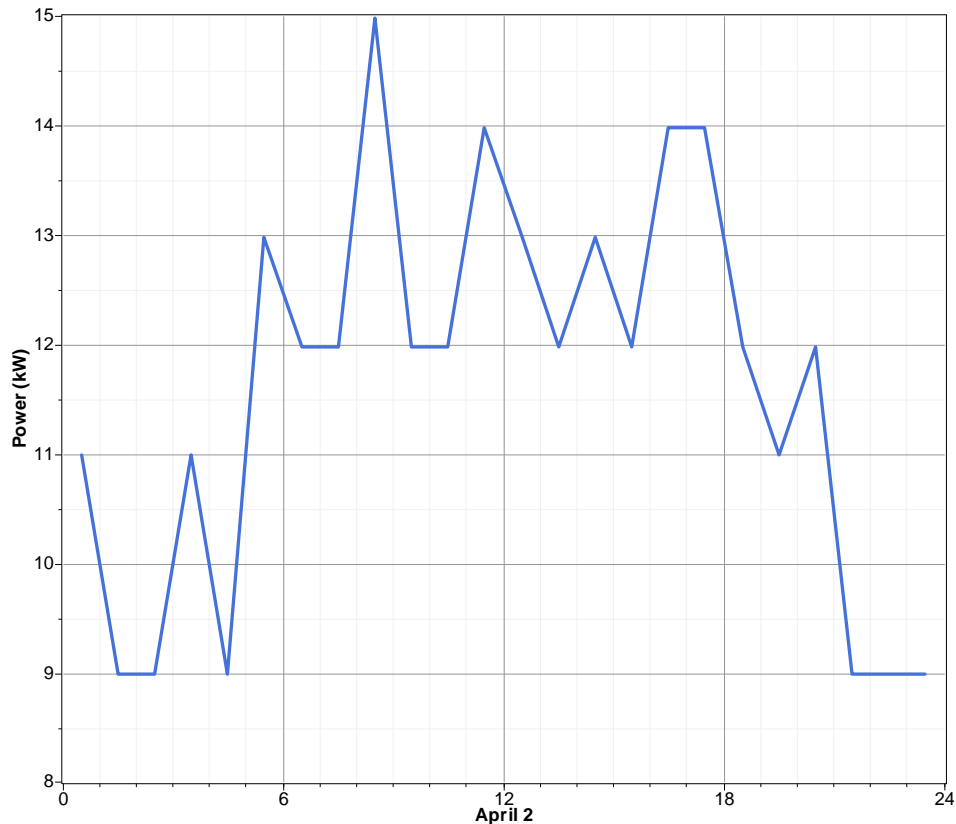
Figure 13.   HOMER Graph Displaying the Hourly Load Profile for One Day

To insert the load for the days of the experiment only, a spreadsheet with 8,760 components was created by the author to match the hours in a year. Then, the number *zero* was inserted into each time slot until the 0100 time slot on April 2. Additionally, a zero was inserted for every time slot beginning with the 0000 time slot on May 2 and continuing through the 8,760th slot. This spreadsheet was then imported into HOMER. The result was a load that represented 8,358 kWh of demand for the period of April 2–May 1.

b.   *Components*

The components selected were PV and Converter.   Additionally, the Equipment is connected to the *grid* button was selected. An example of these selections is shown in Figure 14.
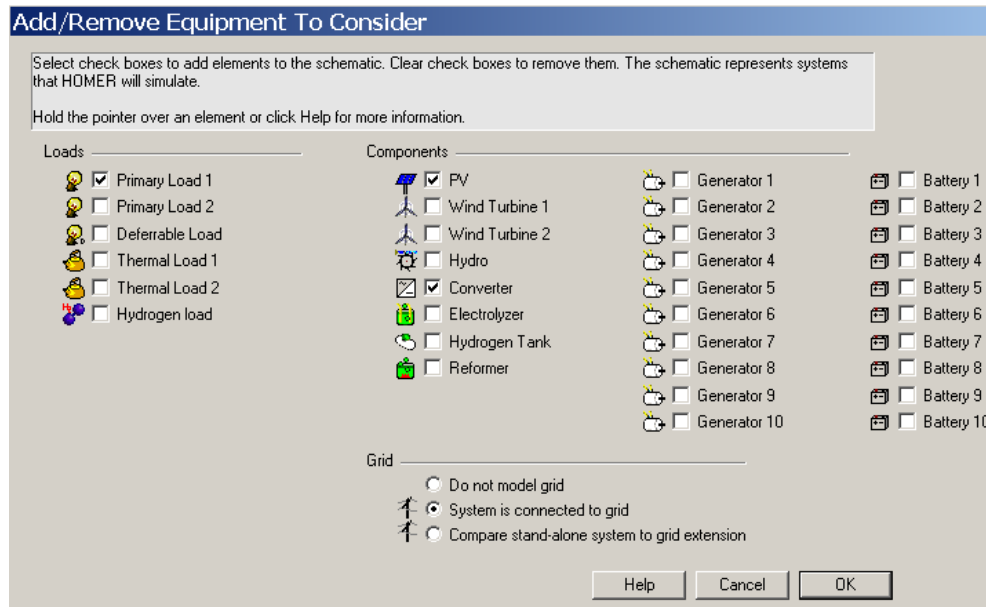
Figure 14.   HOMER Component Selection

c.   PV

The PV inputs are shown in Figure 15.   The initial size chosen by the author was the 205 watts of an individual panel.   The cost considerations were disregarded for the purposes of this evaluation.   The only size to consider included all three arrays as a single 11.48 kW system.   While more sizes to consider could have been input to reflect the three separate arrays, the desired outcome was the use of the entire system, so additional sizes were unnecessary.   The 20-year lifetime is a default HOMER value, and it was irrelevant to the particulars of this experiment.   The 80% derating factor is also a default value that was not altered for the initial simulation.   However, the derating factor will play a critical role in the calibration process discussed later.   The slope and azimuth correspond to the particulars of the actual system.   Ground reflectance was left at the default value of 20%.   Additionally, the temperature effects were not considered at this point in the experiment but did play a role in the calibration process.
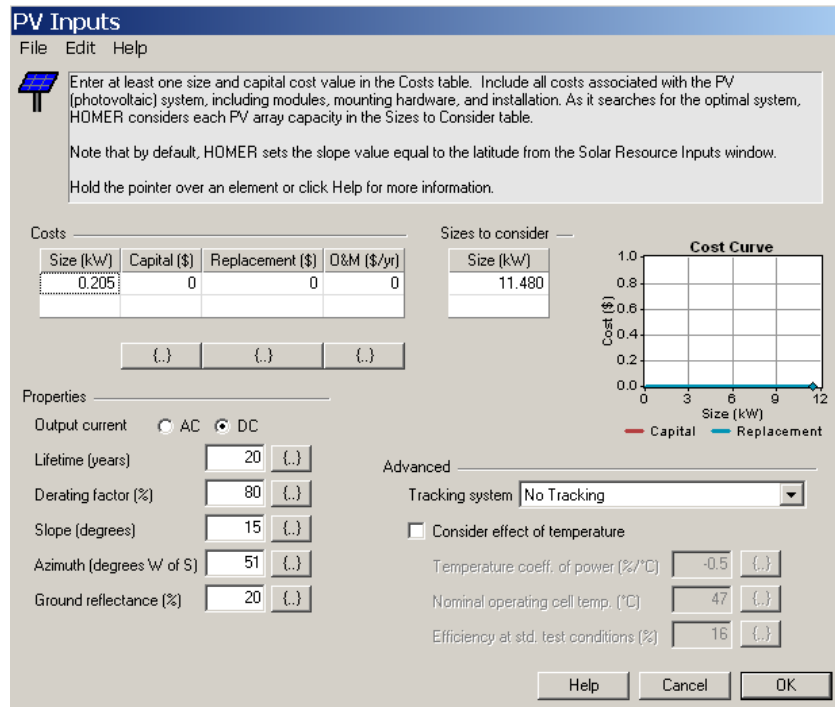
Figure 15. PV Inputs for the Grid-Tied-PV Experiment

d. Converter and Grid

The key input for the converter was the efficiency. The inserted efficiency for the inverter was 94.5%, as discussed in the System Details subsection. It was also important to input inverters that could accommodate the instantaneous power output of the load. Each SunnyBoy 3800U is rated at 3.8 kW [12], so the input for the category labeled *Sizes to consider* was 11.4 kW in order to represent all three. The Converter Inputs page is displayed in Figure 16.
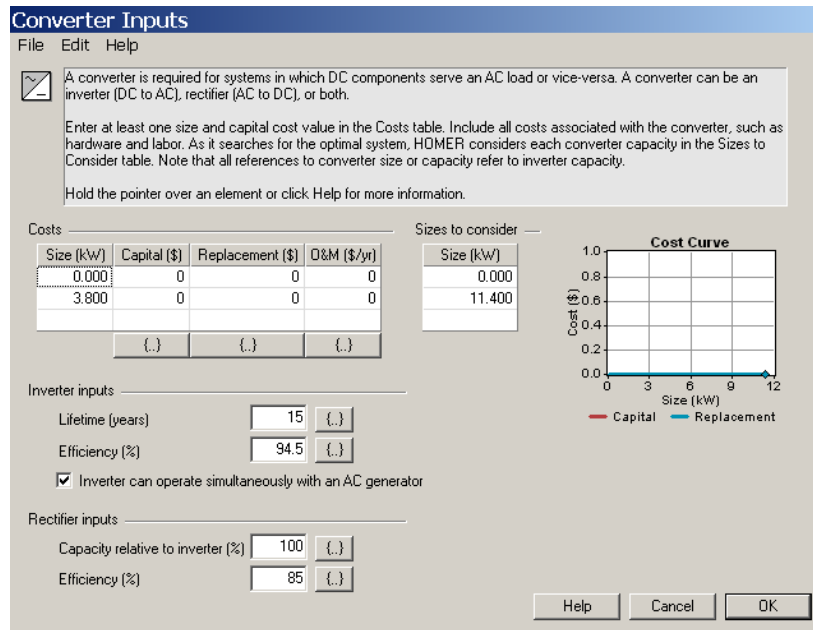
Figure 16.   HOMER Converter Inputs

As for the grid, there were no critical specifications needed. The utility cost of $0.17/kWh is what NPS uses for planning purposes [14]. That cost was added simply to ensure HOMER valued the cost-free PV system over the grid when both options were available.

e.   *Solar Resource*

The initial model utilized HOMER's inherent solar resource estimating capability. This was done by inputting the latitude, longitude, and time zone that corresponded to the actual system. Then, by selecting *Get Data Via Internet*, HOMER populated the monthly averages of the clearness index and daily radiation from NASA's Surface Solar Energy Data Set [15]. An example of the Solar Resource Inputs page is shown in Figure 17.
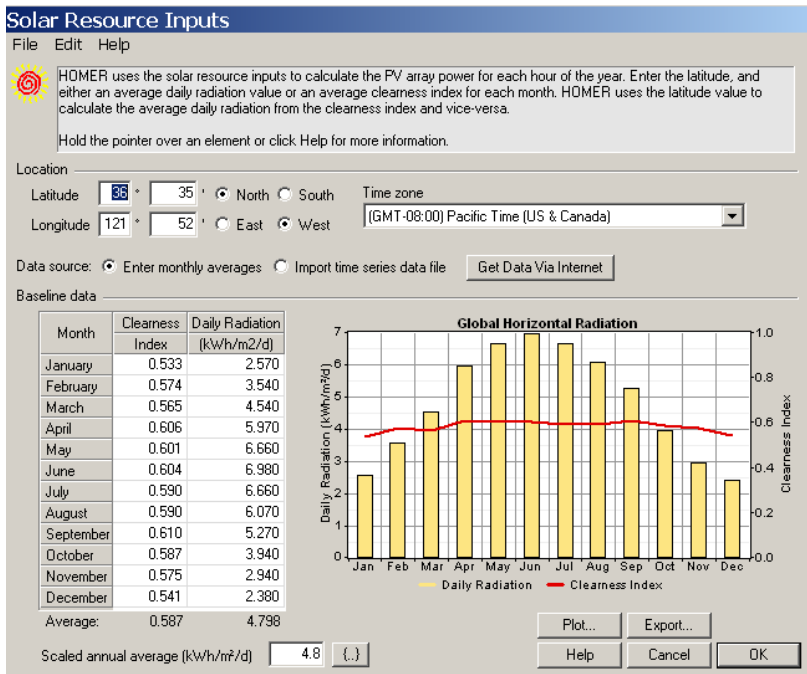
Figure 17.   HOMER Solar Resource Inputs

f.   Results

HOMER's simulation resulted in the power output displayed in Figure 18. The graph reflects the output power following the inversion. Therefore, it incorporates the inverter efficiency.
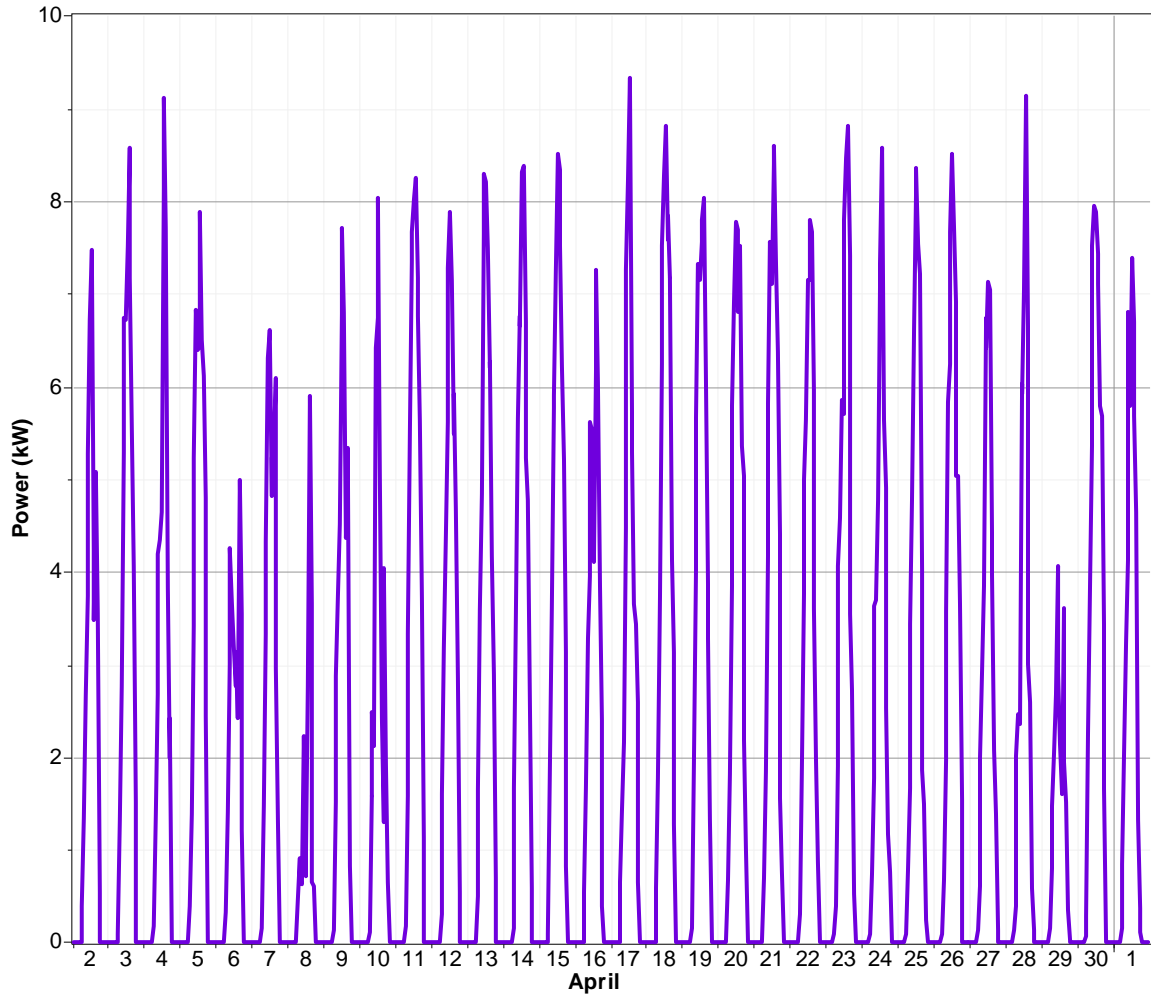
Figure 18.   Inverter Power Output for Uncalibrated HOMER Model

HOMER does not have a graphic that displays daily energy totals in kWh to compare to the measured data shown in Figure 11. The total energy after inversion for the period can easily be derived, as shown in Equation 1.1, by subtracting the grid purchases from the AC primary load found on the Electrical tab of the results. Figure 19 provides a visual of this. The result is the total kWh met by the PV system, rather than the grid.

$$8358 \text{ kWh} - 6746 \text{ kWh} = 1612 \text{ kWh} \tag{0.1}$$

| Cost Summary | Cash Flow | Electrical | PV | | Converter | Grid | Emissions | Hourly Data |

Production	kWh/yr	%		Consumption	kWh/yr	%
PV array	16,977	72		AC primary load	8,358	37
Grid purchases	6,746	28		Grid sales	14,431	63
Total	23,723	100		Total	22,789	100

Figure 19. HOMER Production and Consumption Summary

8. 4. Evaluation

This section is focused on evaluating HOMER's simulation results compared to the actual measured data. The overall effectiveness of HOMER was determined by identifying whether it could be logically manipulated, resulting in an accurate model outcome that corresponded to the actual measured data.

a.   Comparison

How did HOMER's results compare with the measured data? At this point in the analysis, they could be classified only as unfavorable. While the actual energy fed to the grid during the experiment was 1,270 kWh, HOMER's model estimated 1,612 kWh. This is a 27% increase in production. That level of inaccuracy would prove inadequate for the Marine Corps' purposes. However, the uncalibrated HOMER model used up to this point in the analysis corresponded to the most basic of inputs and averages, which may have led to the inaccuracy.

The author had to determine what possible contributors led to HOMER's inaccuracy. For this specific experiment, the author identified three such possibilities: temperature effects, solar irradiance estimates, and the actual performance of the system. Each of these will be covered in further detail later in the thesis and new HOMER simulations will be discussed following each step of the calibration process.

b.   Temperature Effects

It is critical to understand the negative effect on the performance of photovoltaic systems when the panels heat up due to the absorption of solar heat. This is not simply for locations with high ambient temperature. Even in mild climates, there can

be degradation due to the heating of the panels. HOMER has the ability to simulate the temperature effects on a PV panel if the pertinent information is available, as seen in Figure 20. This is the temperature coefficient of power (%/°C), the nominal operating cell temperature (NOTC, °C), and the efficiency at standard test conditions (%). Often these details are listed on or can be derived from the technical data sheets of the PV panel being evaluated.
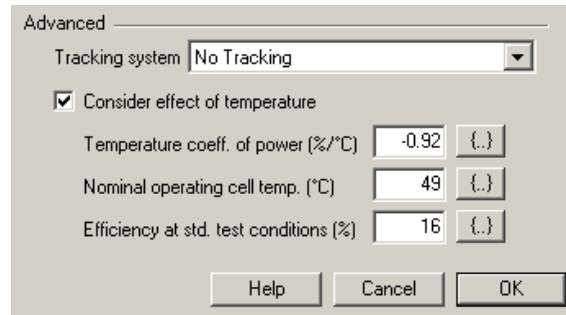
Figure 20.   HOMER Temperature Effects Inputs

In the case of the Kyocera KD205GX, both the NOTC and efficiency at standard test conditions are listed. They are 49° and 16%, respectively [11]. The temperature coefficient of power is not listed and must be derived. Most often, technical data sheets will not list the temperature coefficient in terms of power. Instead, the temperature coefficients of the open-circuit voltage and the short-circuit current will be listed. To achieve a reasonably accurate temperature coefficient of power, Equation 1.2 should be used [16]:

$$\alpha_{V_{oc}} \times I_{mpp} = \alpha_{P} \tag{0.2}$$

In this equation, $\alpha_{V_{oc}}$ refers to the temperature coefficient of the open circuit voltage, I_{mpp} is the maximum power current, and α_{P} is the temperature coefficient of power.

For the KD205GX, the resulting equation is

$$-.120 \frac{V}{°C} \times 7.71A = -.925 \frac{W}{°C} \tag{0.3}$$

When HOMER includes temperature effects in PV simulations, it requires the user to input the ambient temperature for the location of the panels. Once again, HOMER gives the user the option of retrieving this data from [15], which provides an

average ambient temperature for each month. The user also has the option to insert more precise data.

For the purpose of this experiment, the monthly averages from [X] were inserted by the author in HOMER as the ambient temperature. Then, HOMER was used to model the system again, with the new temperature-related inputs. This resulted in a more accurate energy estimation, as seen in Table 4. The new HOMER model estimated that the system would meet 1,539 kWh of the energy load over the course of the month. The inaccuracy, therefore, was reduced from +27% to +21%.

Table 4.   Improved Modeled Energy Estimates Due to Temperature Effects

	PV Usable Energy (kWh)	Accuracy
Measured Data	1270	
HOMER Model	1612	+27%
Add Temp Effects	1539	+21%

c.   *Solar Irradiance*

The next step in calibrating this system within HOMER was to interject a more accurate solar resource than was utilized in the initial model. While the monthly averages provided by [14] were a good starting point, they gave HOMER very little information concerning the true solar irradiance. This problem would be inconsequential when projecting the PV production of a unique system over the course of many years because the average will generally hold true, despite the variance from year to year. However, when comparing actual PV production to a HOMER model, the solar irradiance variance from the average can have substantial effects on the accuracy.

Dick Lind provided the author assistance in retrieving a more accurate solar irradiance for the experimental period. The data he provided was from a weather station positioned at the Monterey Bay Aquarium, which is approximately two miles from NPS. The solar irradiance measurements were in two-minute intervals.   The data was stored in text form, as seen in Table 5. Each two-minute data set was stored with the following information: station (which in this case was the Monterey Bay Aquarium), year, month, day, minute of the hour in Coordinated Universal Time (HrMn UTC), and solar irradiance in watts per meter squared (SW). Table 5 is an example of the data set. When collecting data from a weather station, it is important to clarify whether it is solar radiance, which is direct sunlight only, or solar irradiance, which incorporates refracted light hitting in addition to direct sunlight.   The distinction is important because photovoltaic panels produce power from refracted light as well as from direct sunlight.

Table 5.   Example of Solar Irradiance Data From the Weather Station at the Monterey Bay Aquarium

```
Stn Year Mo Da HrMn   SW(in)
                  UTC   w/sq m
MBA 2010  4  2     0   401.10
MBA 2010  4  2     2   394.90
MBA 2010  4  2     4   388.00
MBA 2010  4  2     6   383.50
MBA 2010  4  2     8   374.30
MBA 2010  4  2    10   363.90
```

To utilize this data for the purposes of HOMER, a user must manually manipulate the data. To manually insert solar irradiance into HOMER, the user must create an Excel spreadsheet with hourly solar irradiance values for the entire year. Similar to the process of uploading the load, the solar irradiance input must have 8,760 values to match the hours in a year. Additionally, the values must be in kilowatts per meter squared.

The author wrote MATLAB code, included in Appendix A, to facilitate the data manipulation required. Before the code could be utilized, the text file from the weather station had to be entered into an Excel spreadsheet. Next, UTC times had to be converted to local Pacific Standard Time (PST), which represented a seven-hour difference. From here, MATLAB code was utilized to create a data set appropriate for HOMER input.

The code was written to pull the two-minute interval data from a spreadsheet and then to plot the one-month period, as seen in Figure 21. Then, the code was used to calculate a mean hourly value from the two-minute intervals within each hour. This result was a relatively accurate solar irradiance reading per hour. Then, the code was used to create an array of 8,760 data points from only one month's worth of data. Because HOMER's power estimation for the rest of the year was irrelevant in the context of this experiment, the solar irradiance for those periods was irrelevant as well. Therefore, the code was written to simply insert the number *zero* for the solar irradiance during those periods. As seen in the code, there were 2,184 hours in the year before April 2. The relevant code was then inserted into the array and represents 720 hourly data points. Again, the number *zero* was inserted for each subsequent hourly data point for the rest of the year. Finally, the code converts the W/m² solar irradiance values to kW/m².
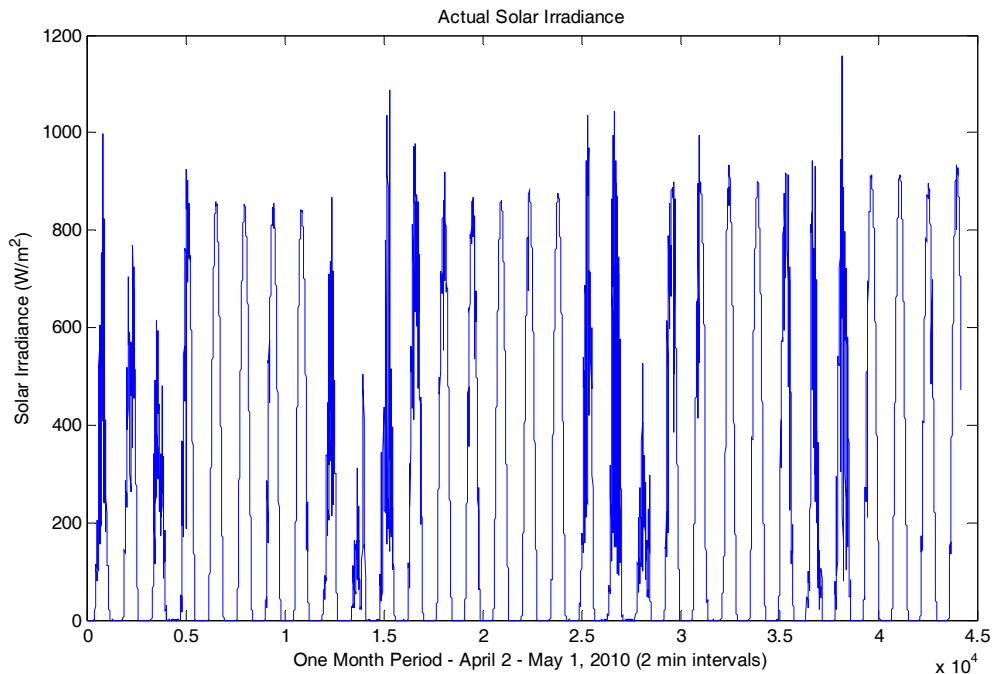
Figure 21.   MATLAB Graph Displaying the Original Solar Irradiance Data from the Monterey Bay Aquarium

Before discussing the insertion of the measured solar irradiance data into HOMER, it is important to look at how HOMER's estimates from average solar irradiance stacked up to the actual data taken from the weather station at the aquarium.

To facilitate this, the author utilized MATLAB once again. To make a comparison between the two data sets, both were integrated over the one-month period. The MATLAB code was written to integrate each of the solar irradiance data sets over the one-month period, and it compares the two values. This led to the results displayed in Table 6.

Table 6.   Comparison Between HOMER's Estimated Solar Irradiance and the Actual Data Taken from the Weather Station at the Monterey Bay Aquarium

	kW/m² (over one month period)
HOMER Estimate	189.8
Aquarium Data	170.0

This comparison indicates that the actual solar irradiance was 9.35% less than HOMER's original estimate. Obviously, this is a significant drop and will certainly result in a decrease in power production from the photovoltaic panels. At this point, it becomes evident that HOMER's estimated solar irradiance was, in fact, one of the factors leading to HOMER's power production calculations far exceeding the actual power produced by the grid-tied-PV. However, it is important to note that the solar irradiance comparison in Table 6 and the resulting 9.35% disparity do not translate into a 9.35% difference in the power production. This is due to the nature of the comparison, which only compared the total kW/m^2 for the month and disregarded when the disparities occurred. This is relevant because photovoltaic panels generally produce the greatest percentage of power during the middle of the day, when the sun is directly overhead. Therefore, a greater disparity in solar irradiance during the noon hour would equate to a far more significant difference in power production. Alternately, if more solar irradiance disparity occurred during the twilight hours, it would result in far less disparity in the power production numbers.

Figure 22 shows graphs of the two solar irradiance data sets as a frame of reference for the disparity between the two. To simplify the view, only the first six days of the period are graphed.
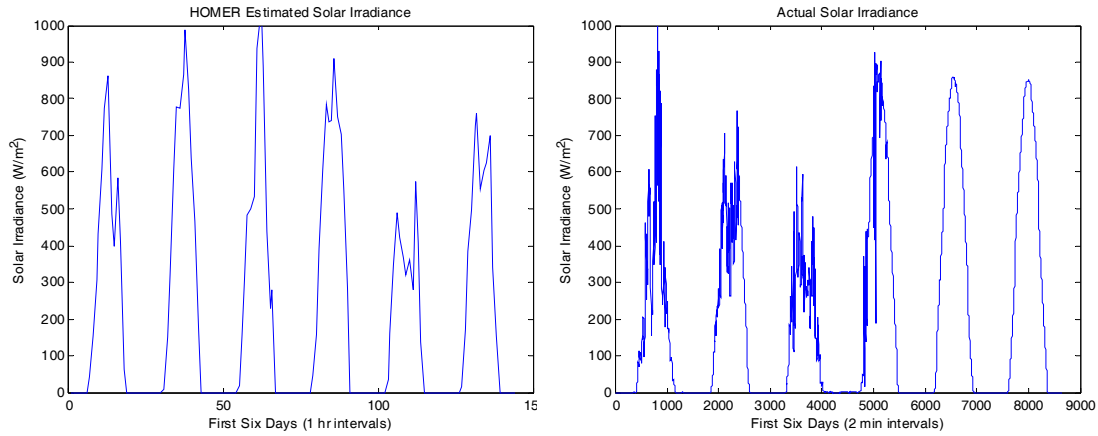
Figure 22. Graphs Displaying HOMER's Estimated Solar Irradiance and the Actual Solar Irradiance

Finally, the true solar irradiance data was input into the HOMER model. As predicted, the power production results from HOMER decreased, bringing the HOMER estimates closer to the actual power production gathered, as seen in Table 7. The HOMER model improved from 21% greater than the actual power production to 17% greater.

Table 7. Improved Model Energy Estimate Due to Accurate Solar Irradiance

	PV Usable Energy (kWh)	Accuracy
Measured Data	1270	
HOMER Model	1612	+27%
Add Temp Effects	1539	+21%
Add True Solar Irradiance	1483	+17%

It is worth noting that HOMER's model dropped by 56 kWh after inserting the true solar irradiance. This represents only a 3.64% drop in power production as compared to the 9.35% drop in solar irradiance.

d.   System Performance

The final step in the calibration process centered on the overall system's performance. This involved the derating factor, which is defined by the programmers in the following quote: "The derating factor is a scaling factor meant to account for effects of dust on the panel, wire losses, elevated temperature, or anything else that would cause the output of the PV array to deviate from that expected under ideal conditions [6]." The default value of the derating factor is set to 80% within HOMER, but it should be altered as a calibration mechanism. This is where first-hand knowledge of the system is necessary.

For the purposes of the experiment, the author lowered the derating factor incrementally until HOMER's power production matched that of the actual collected data. This resulted in a derating factor of 68.5%. With a derating factor of 68.5%, the HOMER model estimated a power production of 1,270 kWh for the one-month experiment, matching the actual collected data, as seen in Table 8.

Table 8.   Improved Model Energy Estimates Due to a Calibrated Derating Factor

	PV Usable Energy (kWh)	Accuracy
Measured Data	1270	
HOMER Model	1612	+27%
Add Temp Effects	1539	+21%
Add True Solar Irradiance	1483	+17%
Vary Derating Factor	1270	--

This decrease of the derating factor is justifiable. After discussions with base personnel [14], the author discovered that the solar panels have rarely, if ever, been cleaned. This led the author to believe that there is a layer of dust on the solar panels, which significantly decreased the kW/m^2 fueling the photovoltaic panels. Therefore, it is reasonable to infer that the overall efficiency of the system has decreased and corresponds to a derating factor of 68.5%.

9. 5. Conclusion

The purpose of this experiment was to evaluate a HOMER model of the grid-tied-PV versus actual measured energy production from the Kyocera KD205GX. The author discovered that part of the process of utilizing HOMER needed to involve a calibration of the model to the particular scenario being modeled. A controlled experiment was the best forum for that calibration.

The grid-tied-PV system proved that HOMER can accurately predict power production if the calibration is done. By applying the three calibration steps of including temperature effects, inputting accurate solar irradiance data, and inferring a more accurate derating factor, HOMER satisfactorily modeled a real-world system. The experiment detailed in the next chapter is an attempt to further test HOMER's modeling capability by utilizing a completely different system all together. The results of the calibration process will be discussed, and the concept of the energy density of power systems will be introduced.

V. CONTROLLED EXPERIMENT: WIND-PV SYSTEM

A. INTRODUCTION

This experiment was an opportunity to evaluate HOMER's modeling of small PV and wind systems. Two different types of PV and one wind turbine were set up on the roof of Spanagel Hall at Naval Postgraduate School. The objective was to compare the measured energy output of these systems to a HOMER model of each. Both the experimental setup and the HOMER model were conducted one system at a time, rather than all together. The PV portion of this experiment showed the effectiveness of HOMER's modeling capability. However, the same cannot be said for HOMER's wind turbine modeling. Wind as an energy resource is much more variable than solar irradiance. Therefore, HOMER's modeling strategy of hourly simulations was insufficient in the context of this experiment and perhaps in the context of expeditionary energy all together. This chapter details the experiments, the HOMER models, and the comparative results.

B. EXPERIMENT

10. 1. Photovoltaics

Two unique types of solar panels were utilized for this experiment. One was a hard panel configuration made by Kyocera and known for its optimal performance and high efficiency. The second panel used was a foldable, flexible panel of thin film cells made by PowerFilm. These panels are known to have a low efficiency but are very durable and light. The two panels are shown in their test position in Figure 23.

**Figure 23.   The Two Solar Panels Utilized for the Wind-PV Experiment
(Note: The Kyocera panel is in the foreground and the PowerFilm
panel is in the background.)**

a.   *Kyocera*

A Kyocera KC50T High Efficiency Multicrystal Photovoltaic Module was one of the three systems used in this experiment. It is rated at 54 watts under standard test conditions. The KC50T is reported to be over 16% efficient. It has a hard panel structure and can be configured in an array of multiple solar panels. The dimensions are 0.652 meters by 0.639 meters, for an area of 0.417 meters squared. The I-V curve, illustrated in Figure 24, shows the panel's performance at different irradiance levels. It was chosen as a compliment to the PowerFilm flexible solar panel discussed in the next subsection

.
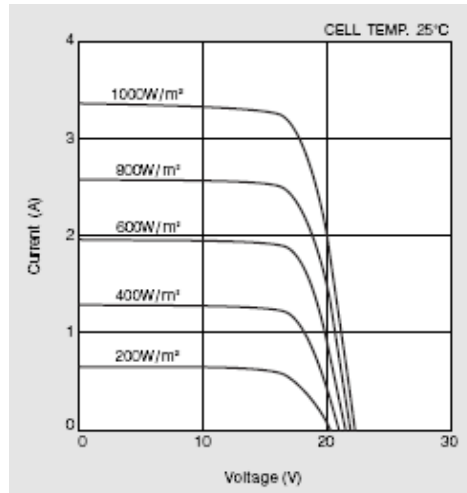
**Figure 24. Current-Voltage Characteristics of KC50T at Various Irradiance
Levels, From [22]**

b. *PowerFilm*

A PowerFilm FM15-3600 was the other solar panel used for this experiment. It is flexible and foldable. PowerFilm markets the FM15-3600 as being "designed for users who need lightweight and portable power for laptop, cell and satellite phones, GPS units and more [17]." PowerFilm lists it as a solar charger and gives it a power rating of 60 watts. It is much less efficient than the KC50T multicrystal structure, but PowerFilm does not publish any details concerning its efficiency. In fact, PowerFilm publishes very little concerning the performance of the system. The only published information is the operating voltage (15.4 volts) and the operating current (3.6 amps) at standard test conditions. When employed, the panel is 1.499 meters by 1.092 meters, for an area of 1.632 meters squared.

c. *Set Up*

Next to the solar panels, a pyranometer was set up to accurately measure the solar irradiance level at that exact location. The pyranometer was an Apogee SP-110 and was set up and maintained by Dick Lind of the NPS Meteorology Department. Each of the PV systems was mnitored for a one-month period, from April 24–May 23, 2010. Each solar panel was connected to a high-power variable resistor, which could be varied

between 1 and 7 ohms. A maximum power point tracker (MPPT) was not utilized for the experiment. Instead, a relative maximum power point (MPP) was calculated.

The MPP of a solar panel is critical to the performance of the system. It is the point on the I-V curve that produces the most power from the solar panel. The concept of MPP is described graphically in Figure 25. The green line represents the I-V curve of a solar panel receiving a certain irradiance level. Since power is equal to current multiplied by voltage, the wattage is drastically different depending on the voltage chosen for that system. However, there is a location on the I-V curve that will produce the highest wattage. This point is referred to as the MPP. The red line represents the wattage as the voltage setting varies across the I-V curve. The voltage level when the red line is at its peak corresponds to the voltage level on the I-V curve where the MPP is. An MPPT continuously monitors the I-V curve of a solar panel and adjusts the voltage level to produce the most power at that instant.
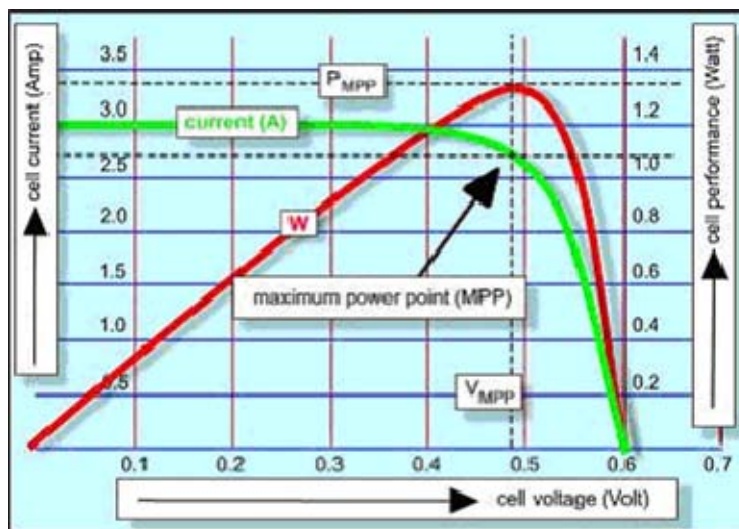
Figure 25.   Maximum Power Point Graphic, From [18]

In lieu of an MPPT, a rudimentary process was undertaken to set the load at an appropriate resistance in order to ensure that the solar panels remained relatively close to the MPP. Each panel was set up on a cloudless day at the noon hour, which corresponded to the highest level of solar irradiance. Each panel was connected to a

variable resistor. The resistance was varied between 1 and 6 ohms, and the current and voltage were recorded for each setting, as seen in Table 9.

Table 9.   **Voltage and Current Measurements Corresponding to Each Resistance Level**

	Kyocera KC50T			PowerFilm FM-15	
Resistance (Ω)	Voltage (V)	Current (A)		Voltage (V)	Current (A)
1	2.1	3.2		3.6	4.7
2	5.7	3.3		8.2	4.4
3	9.2	3.3		11.1	4
4	11.5	3.2		12.2	3.6
5	12.6	3.1		12.7	3.1
6	13.2	2.9		12.8	2.7

This data was then utilized in MATLAB to create the I-V curves and corresponding power graphs seen in Figures 26 and 27. The relative MPP was selected by evaluating the I-V curve graphs.   The blue line with red circles represents the measured I-V data points and the resulting curve. The green line represents the power curve, resulting from the multiplication of the current and voltage corresponding to the data points. The I-V data point, which resulted in the highest power output, was chosen. This analysis led to the selection of a 4-ohm load for the KC50T and a 3-ohm load for the FM-15 3600 to simulate the MPP. Certainly, a more accurate maximum power point could have been solved for, but that level of precision was deemed unnecessary. Even if a precise MPP was chosen for the scenarios presented in Table 9, it would no longer be applicable once the solar irradiance level changed, which it does continuously. As soon as the solar irradiance level changed, the load setting would have become less efficient, regardless of how precise the calculations had been. The bottom line is that with the absence of an MPPT, PV production will never be efficient. However, the objective of this experiment was to calibrate HOMER to the particulars of a unique circuit—whether that circuit operates at maximum efficiency is irrelevant. Once a HOMER model is calibrated to a circuit, it can accurately model the setup of that circuit anywhere in the world.
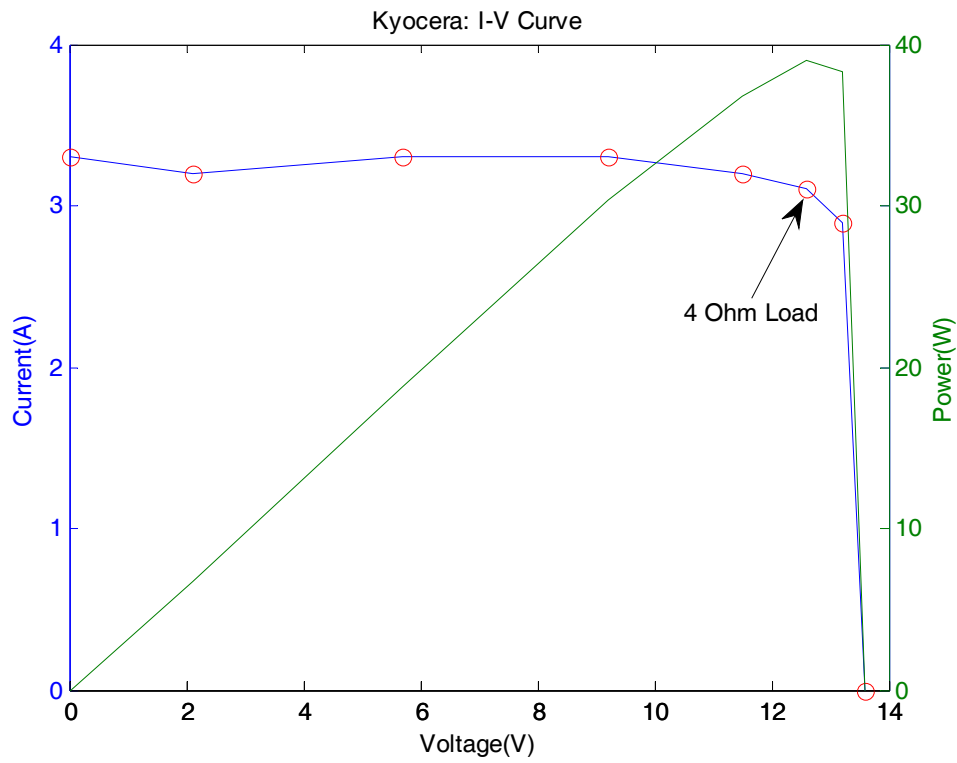
Figure 26.   I-V Curve from the Variable Resistance Connected to the Kyocera KC50T (Blue line = I-V Curve, Green line = Power Curve)
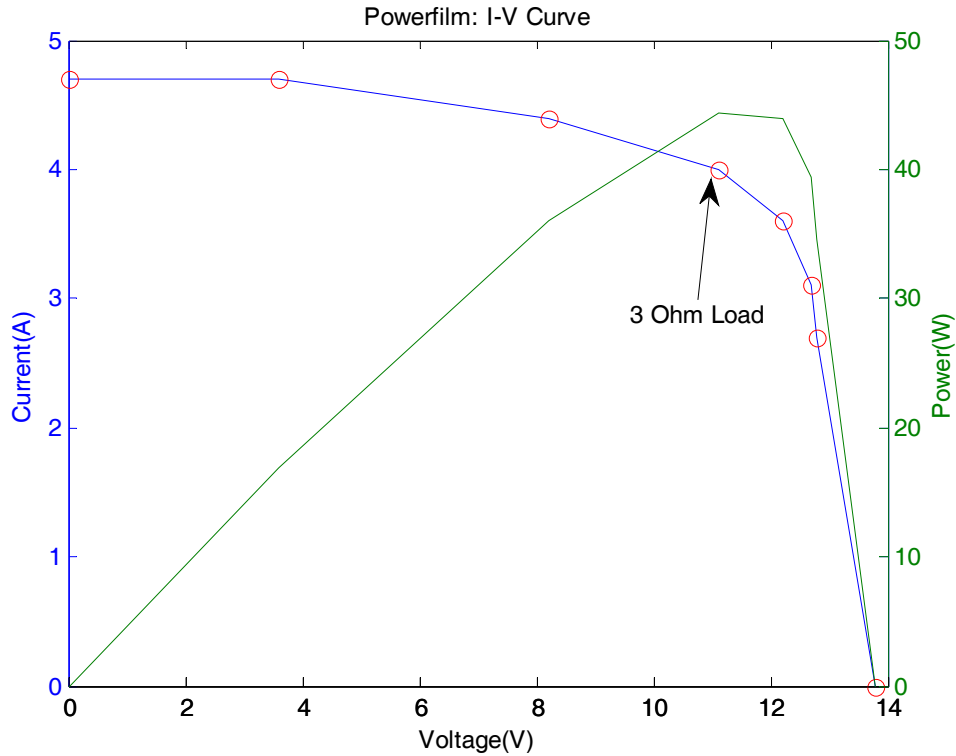
Figure 27. I-V Curve from the Variable Resistance Connected to the PowerFilm FM-15 3600 (Blue line = I-V Curve, Green line = Power Curve)

The circuit shown in Figure 28 depicts the PV experiment. A LabView program was written by Jeff Knight, the NPS Electronics Lab technician, to collect the data from the PV experiments. A block diagram of the program is shown in Appendix B. The program was created to collect the time, instantaneous current, and instantaneous voltage reading every minute.
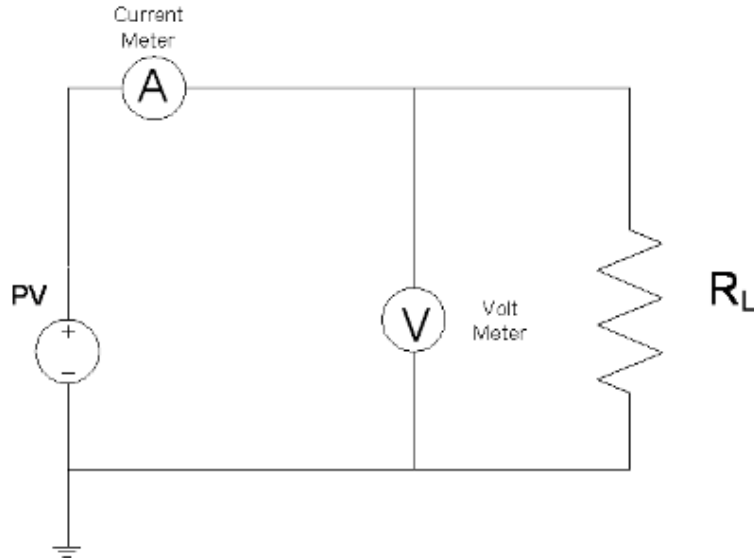
Figure 28.   Generic PV Circuit Setup for Experiment (R_L represents the load resistance)

d.   Data Collected

The data for both the Kyocera and PowerFilm panels was collected over the one-month period from April 24–May 23, 2010.   It was collected in one-minute intervals, consisting of a date and time stamp, the instantaneous current, and the instantaneous voltage, as seen in Table 10.

Table 10.   Sample of Kyocera KC50T Data Measured During Experiment

DATE	TIME		CURRENT (A)	VOLTAGE (V)
5/5/2010	9:17:53 AM		1.93E+00	9.60E+00
5/5/2010	9:18:53 AM		1.95E+00	9.72E+00
5/5/2010	9:19:53 AM		1.94E+00	9.69E+00
5/5/2010	9:20:53 AM		1.95E+00	9.72E+00

From this data, instantaneous power was calculated for each one-minute sample by multiplying the current and voltage. A sample of this power data is shown in Figure 29 and represents the first three days of the experiment period. Notice how the power profile on Day 3 looks different than the power profile on the first two days. This

was due to the intermittent cloud cover on that day, which resulted in drastic fluctuations in the solar irradiance.
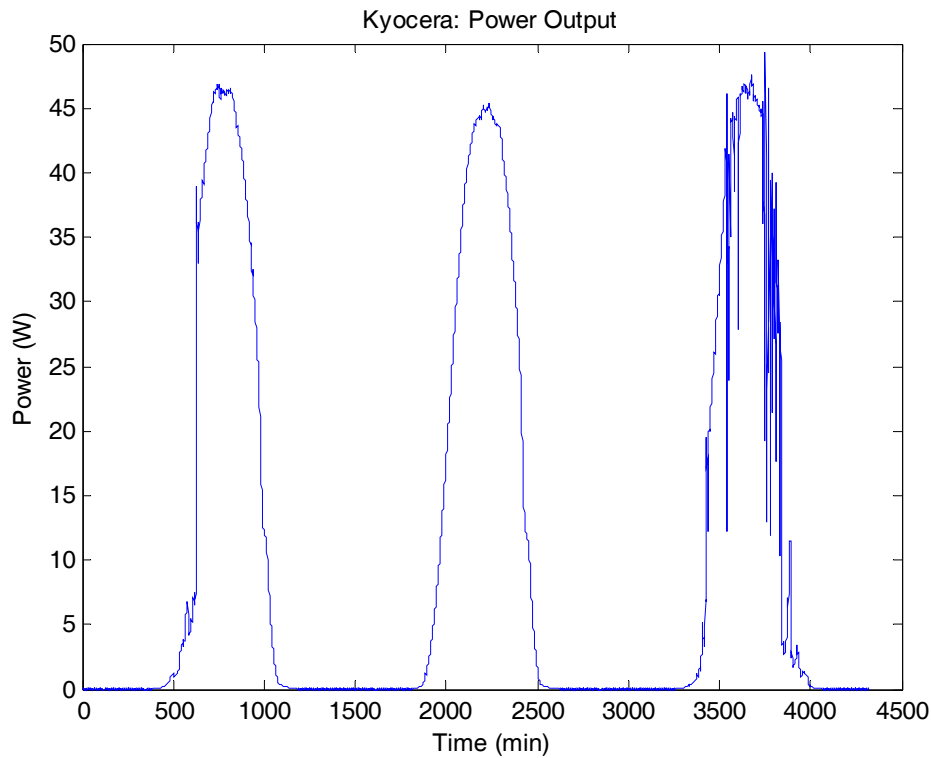
Figure 29.   MATLAB Plot of KC50T Instantaneous Power in One-Minute Intervals over the First Three Days of the Experiment

MATLAB was also used to extrapolate the energy production of each panel for the entire one-month period. First, the instantaneous power at each minute sample was assumed to be constant throughout the one-minute period. Obviously this was not the case, but the variations were negligible when looking at monthly totals. Next, each power point was multiplied by the one-minute interval to give a watt-minute energy level. Next, each value was divided by 60 to display energy in watt-hours (Wh). Then, all values for the entire month were summed to give watt-hours per month. This process is shown in Equation 1.4, where E_{mth} refers to the energy produced throughout the month and P_i refers to the instantaneous power.

$$E_{mth}=\Sigma\left[P_i(1\text{ minute})\left(\frac{1\text{ hour}}{60\text{ minute}}\right)\right] \tag{0.4}$$

Using this process for both solar panels resulted in the energy levels shown in Table 11. The Kyocera KC50T produced 5.312 kWh during the one-month period. Meanwhile, the PowerFilm FM-15 3600 produced 4.781 kWh during the month. The daily average, as watt-hours per day, is displayed in Table 11.

Table 11.   Solar Panel Energy Production for Duration of the Experiment and Daily Average

	Energy Produced Apr24 - May23 (kWh)	Daily Energy Production (Wh/d)
Kyocera KC50T	5.312	177
PowerFilm FM-15 3600	4.781	159

11. 2. Wind Turbine

The small-scale wind turbine used for this experiment was an Air X, manufactured by Southwest Windpower. The Air X turbines were owned and maintained by the NPS Oceanography Department, specifically by Professor Timothy Stanton. The turbines were being operationally tested prior to their employment in the Arctic. Professor Stanton was gracious enough to modify the test circuit in order to facilitate this experiment. Three turbines were utilized in succession during this experiment. The replacement downtime, the time when the turbines were swapped, only totaled a combined four hours. Therefore, it had little impact on the 30-day energy totals. The turbine was affixed atop a pole on the roof of Spanagel Hall on the NPS campus. An RM Young 8500 Ultrasonic Anemometer was set up next to the turbine to monitor the wind speed [19]. Figure 30 is a photograph of this setup.

Figure 30.   Photo of the Air X and Adjoining Anemometer Used in the Wind-PV Experiment

a.   Air X

The Air X is considered a small-scale wind turbine. It is rated at 400 watts at a 12.5 m/s wind speed. It has an internal charge controller and peak power tracker [20].   The   Southwest   Windpower   website   http://www.windenergy.com/products/air_x.htm) details the function of the charge controller:

> The Air X charge controller periodically stops charging, reads the battery voltage, compares it to the voltage setting and if the battery is charged, it completely shuts off all current going to the battery. This function is performed within a few milliseconds. The closer the battery is to reaching its full state of charge, the more often the Air X circuit repeats this action. When the battery has reached its charged state, the Air X will slow to an almost complete stop. [20]

This information was critical to the experiment. The objective of the experiment was to measure the total energy produced over a one-month period, compare it to the HOMER model, and then calibrate the model. Due to the advanced design of the controller to stop producing power when the battery is charged, the measurements taken in this experiment are not simply a reflection of the energy production capability of the Air X. Rather, they are a reflection of the energy production capability of the Air X in the confines of the circuit it is connected to. In other words, HOMER will be calibrated to the particulars of the circuit the wind turbine is a part of. The results of the HOMER calibration are then applicable to the setup of this exact circuit at any location on earth. This circuit is discussed in the following section.

b.   Setup

The turbine was connected to a 12-volt battery. A circuit was designed in parallel to the battery to ensure that it had a constant load drawing power from it, but that it was prevented from dropping below 12.4 volts. The circuit diagram is shown in Figure 31. Four 25-ohm resistors provided a constant 100-ohm load (R_L) on the battery to ensure that the battery did not remain fully charged. The zener diodes were included to ensure that the battery did not drop below about 12.4 volts by essentially turning off the load when the battery dropped to that voltage. The circuit was designed to ensure that the battery did not discharge too low or too often, which would have decreased the lifespan of that battery.
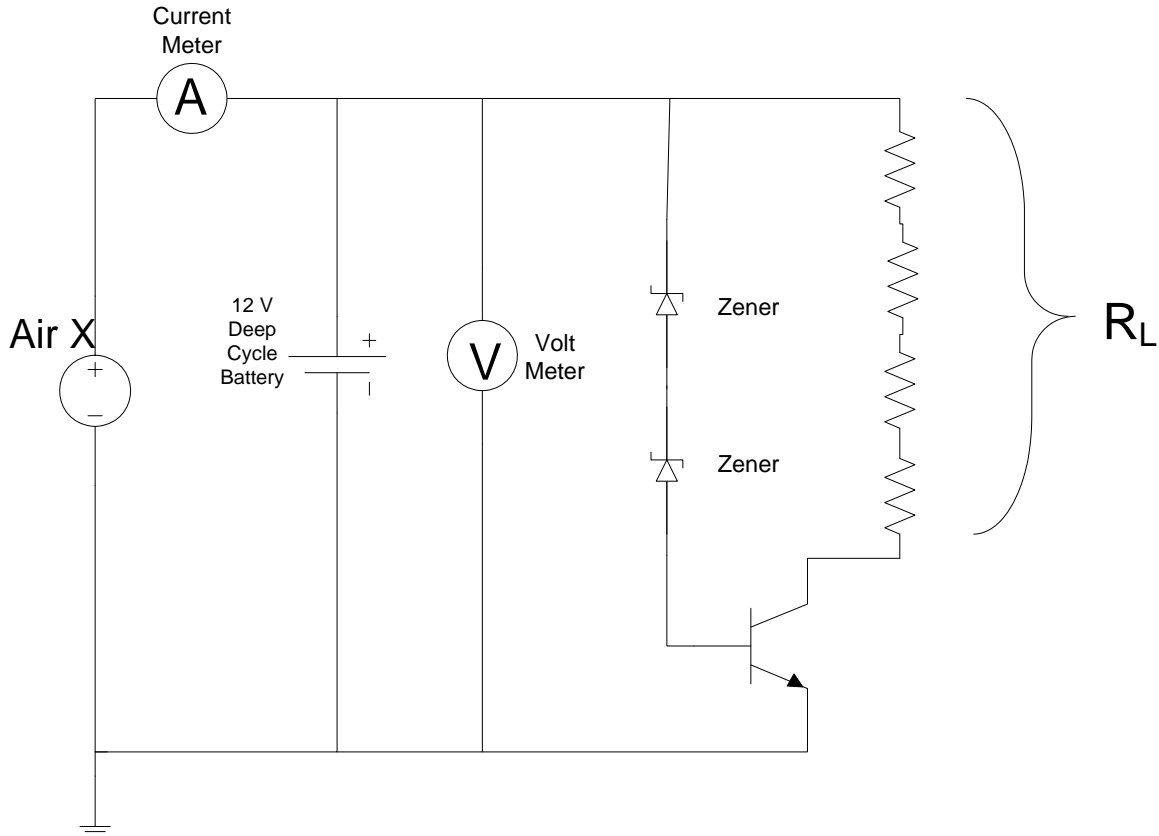
Figure 31.   Circuit Diagram of the Air X Experiment

The data was collected via a MAXIM MAX4080 [21] in 10-second intervals. The data format is shown in Table 12. The first seven columns represent the date/time stamp. The eighth column is the wind speed reading from the anemometer. The anemometer recorded the wind speed in terms of voltage, with a standard conversion of 5 volts being equal to 100 m/s [19]. The wind speed was converted to m/s via Excel, but is not shown in Table 12. The ninth column is the instantaneous battery voltage. Column 10 is the current leaving the wind generator. The final column represents the mean power over the 10-second interval. The MAX4080 chip took a sample of the battery voltage and of the generator current ten times a second. Then, it calculated a mean value for the battery voltage and the generator current across the 10-second period and multiplied those mean values to produce an average power value for the period.

Table 12.   Collected Data During Air X Experiment

Yr (1900+)	mth	day	hr (UTC)	min	sec	millisecond	wind speed votls (5v=100m/s)	battery voltage (V)	wind generator current (A)	Avg. Power (W)
110	4	23	19	34	12	403894	0.217	12.71	0.032	0.412
110	4	23	19	34	22	413219	0.284	12.713	0.093	1.188
110	4	23	19	34	32	423545	0.292	12.76	0.689	8.794

c.   *Data Collected*

MATLAB code was written by Professor Stanton to view the data and extract an energy production value. Over 250,000 samples were collected during the 30-day experiment. In Figures 32 and 33, four graphs are shown to display different aspects of the data. For simplicity, only Days 4–6 were graphed. The graphs show the measured wind speed, battery voltage, wind turbine current, and mean wind turbine power, respectively; each measurement is shown versus time, which is in 10-second segments.
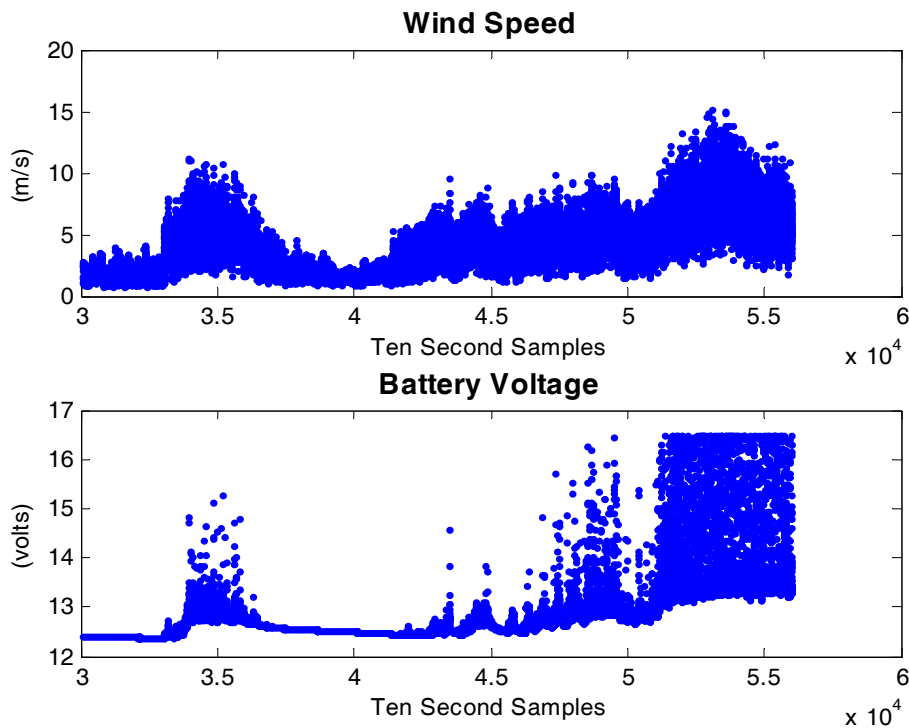
Figure 32.   Air X: Wind Speed and Battery Voltage (Days 4–6)
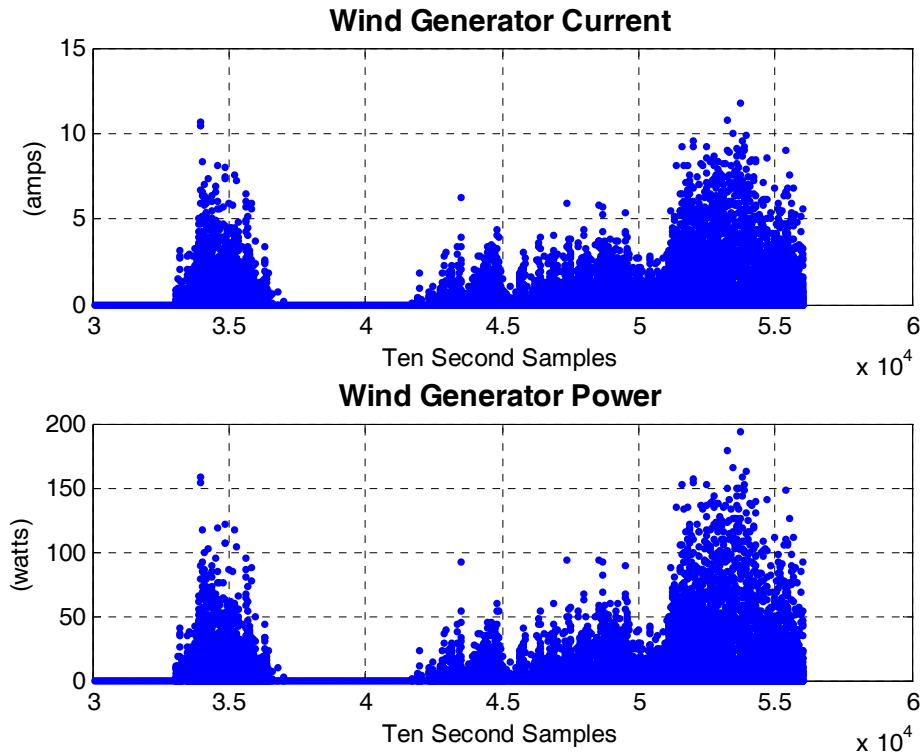
Figure 33.   Air X: Current and Mean Power (Days 4–6)

Further analysis of the data shows how the Air X produced power in relation to the wind speed. Southwest Windpower publishes a power versus wind speed graphic that details the Air X's expected performance, displayed in Figure 34. For the sake of comparison, the actual measured data is displayed in a power versus wind speed graph in Figure 35. Only the first 10 days are graphed, for simplicity's sake. A visual comparison between the two graphs indicates that the Air X in the experiment generally performed as the manufacturer stated.
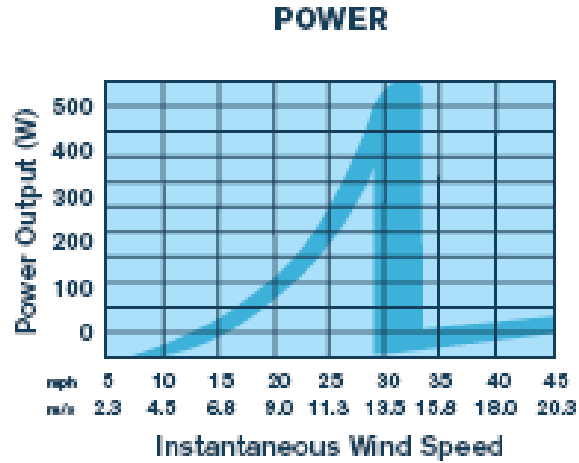
POWER

Figure 34.   Air X: Published Power Versus Wind Speed Graph, From [10]
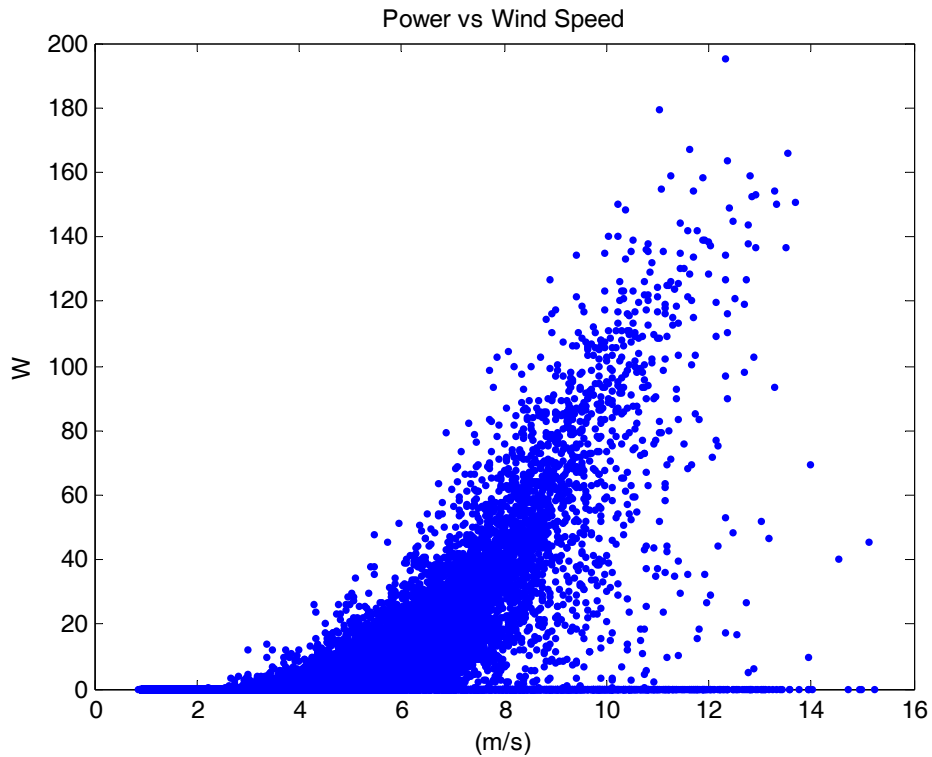
Figure 35.   Air X: Power Versus Wind Speed (Days 1–10)

However, two attributes of note are displayed in Figure 35. One is the inconsistency of the power production at each wind speed. For example, the power production at 9 m/s ranges from 130 watts down to 0 watts. This range is much greater

than the range shown in the manufacturer's graph in Figure 34. This inconsistency was due to the effects of turbulence in the area of the turbine. Turbulence and its effect on wind power will be discussed further in the section III.C.4.

The other noteworthy attribute in Figure 35 is the result of the turbine's performance when the battery was fully charged. Figure 36 is shown to highlight this; it has a more narrow scope of the same data shown in Figure 35. The inconsistency of the circuit is best revealed by the numerous points in Figure 36, where the power output is close to 0 watts, despite the wind speed being in excess of 6 m/s. This is the result of the charge controller stopping the power production of the turbine.
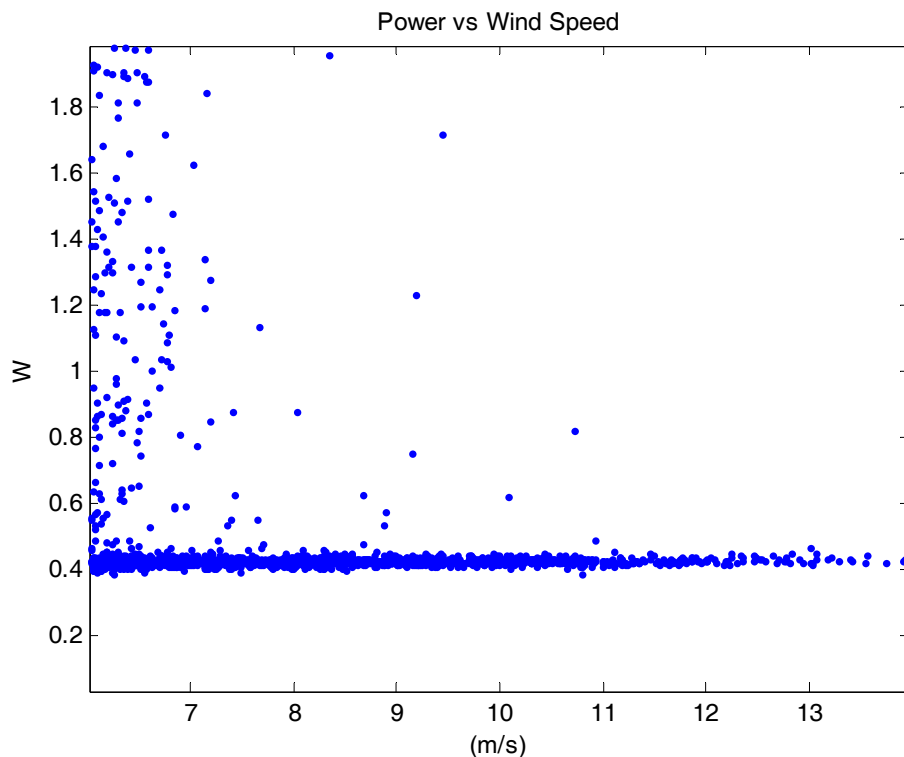
Figure 36.   Air X: Power Versus Wind Speed, Zoomed in to Display All Samples That Had Wind Speeds Greater Than 6 m/s, Yet Produced No Power Due to the Circuit Configuration (Days 1–10)

The total energy produced by the Air X during the 30-day experiment was calculated via the MATLAB code written for this experiment. First, the mean power data was filtered to remove any values less than 0.05 watts. These values represented noise in

the system, when the turbine was not spinning, and therefore were negated. Next, the mean power output for each 10-second sample was integrated across each hour to produce an energy level of watt-hours for each hour of the period. This was accomplished by using Equation 1.6. In this equation, E_{mth} represents the energy produced by the Air X during the month, and $P_{mn>.05}$ represents all mean power values greater than 0.05 watts. These power values were multiplied by 10 seconds to produce energy in watt-seconds for each sample period. Next, each of these energy values was converted to watt-hours. Finally, these hourly values were summed to produce an energy total for the entire period. The final result was 1.538 kWh for the 30-day period, which equates to 51 Wh a day, as seen in Table 13.

$$E_{mth} = \Sigma \left[P_{mn>.05} (10 \text{ seconds}) \left(\frac{1 \text{ hour}}{3600 \text{ seconds}} \right) \right] \tag{0.5}$$

Table 13.   Total and Average Daily Energy Produced by the Air X During the Experiment

	Energy Produced Apr24 - May23 (kWh)	Daily Energy Production (Wh/d)
Air X	1.538	51

Certainly, the energy production was much lower than anticipated for a wind turbine rated at 400 watts. The next section will discuss the HOMER model and detail the comparison of the wind energy data measured and modeled. Additionally, justification for the poor power production of the Air X will be detailed.

C.   HOMER ANALYSIS

12. 1.   Inputs

The initial inputs for the HOMER model of each of the systems were virtually the same. The inputs that relate to all models will be discussed in this section, while the inputs unique to a particular model will be discussed in the respective section of each system. First, the equipment selected was *Primary Load 1*, *PV*, *Converter*, and

Generator 1. Also, *Do not model grid* was selected. Unlike the grid-tied-PV experiment discussed in Chapter IV, the grid was not used for this experiment. Instead, a generator was chosen to simulate the power production not met by the alternative power systems.

Before discussing the generator selected, it is important to discuss the load inserted into HOMER for this micropower system. As in the first experiment, the desire was to maintain the use of the ExFOB load, shown in Figure 13. The load, however, was too large for the purposes of this experiment. Therefore, it was scaled down uniformly by a factor of five. This scaled-down load is shown in Figure 37. As in the grid-tied-PV experiment, an hourly load profile was created for the entire year. The scaled load was inserted to HOMER for the period of the experiment, April 24–May 23, 2010, only. The load for the rest of the year was input with the number *zero*. This file was then uploaded to HOMER.
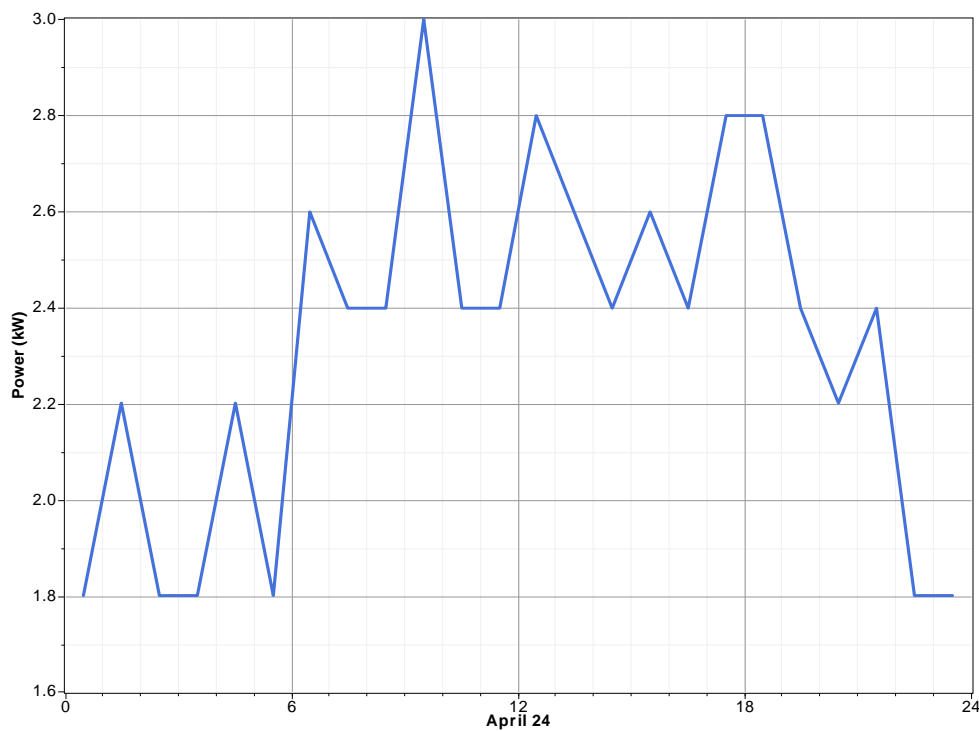
Figure 37.   Load for Wind-PV HOMER Model, Taken from Scaled-Down Version of ExFOB Load

The generator chosen for the modeling portion of this experiment was the Mobile Electric Power–802A, known simply as MEP–802A. It is the 5-kW generator in the

Marine Corps' inventory. It was chosen due to the nature of the load, which does not exceed 3 kW. Therefore, the generator would not be under- or overloaded. The fuel selected was JP-8, which was added into HOMER's fuel inventory during the grid-tied-PV experiment.

The converter efficiency is identified to be 100%. This is because the measured data included no converter and remained DC. Therefore, to appropriately compare the measured and modeled energy production, it was preferable to have no losses due to the inversion—however impractical that may seem in real life.

The grid coordinates for the solar resource matched the NPS location. They were 36°35'north and 121°52'west. The initial solar resource for each PV model was acquired via the *Get Data Via Internet* button. The *Slope* and *Azimuth* of the PV systems were both input with the number *zero* because the systems were flat on the ground during the experiment.

13. 2. Kyocera

The PV inputs are the only inputs not mentioned in the previous subsection. Therefore, they are the only inputs unique to the HOMER model of the Kyocera KC50T. In Figure 38, the initial PV inputs of the precalibrated model are shown. The 54-watt rating of each panel was included as the baseline size. In order to show more power production, the micropower system was modeled with 30 KC50T panels. The resulting 1.62-kW system is seen in the *Sizes to consider* column. The costs were deemed irrelevant to this exercise, so the number *zero* was input into each position. All other values in Figure 38 represent the default values within HOMER.
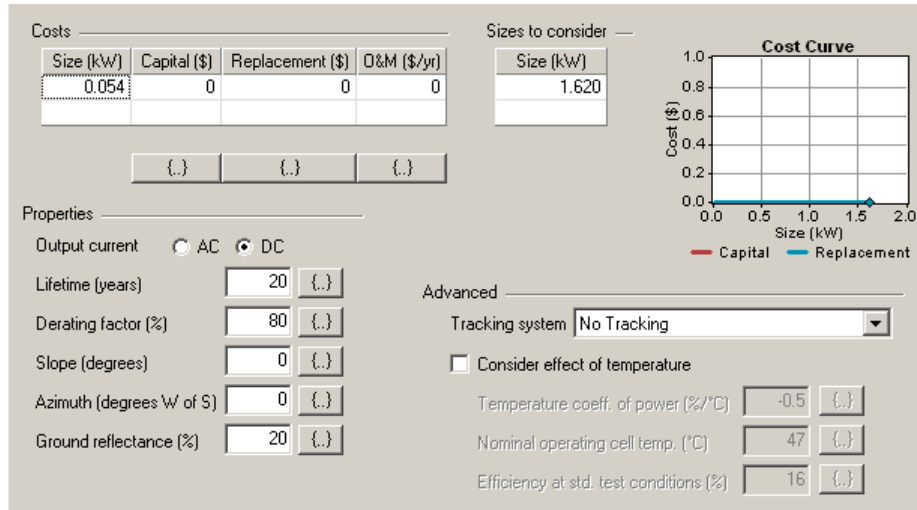
Figure 38.   PV Inputs of the Precalibrated KC50T Model

The measured energy from the KC50T experiment was 5.312 kWh, as discussed in the Kyocera Data Collected subsection. As shown in Table 14, 30 panels would equal the rounded value of 159 kWh, all things being equal. This served as the baseline for the calibration of the Kyocera KC50T model.

Table 14.   Kyocera KC50T Scaled Usable Energy from Measurements

	PV Usable Energy (kWh)
Measured Data (1 panel)	5.312
Measured Data (Scaled to 30 panels)	159

The precalibrated HOMER model resulted in an estimation of 233 kWh of usable energy, which was 47% higher than the measured data. The following section will show the calibration process used to align the HOMER model with the measured data.

a. Calibration

The same calibration process described in Chapter IV was utilized for the Kyocera KC50T portion of this experiment. The results of the first two steps of the calibration process are displayed together in Table 15. First, temperature effects were included in the model, as shown in Figure 39. The NOTC and efficiency at standard test conditions were taken directly from the Kyocera KC50T Specifications Sheet [22]. Meanwhile, the temperature coefficient of power was calculated using Equation 1.2, given in Chapter IV. Additionally, the average monthly temperature at the Naval Postgraduate School was included as an input, as detailed in Chapter IV.

Figure 39.   PV Inputs for Kyocera KC50T Temperature Effects

The second step of the calibration process involved inserting the actual solar irradiance data measured at the location of the experiment. This data replaced the monthly average irradiance and corresponding hourly data used in the precalibrated model.

Table 15. Results of the First Two Steps in the Kyocera KC50T Calibration Process

	PV Usable Energy (kWh)	Accuracy
Measured Data (Scaled to 30 panels)	159	
HOMER Model	233	47%
Add Temp Effects	232	46%
Add True Solar Irradiance	225	42%

Finally, the derating factor had to be altered to reduce the modeled energy production and concluded the calibration process. This was done by making use of the sensitivity analysis capability within HOMER. The sensitivity analysis capability allows a user to insert multiple values for any of the variables inputs. Then, the model is simulated with each of the values and the results are displayed graphically. In this case, sensitivity analysis was used for the derating factor. This was done by selecting the *{…}* button next to *Derating factor* on the *PV Inputs* page. Then, a range of values was inserted, as seen in Figure 40.

Figure 40.   Sensitivity Values for the Derating Factor in Kyocera KC50T

Following the recalculation of the HOMER model, the results of the sensitivity analysis were evaluated. This was done by selecting the *Sensitivity Results* tab and selecting *PV Production* as the *Primary*. The resulting graph is shown in Figure 41. The appropriate derating factor can be found by locating where the line in the graph corresponds to 159 kWh, which corresponds to the actual measured data. The line shows that the derating factor for this experiment should be 52%.
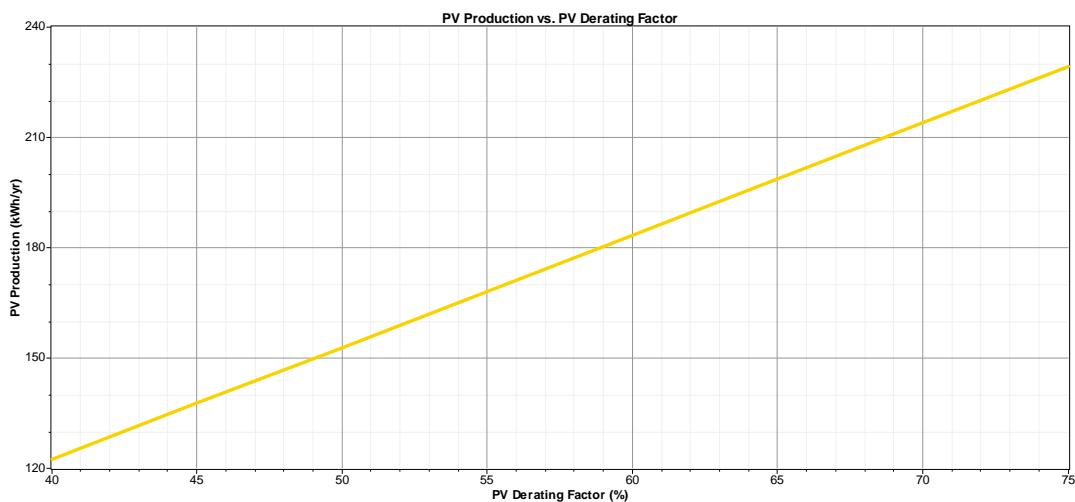
Figure 41.   Sensitivity Results: PV Production Versus PV Derating Factor

b. Results

The results of the calibration process are shown in Table 16. It is important to ask if these results pass the logic test. Obviously, very little difference was made in the model by including the temperature effects and the actual solar irradiance. Meanwhile, the derating factor had to be drastically lowered from the default value of 80%.

Table 16.   Kyocera KC50T HOMER Calibration Results

	PV Usable Energy (kWh)	Accuracy
Measured Data (Scaled to 30 panels)	159	
HOMER Model	233	47%
Add Temp Effects	232	46%
Add True Solar Irradiance	225	42%
Vary Derating Factor	159	--

The most logical reason behind the substantial derating factor drop is the lack of an MPPT in the experiment. This drop in performance was not a surprise, as the effect of no MPPT can be substantial. The absence of the MPPT required a significant decrease in the derating factor in order to account for the inefficiency of the system. The variance in the derating factor is not a reflection of poor modeling capability within HOMER; rather, it shows the importance of calibrating HOMER to the particulars of each system in a controlled experiment. Following this calibration, a user can set up the same circuit anywhere in the world, and HOMER will be accurately calibrated to that system.

14. 3. PowerFilm

For the HOMER modeling of the PowerFilm FM-15 3600, the same process was undertaken as with the Kyocera panels. One input difference was the rated power of the panel—60 watts compared to 54 watts for the Kyocera panels. This resulted in a 30-panel rating of 1.8 kW for the PV in the model. Another difference was the lack of performance details published by PowerFilm. This prevented the first step of the calibration process, the inclusion of temperature effects.

As shown in Table 17, the measured data for the single PowerFilm FM-15 3600 was 4.781 kWh for the one-month period. To incorporate the 30 panels being modeled, that value was multiplied by 30 and resulted in a rounded value of 143 kWh. Therefore, 143 kWh was the baseline the HOMER model was compared to.

Table 17.   PowerFilm FM-15 3600 Scaled Usable Energy From Measurements

	PV Usable Energy (kWh)
Measured Data (1 panel)	4.781
Measured Data (Scaled to 30 panels)	143

The precalibrated HOMER model resulted in an estimation of 251 kWh of usable energy, which was 76% higher than the measured data. The following section will show the calibration process used to align the HOMER model with the measured data.

a.   *Calibration*

As mentioned in the previous subsection, the temperature effects were not included in the calibration process for the PowerFilm FM-15 3600. Therefore, the calibration began with the inclusion of the actual solar irradiance. The irradiance levels measured at the location of the panel were compiled into hourly averages. Then, this data was uploaded to the model. This modified HOMER's estimated power production down to 238 kWh, 66% higher than the measured data, as shown in Table 18.

Again, the derating factor was evaluated via the sensitivity analysis capability in HOMER. A range from 40–70% was inserted for the derating factor. The results are displayed in Figure 42. The derating factor of 41.5% was chosen because it corresponded to the PV production of 143 kWh.
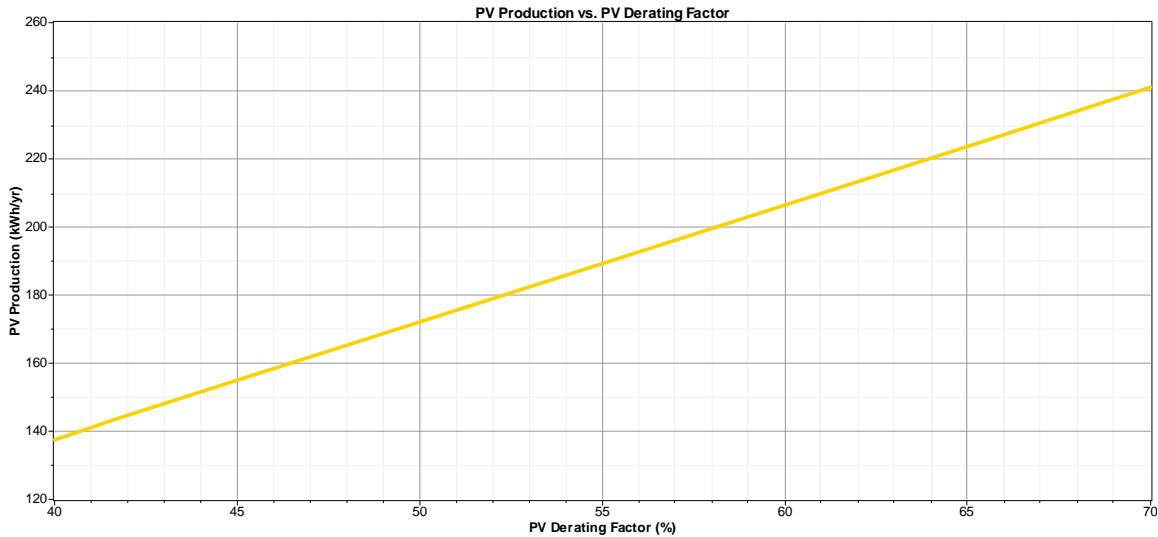
Figure 42.   Sensitivity Results: PV Production Versus PV Derating Factor

b.   *Results*

The calibration process results are shown in Table 18. Notice that the derating factor had to be lowered well beyond that of the Kyocera KC50T model, which was at 52%. Certainly, some of that was the effect of the MPPT absence, as was the case with the Kyocera experiment. Additionally, the lack of performance details provided by PowerFilm was a large part of the derating factor decrease. The only time HOMER incorporates the efficiency of the panel is when the temperature effects are monitored. In fact, that is the only time the user is asked to insert the efficiency. This is because the designers of HOMER simply trust the power rating factor of the respective PV manufacturer. Because the PowerFilm FM-15 3600 is made of thin film photovoltaic cells and has a substantially lower efficiency than the Kyocera panel, it may have performed differently at different solar irradiance levels and angles of the sun.

Table 18.   PowerFilm FM-15 3600 HOMER Calibration Results

	PV Usable Energy (kWh)	Accuracy
Measured Data (Scaled to 30 panels)	143	
HOMER Model	251	76%
Add Temp Effects	--	--
Add True Solar Irradiance	238	66%
Vary Derating Factor	143	--

15. 4. Air X

The Air X HOMER model had the same basic inputs discussed in the beginning of Section V.C., which were applied to the PV models as well. However, there were inputs particular to the modeling of wind turbines that have yet to be discussed in this thesis. Therefore, those inputs will be covered in this section, beginning with the initial uncalibrated model.

The initial model consisted of the same equipment types as the PV models, except for the obvious: the *PV* was unchecked, while *Wind Turbine 1* was selected. On the Turbine Inputs page, the *SW Air X* was chosen out of the stock wind turbines already loaded in HOMER. One turbine was input as the *Quantity*. Unlike the PV models, multiple systems were not included in the model in order to prevent confusion when discussing the complexities of modeling wind turbines. That complexity has to do with turbulence.

Turbulence, in the meteorology context, is defined as "irregular motion of the atmosphere, as that indicated by gusts and lulls in the wind" [23]. This "irregularity" in the wind substantially hinders the power production capability of wind turbines. Mick Sagrillo wrote an article published in the March issue of *Solar Today* magazine [24] that

gives an excellent description of the effects of turbulence on wind turbines. Sagrillo used the example of water flowing in a river to give a visual illustration:

> When we toss a twig into the water near the bank, it moves slowly downstream. It also spins as it moves, caught in eddies. Toss the twig into the strong smooth current in the middle of the river and the random spinning is considerably reduced. Near the bank, we see the effect of turbulence on a moving fluid, a swirling, apparently chaotic motion. Swirling results from the water tumbling as it passes around obstacles. In the river: rocks, tree stumps, branches, even the bank itself. The progress of the water downstream is compromised not only by friction with the bank, which reduces its velocity, but also by turbulent flow. The energy of turbulent water is diverted sideways, downward and even backward. It wouldn't be much use in turning a water wheel. [24]

Sagrillo continued by explaining, "the amount of kinetic energy in the wind that can be extracted to generate electricity is considerably reduced by turbulence [24]." The issue of turbulence is a hindrance to all wind turbines, but none more so than small-scale turbines. Today, large wind farms usually consist of wind turbines 80 meters in the air. This is because turbulence is greatly reduced the higher the clearance is above obstacles. This concept is called "ground drag" and results in an exponential increase in wind speeds the higher one climbs above the earth's surface. (Sagrillo explained the concept of ground drag in his article in the January/February 2010 edition of *Solar Today* [25].) Unfortunately, large-scale wind turbines are incompatible with expeditionary energy. The permanence of the structures, along with the extreme profile, does not fit with the term *expeditionary*. Small-scale wind turbines, however, should be considered for expeditionary energy, but only with an understanding of the performance limitations presented by turbulence.

This experiment exposed the reality of the effects of turbulence on wind turbines. Additionally, it illustrated the difficulty in simulating wind turbines. The dynamic performance of wind turbines is extremely complex due to the fluctuations of the wind. Unlike solar irradiance, which can only gradually change as a cloud moves between the sun and a solar panel, wind fluctuates in speed and direction constantly. Therefore, any attempt to model wind turbine performance, especially in turbulent locations close to obstacles, cannot help but be flawed. This was the case with HOMER's hourly

simulation strategy. The following section will highlight the limitations of HOMER's wind power model. The initial uncalibrated HOMER model resulted in a 60-kWh energy estimate, which was 40 times the actual measured data, as seen in Table 19.

Table 19.   Air X HOMER Uncalibrated Results

	Wind Usable Energy (kWh)	Accuracy
Measured Data (1 turbine)	1.5	
HOMER Model	60	3796%

a.   *Calibration*

(i) Step 1. The first step in calibration was to integrate the actual measured data into the HOMER model. This was done in similar fashion to the integration of the solar irradiance data for the PV models. MATLAB was used to retrieve the wind speeds in 10-second samples and to convert them into hourly averages. Then, a file of 8,760 hourly wind speeds was created to match the hours in the year. The averages calculated from the measured data were inserted to represent the period of the experiment, while all other hourly inputs were given the number *zero*. This file was then uploaded as the wind resource. The new simulation resulted in a reduction of energy to 9 kW, as seen in Table 20.

Table 20.   Air X HOMER Results of First Step of Calibration, Loading Hourly Wind Averages from Anemometer Data

|	Wind Usable Energy (kWh)	Accuracy
Measured Data (1 turbine)	1.5	
HOMER Model	60	3796%
Add Anemometer Data	9	484%

While the improvement was substantial, it was not acceptable because the estimate remained six times higher than the actual measured data. This level of resolution would be worthless to Marines for pre-deployment purposes. The next step of calibration made use of the sensitivity analysis within HOMER and facilitated the calibration of HOMER to the experiment. However, it remains unclear whether this step would be helpful in a pre-deployment context.

(ii) Step 2. The final calibration step involved the variance of two variables in order to force the model to achieve an accurate energy level of 1.5 kWh. The only realistic way to do this was to simulate turbulence into the model, but that was not an option afforded by the HOMER software. HOMER's hourly simulation treats the hourly average wind speed inputs as if they were consistent throughout that hour. It uses the turbine manufacturer's power versus wind speed chart (see Figure 34) to calculate the power during that hour as if the wind were not fluctuating. As mentioned before, wind speeds and the resulting power production are infinitely more complex than that. HOMER does not account for turbulence.

HOMER does incorporate the ground drag concept, but that is only when the anemometer height is different than the actual turbine hub height; in this case, it was not different. The location of NPS is known to be a highly turbulent area, and although the wind turbine is on the top of a six-story building, the building creates turbulence. Turbulence is the critical factor in the disparity of measured and modeled energy levels, as seen by a comparison of the graphs in Figures 43 and 44. The top graph displays every mean wind power reading taken during the experiment and compares them to the 250,000-plus samples. The bottom graph is a HOMER product that displays the power profile of the HOMER model. The consistency of the highs and lows on each graph reveal that their time frames are consistent. The first impression when comparing the two graphs is that the outline of the power production looks the same in both. This is a false impression. Under closer scrutiny, the disparity between the two is obvious. Focus on the large spike in the 5,000-sample range of the top graph. There are data points that fill in the entire spike, which means that during that time frame, there were power outputs ranging from 0 to over 140 kWhs. The same spike on the HOMER graph,

which covers April 28 and 29, is not filled in with highly variable power outputs; instead, HOMER estimated the power output to be relatively high throughout those two days. This is proof of HOMER's inability to incorporate turbulence.
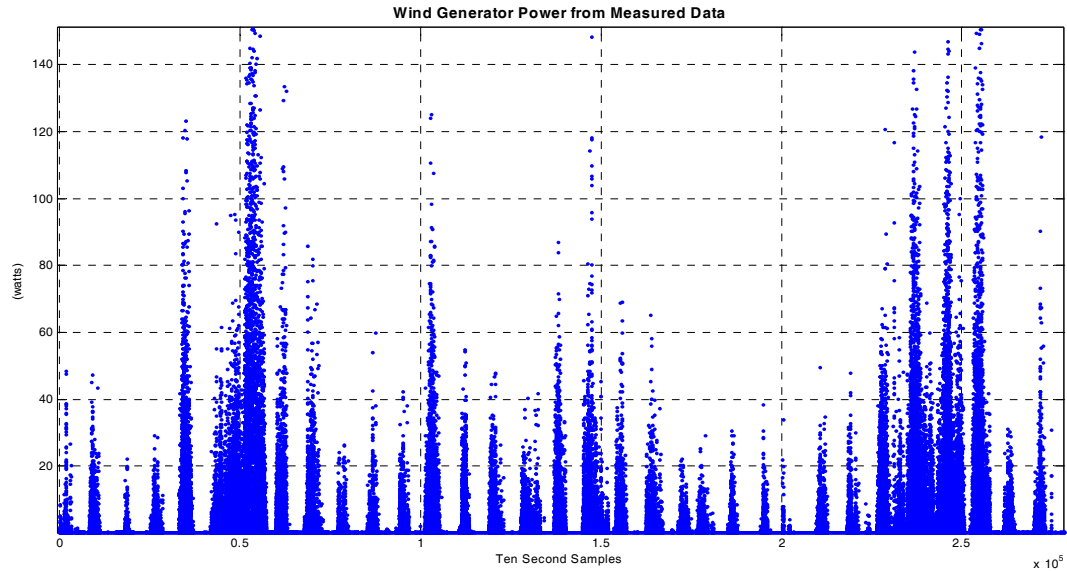
Figure 43.   MATLAB Graph of the Actual Measured Data from the Air X During the Experiment Period
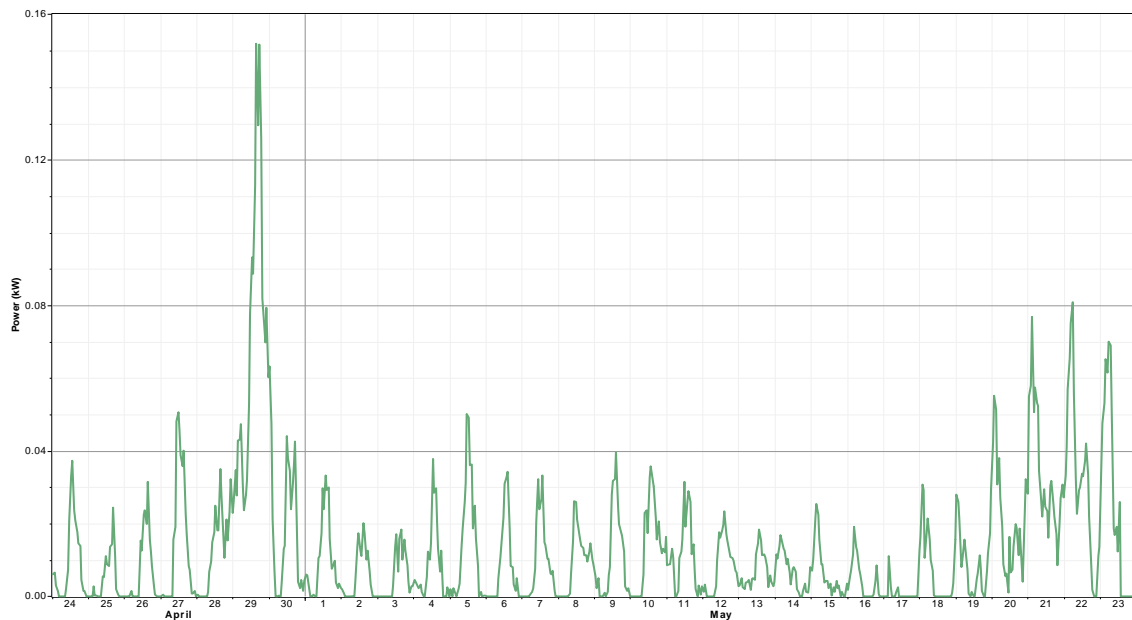
Figure 44.   HOMER Graphic Displaying the Estimated Power Profile of the Air X During the Experiment Period

Despite all of these inconsistencies, HOMER was still calibrated to match the measured data. This was done by varying the hub height and the surface roughness length. On the Wind Turbine Inputs page, the hub height input was given a range from 10 to 40 meters. This, of course, was inaccurate because the hub height was known, but varying the height in relation to the anemometer in the model was the only way to force HOMER to incorporate the surface roughness length variable. The *Surface roughness length* input can be found by clicking the *Vary With Height* button on the Wind Resource Inputs page. The HOMER help menu defines surface roughness length as "a parameter that characterizes the roughness of the surrounding terrain." The surface roughness length affects the logarithmic profile as explained in the following excerpt from the help menu:

> Ground-level obstacles such as vegetation, buildings, and topographic features tend to slow the wind near the surface. Since the effect of these obstacles decreases with height above ground, wind speeds tend to increase with height above ground. This variation of wind speed with height is called *wind shear*. Wind energy engineers typically model wind shear using one of two mathematical models, the logarithmic profile or the power law profile. [26]

The logarithmic profile assumes the wind speed is proportional to the elevated height above the earth's surface. The logarithmic profile does incorporate some components of turbulence, such as speed fluctuations, but it does not seem to account for direction changes. Equation 1.7 is used by HOMER to account for the change in wind velocity (v) from the anemometer height (z_{anem}) to the turbine hub height (z_{hub}) and to incorporate the surface roughness length (z_0).

$$\frac{v(z_{hub})}{v(z_{anem})} = \frac{\ln(z_{hub} / z_0)}{\ln(z_{anem} / z_0)} \tag{0.6}$$

Figure 45. HOMER Surface Roughness Length Scale

        The scale of the surface roughness length values is shown in Figure 45. The sensitivity analysis for the calibration process in this experiment incorporated a surface roughness length range of 0.1 to 1.5 meters. This varied the surface type from *Few trees* to *Suburbs*. The surface-roughness length variable and the hub height variable combined to provide the sensitivity analysis surface plot displayed in Figure 46. The colors vary according to the energy output capability of the wind turbine, as seen in the legend. Recall that the measured energy production was 1.5 kWh. This matches the dark-blue zone found in the bottom right corner of the graph. From this dark-blue region, a hub height of 10 meters and a surface roughness length of 1.5 meters were selected. With these inputs, the HOMER model matched the measured energy level of 1.5 kWh.
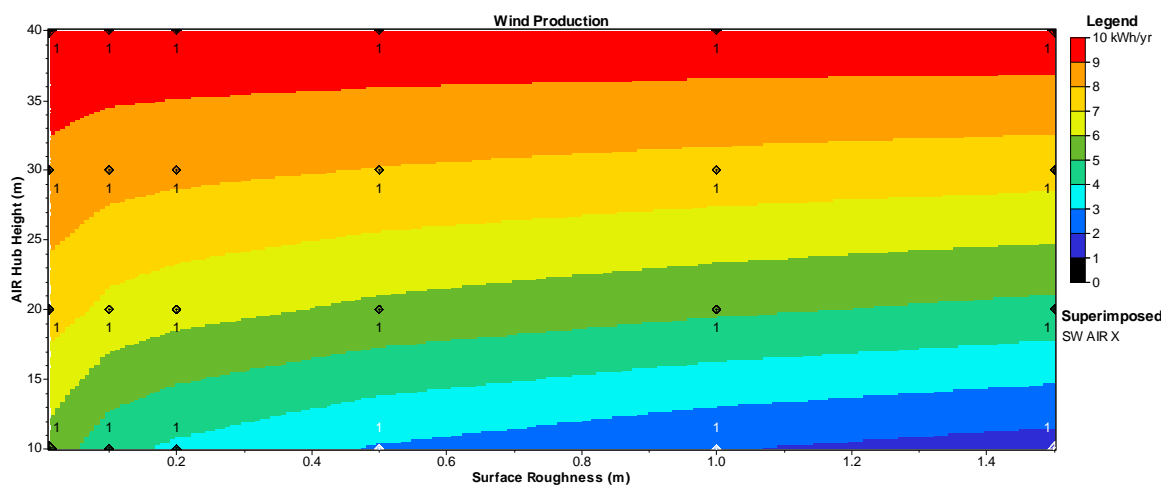
Figure 46. Air X HOMER Sensitivity Analysis, Varying Hub Height and Surface Roughness

b. *Results*

The results of the calibration process are displayed in Table 21. The accuracy column represents the comparison of the HOMER model's energy estimate to the measured energy. For example, 484% means the estimate was 484% higher than the actual data. As previously discussed, it is unclear if the success of this calibration would carry over for pre-deployment purposes. Further experiments should be conducted that test the specifics of the calibrated model against the employment of the same system in another region of the world.

Table 21.   Air X HOMER Calibration Results

	Wind Usable Energy (kWh)	Accuracy
Measured Data (1 turbine)	1.5	
HOMER Model	60	3796%
Add Anemometer Data	9	484%
Vary Hub Height and Surface Roughness	1.5	--

D.   EXPEDITIONARY ENERGY DENSITY

The term *energy density* has different meanings depending on the context in which it is used. In the context of stored energy, it means the energy per volume (kWh/m^3) that can be stored within a battery or fuel cell, for example. In the context of solar irradiance, it means the solar energy reaching the earth within a square meter (kWh/m^2). A new meaning for energy density should be applied within the realm of expeditionary energy that focuses on the energy production capability of a system versus the area the system consumes within a secured FOB.

16. 1. Concept

Expeditionary energy density provides a metric to evaluate how a system will perform in the context of how much valuable space it consumes within a FOB. HOMER is used to estimate the energy production capability of a system in a specific location over a defined time frame. Then, that energy estimate is divided by the area of the system in squared meters and by the number of days. The result is an energy density in a kilowatt-hour per meter squared per day (kWh/m²/d) value.

17. 2. Comparison of Systems

The expeditionary energy density concept was established as part of the wind-PV experiment detailed in this chapter. Calculations were performed to value each of the three alternative power systems in terms of expeditionary energy density. In Equation 1.8, the total energy (E_{Tot}) divided by the consumed area of the system (A) is the expeditionary energy density per day (D_{EE}). The expeditionary energy density is then divided by the number of days taken to acquire E_{Tot} to find the kWh/m²/d value.

$$D_{EE} = E_{Tot} / A \hspace{4cm} (0.7)$$

The consumed area of each system requires an explanation. It is fairly straightforward in regard to PV systems. The length and width of each system represents the area the system consumes. This area calculation can become more complex when incorporating the angle of the PV panels or the measures taken to ensure minimal shading. In the context of this experiment, only the length and width of the system was considered.

The consumed area of a wind turbine is more complex, however. Due to the effects of turbulence, obstacles, including other wind turbines, must be managed. Multiple wind turbines should be positioned in a line perpendicular to the direction of the prevailing wind. This concept is eloquently explained in "Wind Power Project Site Identification and Land Requirements," which is one of the publications in the *New York State Energy Research and Development Authority (NYSERDA) Wind Energy Tool Kit*

[27]. This document defines the ideal spacing between wind turbines to be 3 by 10 rotor diameters. This is illustrated in Figure 47.
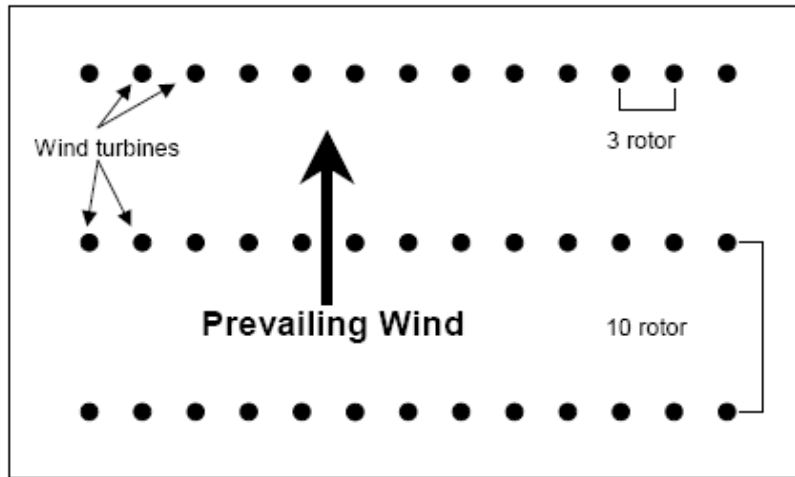
Figure 47.   Illustration of Turbine Spacing, From [27]

This turbine spacing concept was used in the context of this experiment to account for the consumed area of a wind turbine and is illustrated in Figure 48. Since each turbine would have 3 rotor diameters in each perpendicular direction to the wind and 10 rotor diameters in each parallel direction to the wind, the consumed area around each turbine would be 6 by 20 rotor diameters. However, only half of this spacing in each direction should be claimed by that single turbine. The other half of the spacing must be attributed to the adjoining turbine. This logic leads to the assumption that a 3 by 10 rotor diameter should be considered the consumed area of a single turbine. In the case of the Air X, which has a rotor diameter of 1.15 meters, the length (10 rotor diameters) becomes 11.5 meters and the width (3 rotor diameters) becomes 3.45 meters. These calculations were used in the expeditionary energy density calculations for the Air X.
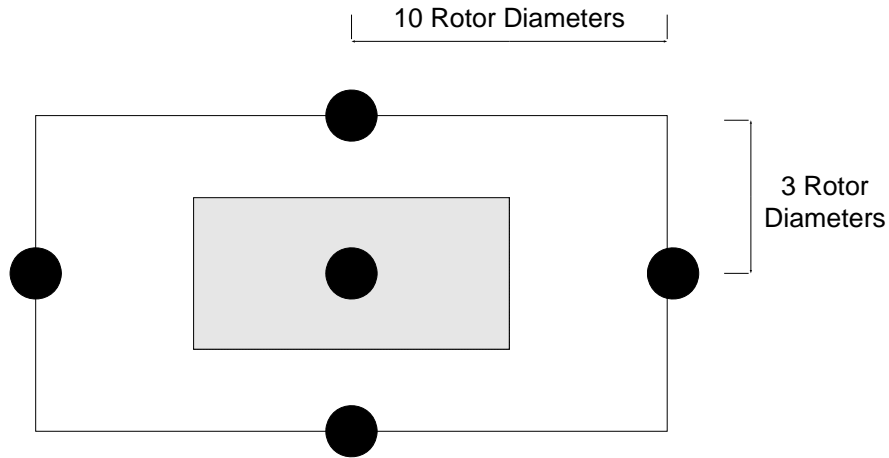
Figure 48. Air X Consumed Area by Applying the Turbine Spacing Concept Shown in Figure 47

The expeditionary energy density results for each wind-PV experiment system are shown in Table 22. The results reflect the energy production capability in the context of the location and setup in which each system was employed. The results can drastically change with a change of location, which would affect the solar and wind resources, or with an altered circuit, which would affect the efficiency of the system.

Table 22. Expeditionary Energy Density Calculations From Wind-PV Experiment

	Energy Total (kWh)	System Length and Width (m x m)	Consumed Area (m²)	Exp. Energy Density (kWh/m²)	No. of days in period	Exp. Energy Density per day (kWh/m²/d)
Kyocera KC50T	5.367	0.639 x 0.652	0.417	12.881	30	0.429
PowerFilm FM-15 3600	4.781	1.499 x 1.092	1.637	2.921	30	0.097
Air X	1.538	11.5 x 3.45	39.675	0.039	30	0.001

E. CONCLUSION

The wind-PV experiment shows the merits and limitations of using HOMER to estimate energy production for wind turbines and PV systems. While each HOMER

model was effectively calibrated to the experiments, it is unclear whether that calibration would be effective in future employments of the Air X. Therefore, further research to include the calibration and subsequent setup in a new locale should be explored.

Another concept that should be researched further is the concept that was defined and explored in this chapter of expeditionary energy density. It can be used as a metric for the selection of power systems and can help to prioritize systems being considered during pre-deployment.

THIS PAGE INTENTIONALLY LEFT BLANK

VI.   EXPERIMENTAL FORWARD OPERATING BASE

A.   BACKGROUND

The Experimental Forward Operating Base (ExFOB) concept was first established in September 2009. It was designed as Step 3 of the Commandant of the Marine Corps' new emphasis on expeditionary energy. Step 1 was the formation of the Afghanistan Marine Energy Assessment Team and their mission to Helmand Province. Step 2 was the creation of the Expeditionary Energy Office (E2O). Step 3 was the tasking of E2O to conduct the ExFOB concept to evaluate COTS solutions that could meet the Marine Corps' expeditionary energy needs.

The mission of the ExFOB was to establish a mock forward operating base (FOB) that simulated the fuel and water demands of an FOB in Afghanistan in order to evaluate expeditionary energy solutions. In December 2009, a Request for Information (RFI) was distributed to industry, soliciting companies that had capabilities that would meet the intent of the ExFOB. The following excerpt from that RFI best describes the intent of the ExFOB:

> The Office of Naval Research in support of USMC technology requirements is interested in understanding the currently available technologies that could enhance the logistics sustainability of remote Forward Operating Bases (FOBS) engaged in combat operations. Specific areas of interest for this RFI include 1) water purification and distribution, 2) electric power generation and distribution, and 3) energy efficient structures. Technologies of interest are those that would most effectively enhance self sufficiency of a Forward Operating Base roughly the size of a Marine Corps Company (approximately 200 Marines). [28]

Obviously, this thesis is aligned with the second area of interest listed in the RFI, "electric power generation and distribution."

18. 1.   ExFOB Process

The ExFOB process began with the receipt of proposals from manufacturers with technologies relevant to the ExFOB's intent. Then, technologies of interest were selected

to be evaluated during the initial ExFOB evaluation period in March 2010. This initial ExFOB evaluation was held in Quantico, Virginia, aboard Marine Corps Base Quantico. Details concerning how the technologies were evaluated were unclear to the author and, therefore, are not covered in this thesis. Following the evaluation, four power generation technologies were selected by the Marine Corps, all of which are PV technologies and will be discussed in the next section.

The next step in the ExFOB process was a Field User Evaluation (FUE) of the systems during the African Lion exercise in Morocco in May 2010. The technologies were integrated into the setup of the Marine Corps unit that was involved in the exercise. Once again, the technologies were evaluated for performance. The details of that evaluation are unclear to the author as well.

The final step of the ExFOB process, as it pertains to these technologies, is the scheduled shipment and employment of these technologies to Afghanistan to be integrated into actual combat FOBs within MEB–A. This is scheduled to take place in October 2010 [29].

The overall timeline and locations of the ExFOB process are relevant to the HOMER discussion within this chapter. Solar radiation maps for each location are in Appendix C. The technologies selected have been modeled within HOMER. Additionally, HOMER models matching the three locations—Quantico, Virginia; Morocco; and Afghanistan—and the respective month tied to those locations were used. However, a discussion of the technologies selected via the ExFOB process is first necessary.

19. 2. Selected Systems

Four power production technologies were selected following the initial ExFOB evaluation in Quantico, Virginia. Each technology is a PV system, but they share little else in common. The PV technology used to manufacture each system and the marketed purpose of each system vary greatly. Additionally, some items are considered stand-alone end items, while others are simply considered as a component of a larger system. Each technology is discussed below.

a.   Solar Field Shelter

The PowerFilm Solar Field Shelter is a flexible shelter that can be set up above the tent structures currently used in combat operations. The shelter has flexible thin film PV cells attached to the exterior. The Solar Field Shelters come in two sizes, which are distinguished by the power rating of each, 1 kW and 2 kW. The 1 kW size was selected for ExFOB. The shelter is shown in Figure 49.

As with the FM-15 3600 discussed in Chapter V, PowerFilm publishes very little technical or performance specifications. This leads to much more variability within the HOMER model. Despite the lack of published specifics, there are several factors that should be kept in mind when evaluating the system. One is the fact that thin film PV has a much lower efficiency than multicrystal PV.   Another is the thermal advantage afforded by using shelters. The shelter reduces the temperature of the shielded tent by blocking the solar irradiance from reaching the tent. This, in turn, reduces the demand for air conditioning and results in a reduction in the power and fuel demand. Also, the shelter takes up very little additional space within a FOB. The use of shelters does increase the footprint of a tent, but only slightly. Therefore, the shelter affords the opportunity to produce power, albeit at a lower efficiency, with minimal space being wasted.

Figure 49.   Photo of PowerFilm 2kW Solar Field Shelter, From [17]

b.   GREEN

The Ground Renewable Expeditionary Energy Network (GREEN) is a program within the Marine Corps Systems Command (MARCOR SYSCOM). The

program is centered on the collection, management, and distribution of electric power. It is not tied to certain technologies; rather, it is designed to accommodate different types of renewable energy production equipment. For the purposes of the ExFOB, GREEN consisted of eight Sanyo HIT Power 205 solar panels, shown in Figure 50 [30].

Figure 50. GREEN Solar Panels, From [30]

Other components of GREEN are an OutBack Extreme Rugged Water Resistant Inverter/Charger and four lead acid batteries. The solar panels are the critical component for this thesis. The critical technical specifications for the purposes of creating a HOMER model are shown in Figure 51. They were taken from the GREEN Performance Specification packet [30]. The GREEN system allows the user to position the solar panels at one of three angles: 0°, 30°, or 60° [31]. Additionally, the I-V curve is shown in Figure 52.

Temperature coeff. of power (%/°C)	-0.29
Nominal operating cell temp. (°C)	46.9
Efficiency at std. test conditions (%)	17.7

Figure 51. Sanyo HIT Power 205 Technical Specifications for Including Temperature Effects
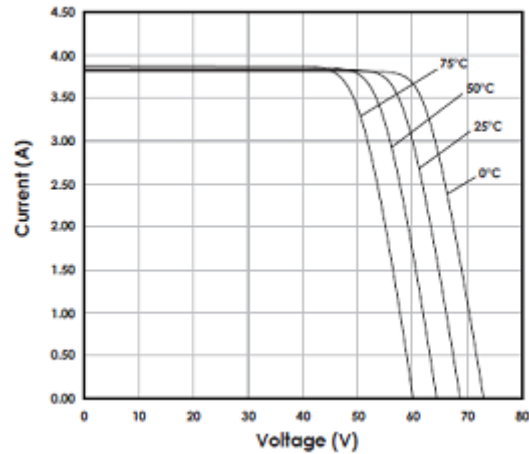
Figure 52.   **Sanyo HIT Power 205 Dependence on Temperature I-V Curve, From [30]**

c.   *ZeroBase*

The ZeroBase Energy Regenerator consists of five solar panels rated at 300 watts apiece. Other than being identified as Unicor Federal Prison panels, no other information about the panels was available [32]. Based on the photograph in Figure 53, it was inferred that the panels could be positioned at a 45° angle, so that was the angle used in the HOMER model.

Figure 53.   **Photo of ZeroBase Energy Regenerator During Evaluation in Morocco, May 2010, From [32]**

d. NEST

The NEST Energy Systems Solar Light Trailer, shown in Figure 54, is a remote lighting capability that does not require external power. It consists of four solar panels, rated at 175 watts apiece, a solar controller, and eight lead acid batteries. For the purposes of this thesis, only the power production capability of the solar panels is important. The NEST PV power production capability was considered to be displacing generator power, even though that is not completely true in real life. The temperature effects were not included in the HOMER models of NEST because insufficient information was provided in the technical specifications [33]. The panels can be set at one of two angles, identified as summer and winter. However, the vice president of NEST Energy Systems recommended leaving them at the winter angle, 55°, year round [34]. Therefore, the 55° angle was used for HOMER modeling.

Figure 54.   Photo of NEST Solar Light Trailer, From [32]

B.   HOMER UTILIZATION

This section discusses the HOMER modeling of the power generation equipment selected during the ExFOB. The four systems are unique, and the technical performance of each differs greatly, which forces the HOMER user to choose between two modeling

strategies. HOMER only allows one PV input when selecting equipment to be modeled. Therefore, one strategy was to treat all four technologies as one large PV array, add up the total power ratings, and input them as the rating of the entire system. The second strategy was to create a model of each technology, accumulate the energy produced from each, and present that total energy demand as being displaced by the PV systems. Both of these modeling strategies were used for this thesis. Each will be discussed, and the results will be compared at the end of this section.

The quantity of each system used for all models was taken from the recommended distribution scheduled for the Afghanistan installment. A company-level FOB was scheduled to receive the following quantities of each system: 2 Solar Field Shelters, 3 GREEN systems, 3 ZeroBase systems, and 10 NEST Solar Light Trailers [32]. Therefore, each HOMER model was input with the appropriate power rating to match the quantities, as seen in Table 23.

Table 23.   Total Power Ratings for All Power Systems Being Deployed to a Company-Sized FOB in Afghanistan

COMPANY EQUIPMENT					
	Rated Pwr / Panel (kW)	No. of Panels	Rated Pwr / System (kW)	No. of Systems	Rated Pwr / FOB (kW)
Solar Field Shelter	1	1	1	2	**2**
GREEN	0.205	8	1.6	3	**4.8**
ZeroBase	0.24	5	1.2	3	**3.6**
NEST	0.175	4	0.7	10	**7**
				Total	**17.4**

20. 1. Inputs

The only inputs that applied to all HOMER models discussed in this chapter were the loads and the locations. However, the inputs do vary somewhat. The approach taken throughout the ExFOB modeling was to create a micropower system model and to simulate it in the three different locations detailed in the ExFOB process: Quantico, Virginia; Morocco; and Afghanistan. For each location, the load was altered to match the month in which the systems were employed in each location. Therefore, the Quantico models were uploaded with a load for March only. Meanwhile, the Morocco and Afghanistan models had a load for only one month as well: May and October, respectively. The hourly load discussed in Chapter III (Figure 13) was the same load used for all ExFOB models. Only the first 30 days of each month were given a load, for the sake of continuity. In Table 24, the inputs relating to each location are displayed.

Table 24.   HOMER Inputs for Each ExFOB Location (GMT stands for Greenwich Mean Time)

	Quantico	**Morocco**	**Afghanistan**
Load Month	March	May	October
Energy Load (kWh)	8650	8650	8650
Latitude	38° 31' N	28° 57' N	30° 53' N
Longitude	77° 19' W	10° 37' W	64° 05' E
Time Zone	GMT -05:00	GMT	GMT +04:30

The inputs that relate to all models will be discussed in this section, while the inputs unique to a particular model will be discussed the respective sections. First, the equipment selected was *Primary Load 1*, *PV*, *Converter*, *Generator 1*, and *Generator 2*. Also, *Do not model grid* was selected. The generator chosen for the modeling portion of this experiment was the MEP-803. The MEP-803 is the 10-kW generator in the Marine Corps' inventory. Two MEP-803 generators were input to ensure the maximum load of 15 kW would be met, even when the PV systems were not producing power. JP-8 was

chosen as the fuel. A 20-kW converter was input with a default efficiency of 90%. The solar resource was input with the *Get Data Via Internet* button for each location.

21. 2. Modeled Together

To create a model that incorporates different systems as one, assumptions must be made. As mentioned earlier, the four types of solar power equipment vary greatly in performance. Additionally, systems like the Solar Field Shelters have very few published specifications. In order to model all systems as one, the choice was made to use the lowest production value for every input in order to ensure that the systems were underestimated rather than overestimated. For example, the Solar Field Shelter is at an angle of 0° when employed, while the other three PV systems can be set at varying angles, yielding more productivity. The angle of 0° was used for the PV input to prevent overestimation. The size of the PV was listed as 17.4 kW, as shown in Table 23. The azimuth was input as 0°, due to the zero angle.

This micropower system, representing the collective sum of all four systems, was simulated for each of the three locations. The results in Table 25 represent the usable energy, meaning the energy after the inverter losses. Also shown in the table is the percentage of the 8,650-kWh energy load being met by the PV systems. The energy levels listed are not consistent and should not be compared to one another because they are each from different months. In other words, the energy levels show that a greater number of kilowatt-hours will be produced in Morocco during the month of May than in Afghanistan in the month of October.

Table 25.   Estimated Usable Energy Totals from Each of the Collective PV Models

	Quantico (kWh)	Morocco (kWh)	Afghanistan (kWh)
PV Combined	**1645**	**2074**	**1984**
Percent of Load	19%	24%	23%

The benefit of these models is that the Marines who are evaluating the systems can take the data shown in Table 25 and plan for it. By using HOMER, they can know

the low bound of what the systems can produce. It is important to point out that this is the low bound due to the input angle of 0°. Once the low bound is know, it is beneficial to fine-tune the estimates. This was done by modeling each system individually.

22. 3. Modeled Individually

The technical specifications available for each power generation system selected in ExFOB were used to calibrate the model and to create the most accurate estimates possible.

a.   Solar Field Shelter

As previously mentioned, little data is published on the performance of PowerFilm products. Therefore, default inputs had to be maintained for the HOMER models of the system. The PV size was input as 2 kW to account for the two shelters. The results for each location are shown in Table 26.

Table 26.   PowerShade Energy Estimates for Each ExFOB Location

	Quantico (kWh)	Morocco (kWh)	Afghanistan (kWh)
PowerShade	191	223	240

b.   GREEN

Unlike the other PV systems selected in ExFOB process, the Sanyo HIT Power 205 panels in the GREEN system do have adequate data published on them to fine-tune the HOMER model for their use. First, 4.8 kW was input as the PV size. Next, the slope was input as 30°. This angle was used for all three locations because it was the closest setting (0°, 30°, and 60°) to the latitude degrees of each location. The converter efficiency was changed from the default value of 90% to 92%, as is listed in the OutBack Power specification sheet [35]. Additionally, the temperature effects were included in the GREEN models by inserting the information shown in Figure 51. The average temperature was taken from the NASA website (http://eosweb.larc.nas.gov/sse/) [15].

These average monthly temperatures were input into the model. The resulting energy estimates are displayed in Table 27.

Table 27.   GREEN Energy Estimates for Each ExFOB Location

	Quantico (kWh)	Morocco (kWh)	Afghanistan (kWh)
GREENS	583	606	675

c.   ZeroBase

Only two inputs were unique for the ZeroBase models. The PV size was input as 3.6 kW, and the slope was input as 45°. Temperature effects were not included due to insufficient data. The results are shown in Table 28.

Table 28.   ZeroBase Energy Estimates for Each ExFOB Location

	Quantico (kWh)	Morocco (kWh)	Afghanistan (kWh)
ZeroBase	430	449	501

d.   NEST

The NEST models were limited in specifics as well. The PV size was input as 7 kW, and the slope was input as 55°. The results are shown in Table 29.

Table 29.   NEST Energy Estimates for Each ExFOB Location

	Quantico (kWh)	Morocco (kWh)	Afghanistan (kWh)
NEST	822	839	940

23. 4.   Comparison

The results of the individual modeling strategy were summed in order to make a comparison to the collective modeling strategy. This comparison is displayed in Table 30. With this knowledge, the Utility Marines responsible for meeting the power demands of their unit can more effectively conduct preplanning.

Table 30.   Comparison of the Two Modeling Strategies

	Quantico (kWh)	Morocco (kWh)	Afghanistan (kWh)
PV Combined	**1645**	**2074**	**1984**
Percent of Load	19%	24%	23%
Individual			
PowerShade	191	223	240
GREENS	583	606	675
ZeroBase	430	449	501
NEST	822	839	940
Cumulative	**2026**	**2117**	**2356**
Percent of Load	23%	24%	27%

C.   POTENTIAL IMPACT OF HOMER

What then does the information presented in this chapter say about the potential benefits of using HOMER in the ExFOB process? The use of HOMER within the ExFOB process would have improved the evaluation process in two ways. One benefit would have been HOMER's use as a tool to evaluate the performance of the PV generation systems at each location. The second benefit of HOMER would have been an improved selection process for the systems that met the Marine Corps' expeditionary energy needs.

To use HOMER to evaluate the performance of the PV generation systems, the first step should have been to treat the ExFOB evaluation in Quantico, Virginia, as a controlled experiment. Conceptually, it should have been similar to the controlled experiments detailed in Chapters IV and V. That is, the power performance of each system should have been closely catalogued. Additionally, the solar irradiance levels should have been monitored. Then, after the evaluation period, this data should have been used to calibrate a HOMER model to each system using the same process detailed in this thesis. Following this calibration, HOMER could have been used to estimate the

energy production capability of each system in the Morocco and Afghanistan setups with greater accuracy than the estimates shown previously in this chapter.

The second benefit of using HOMER within the ExFOB framework centers around fine-tuning the selection process to make more informed decisions on which systems meet the Marine Corps' needs the best. It is no secret that the evaluation of an alternative power system in Quantico, Virginia, for future use in Afghanistan is not an ideal scenario. The two locations have very little in common. One is a heavily wooded area, with high humidity and solar irradiance levels, with solar irradiance levels considered marginal at best. The other is a treeless desert with extremely high solar irradiance levels. Therefore, how does one effectively evaluate a system in Quantico for future use in Afghanistan? The answer is by making use of HOMER. As shown in this chapter, HOMER can be used to produce energy estimates for each system in Afghanistan. However, HOMER's usefulness should extend to the utilization of the expeditionary energy density metric detailed in Chapter V.

Space is an extremely hot commodity in expeditionary locations. Each FOB is considered a secured compound that is not easily expanded. Therefore, how that space is used is very important. One way to best evaluate which alternative power system best suites the expeditionary needs of the Marine Corps is to calculate the expeditionary energy density of each system. As an example, the systems discussed in this chapter will be evaluated for their expeditionary energy density in Afghanistan.

The area required for each system is shown in Table 31. The ZeroBase system was disregarded due to the lack of details about the system. The area consumed by each type of system is the main objective of the table. For simplicity, each system was treated as if it were at an angle of 0°. For greater accuracy, the actual angle could be incorporated to calculate a used area by each system. Additionally, any other components of the systems were disregarded for this example, but should be incorporated when calculating expeditionary energy density to truly evaluate systems.

Table 31.   Area Consumed by Each ExFOB System at a Company-Sized FOB

	Area / Panel (m²)	No. of Panels	Area / System (m²)	No. of Systems	Area / FOB (m²)
Solar Field Shelter	127.09	1	127.09	2	254.18
GREEN	1.16	8	9.28	3	27.84
NEST	1.30	4	5.22	10	52.16

The energy density can be calculated by dividing the Afghanistan energy estimates, shown in Table 30, by the consumed area. The results are shown in Table 32. Evaluation of the data shows that the GREEN system provides the greatest energy capability compared to the area of the FOB it will consume. Of course, this data provides a simplistic view that should not be evaluated in isolation. Mitigating factors, such as the Solar Field Shelter being employed over the top of an existing structure, can be incorporated into the expeditionary energy density calculations as well.

Table 32.   Energy Density of the ExFOB Systems Based on HOMER Estimates for Afghanistan in October

	Area / FOB (m²)	Energy Estimate (kWh)	Monthly Exp. Energy Density (kWh/m²/d)	Daily Exp. Energy Density (kWh/m²/d)
Solar Field Shelter	254.18	240	0.94	0.03
GREEN	27.84	675	24.25	0.81
NEST	52.16	940	18.02	0.60

D. SUMMARY

The integration of HOMER into the ExFOB process could take many different forms. HOMER could be used to model the collective energy production capability of many different systems, which would give a low bound estimate. Each system could be modeled separately to achieve a more precise estimate. The use of HOMER in the initial ExFOB evaluation to calibrate the model would result in even greater resolution on future estimates. Finally, the use of HOMER to calculate the expeditionary energy density of power generation systems would give the Marine Corps the ability to truly evaluate the merit of each system.

THIS PAGE INTENTIONALLY LEFT BLANK

VII. CONCLUSION

A. FINDINGS

HOMER is an exceptional tool. It was developed by experts who truly understand how alternative power systems work and the complexities of micropower systems. It shows great potential for future use as a pre-deployment tool within the Marine Corps.

The alternative power systems in the Marine Corps should be set up in controlled experiments to facilitate the calibration of HOMER to each system. This would enable effective power analysis for the Marine Corps' future needs. While HOMER's calibrated PV modeling process seems reliable, uncertainty remains for HOMER's wind power modeling process. This can be attributed to the hourly simulation scheme that lends itself well to the complexity of optimizing micropower systems, but not to the dynamic performance of wind turbines. Further research should be conducted to more thoroughly evaluate HOMER's modeling of wind power.

The E2O should look for opportunities to integrate HOMER into the ExFOB process. This could greatly enhance the evaluation process of alternative power systems. Additionally, HOMER could facilitate a Marine's understanding of each system's energy production potential unique to any location being considered. HOMER should also be used as a component of the expeditionary energy density concept as a metric for the evaluation and prioritization of alternative power systems.

B. FOLLOW-ON RESEARCH

Additional research should be considered in two areas. One research area should be centered on the modeling of wind turbine energy production. The hourly modeling scheme employed by HOMER is inadequate for properly estimating energy production for small wind turbines due to the effects of turbulence. However, wind turbine models based one one-second modeling schemes are too complex and cumbersome for

HOMER's optimization purposes. Further research should identify the advantages and disadvantages of the different time segment models to meet the Marine Corps' expeditionary energy modeling purposes.

Further research should also be conducted on the full use of HOMER as a pre-deployment tool. This should involve the measuring of the energy production of a particular Marine Corps alternative energy system in a controlled experiment, such as the experiments described in Chapters IV and V. Then the HOMER model calibration of this system should be conducted to match the measured energy production. The final step would be to employ this same system in another location. The energy production from this location would then be used to validate the effectiveness of the calibration method in modeling like systems in different locations.

APPENDIX A

The two sets of MATLAB code in this appendix are the only sources of code included in the body of this thesis. The author determined that no real benefit would result from including more code because all additional use of MATLAB coincided with one of these two provided codes, although values were different.

```matlab
%Pull Aquarium Solar Irradiance data set to plot
clear
B = xlsread('Aquarium Solar Rad.xlsx', 1, 'I213:I22320');
l=length(B);
t=(0:2:2*(l-1))';

plot(t,B);
xlabel('One Month Period - April 2 - May 1, 2010 (2 min intervals)')
ylabel('Solar Irradiance (W/m^2)')
title('Actual Solar Irradiance')

%Build it to 8760
Aq_hr= [];
for i=0:(l/30 -1)
    Aq_hr(i+1) = mean(B(i*30+1:i*30+30));
end

Aq_hr = [zeros(1,2184),Aq_hr(1:720),zeros(1,(8760-2184-720))];  %Insert zeroes
for all hourly data not between April 2 and May 1.
Aq_hr = Aq_hr';
Aq_hr = Aq_hr./1000;   %Convert from W/m^2 to kW/m^2
```

Figure 55.   MATLAB Code for Creating the Solar Irradiance Data to Load to the Grid-Tied-PV HOMER Model

```matlab
%Pull Aquarium Solar Irradiance data set to plot
clear
B = xlsread('Aquarium Solar Rad.xlsx', 1, 'I213:I22320');
l=length(B);
t=(0:2:2*(l-1))';

%integrate in theory - this just gives W/m_squared for entire month
irr = B.*1/30;  %multiply each by 2min then divide by 60 to convert min to hr
tot_irr_B = sum(irr);    %add for the whole month

%%Integrate the solar irradiance from HOMER's estimate
D = xlsread('Hermann_Hall_Irradiance.xlsx', 1, 'B3:B722');
E = D.*1000
tot_irr_E = sum(E);    %B is already in W/m^2 form - add for the whole month

%Compare the two
Comp_irrad_HmrtoAq  =(tot_irr_E  -  tot_irr_B)/tot_irr_B;    %The percentage
HOMER's Irr. is off from actual
```

Figure 56.   MATLAB Code for Comparing HOMER's Estimated Solar Irradiance and the Actual Pyranometer-Measured Data

APPENDIX B.

This appendix shows the LabView display and block diagrams designed to collect the PV data for the wind-PV experiment that was set up on the roof of Spanagel Hall at Naval Postgraduate School.
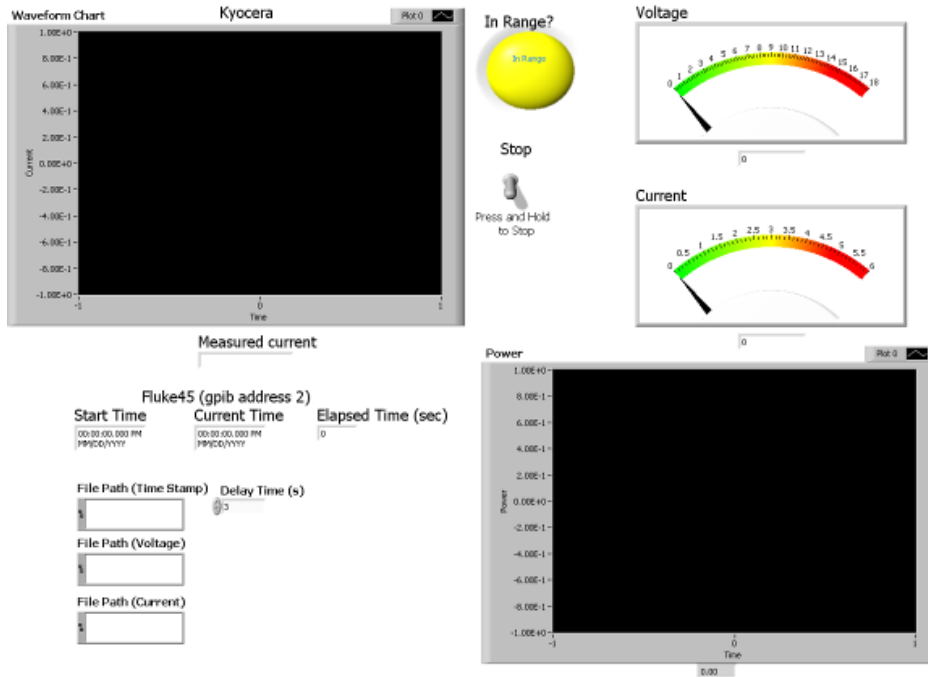
Figure 57.   Display of the LabView Program Used for the PV Measurements During the Wind-PV Experiment
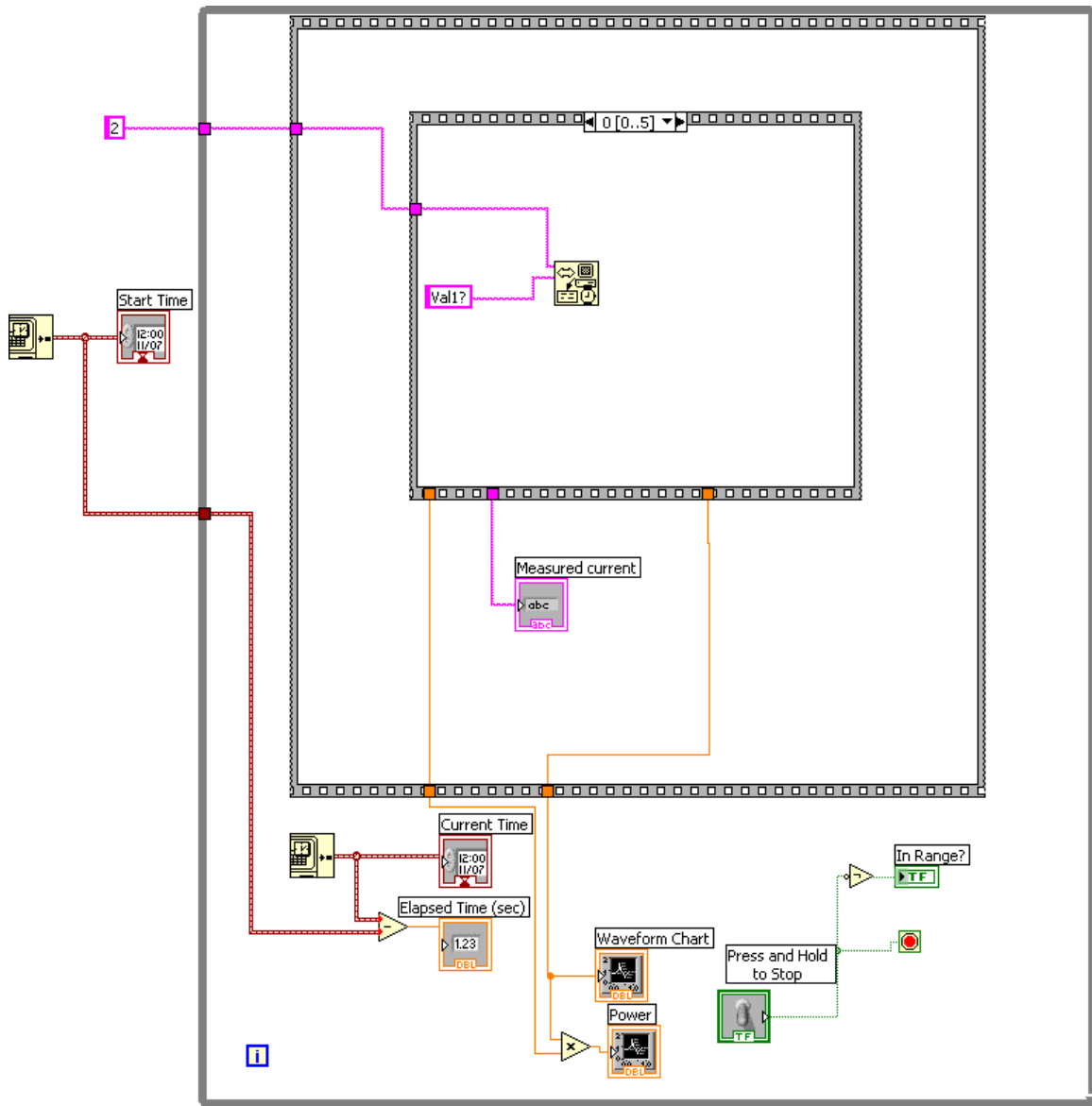
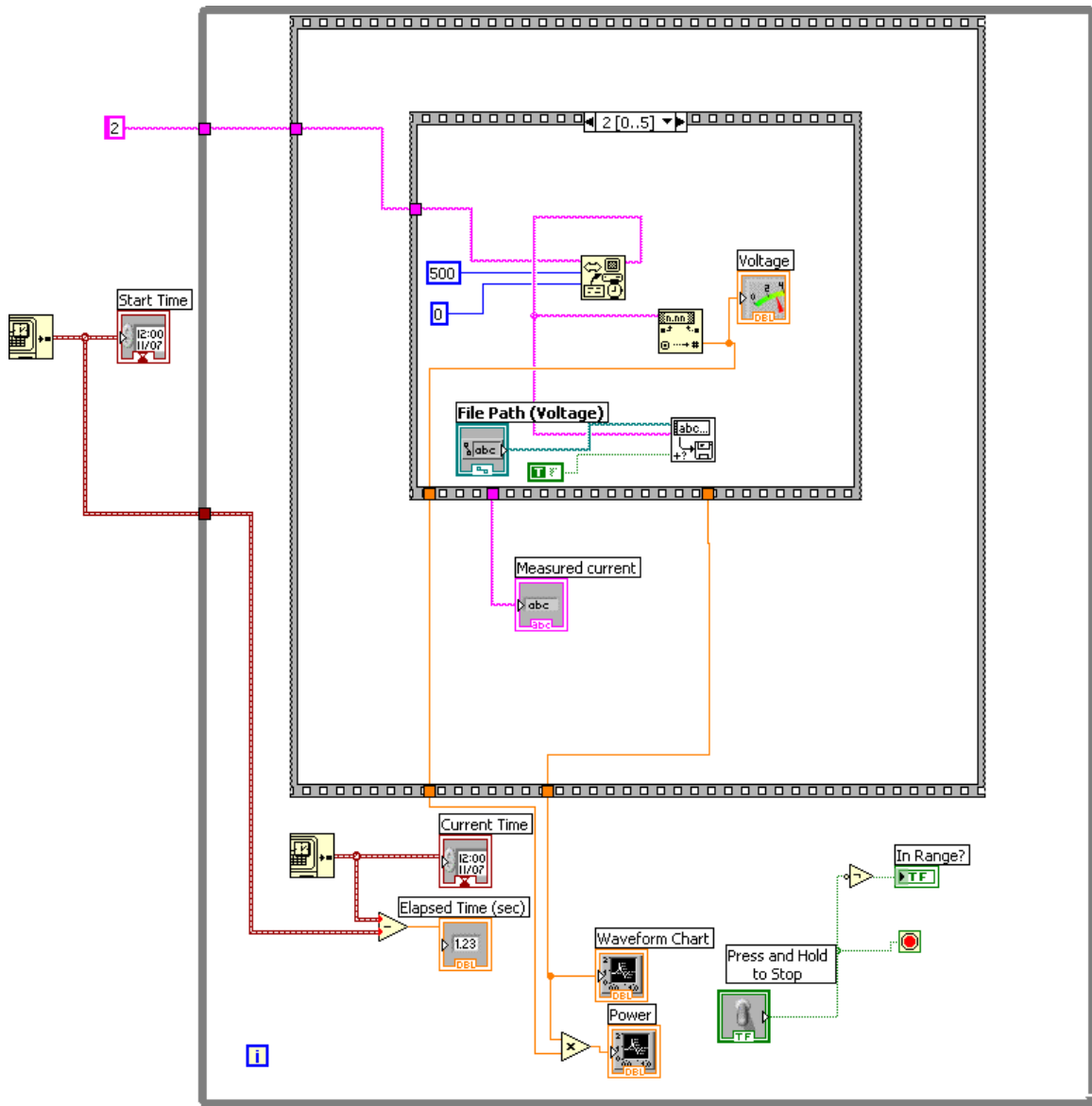**Figure 58.   Block Diagram 1**
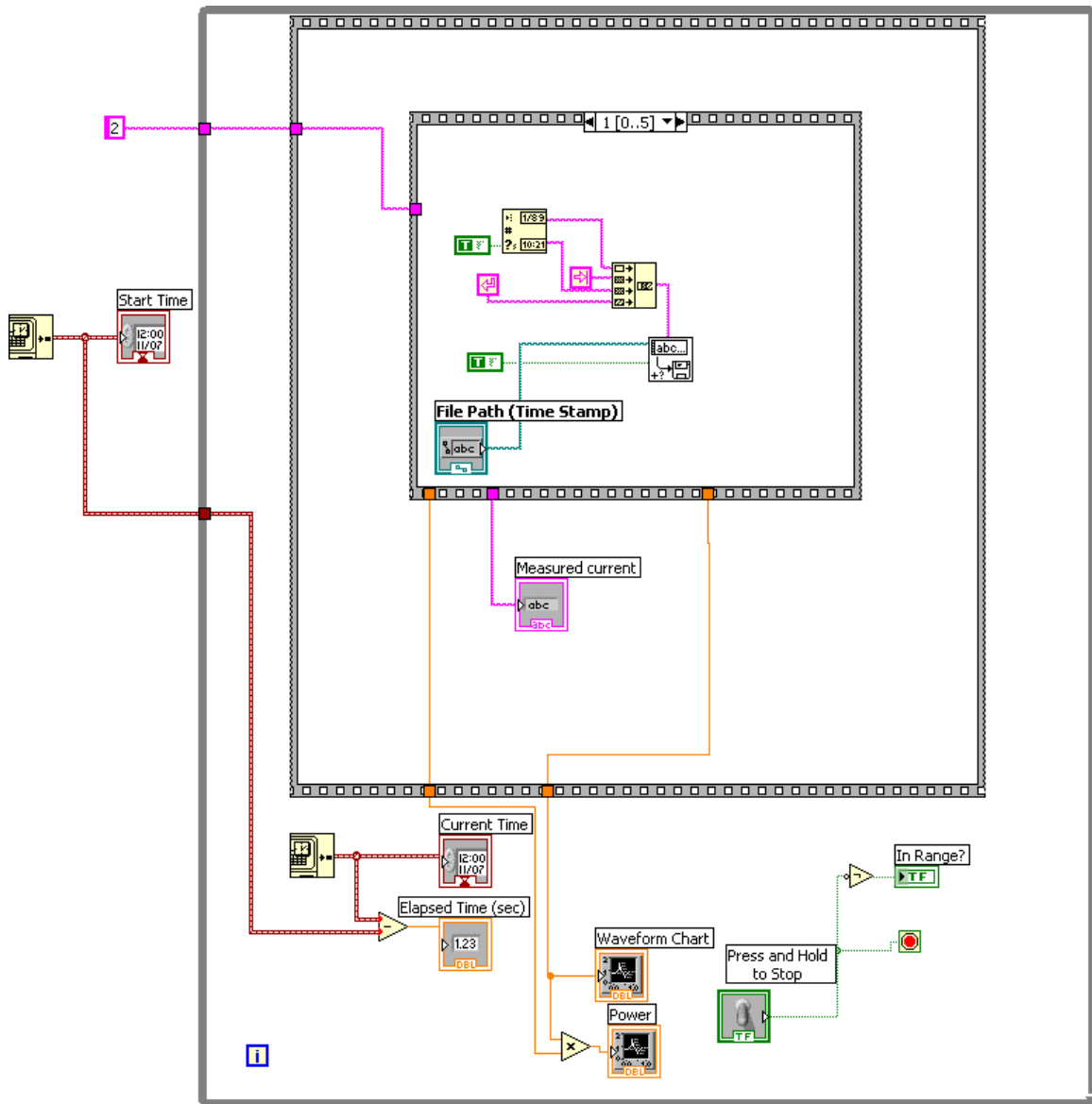
Figure 59.   Block Diagram 2

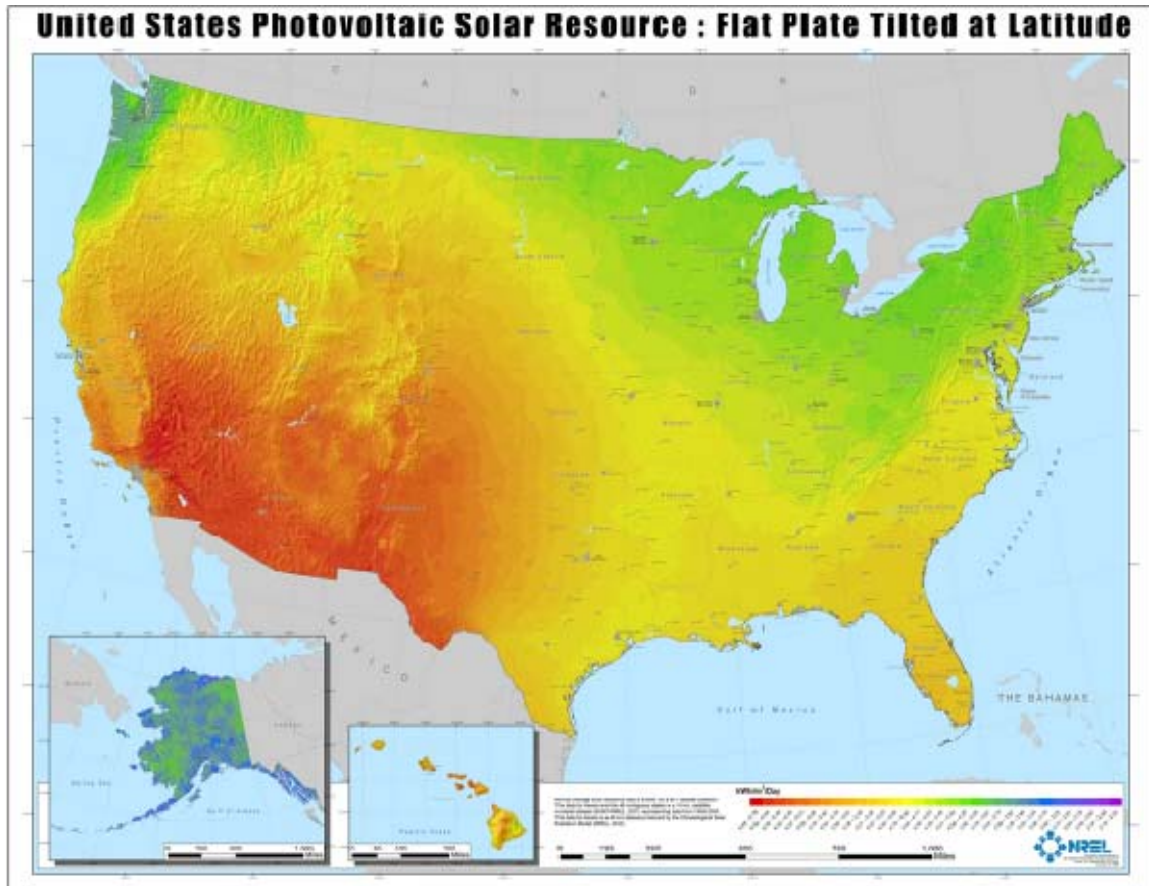**Figure 60. Block Diagram 3**
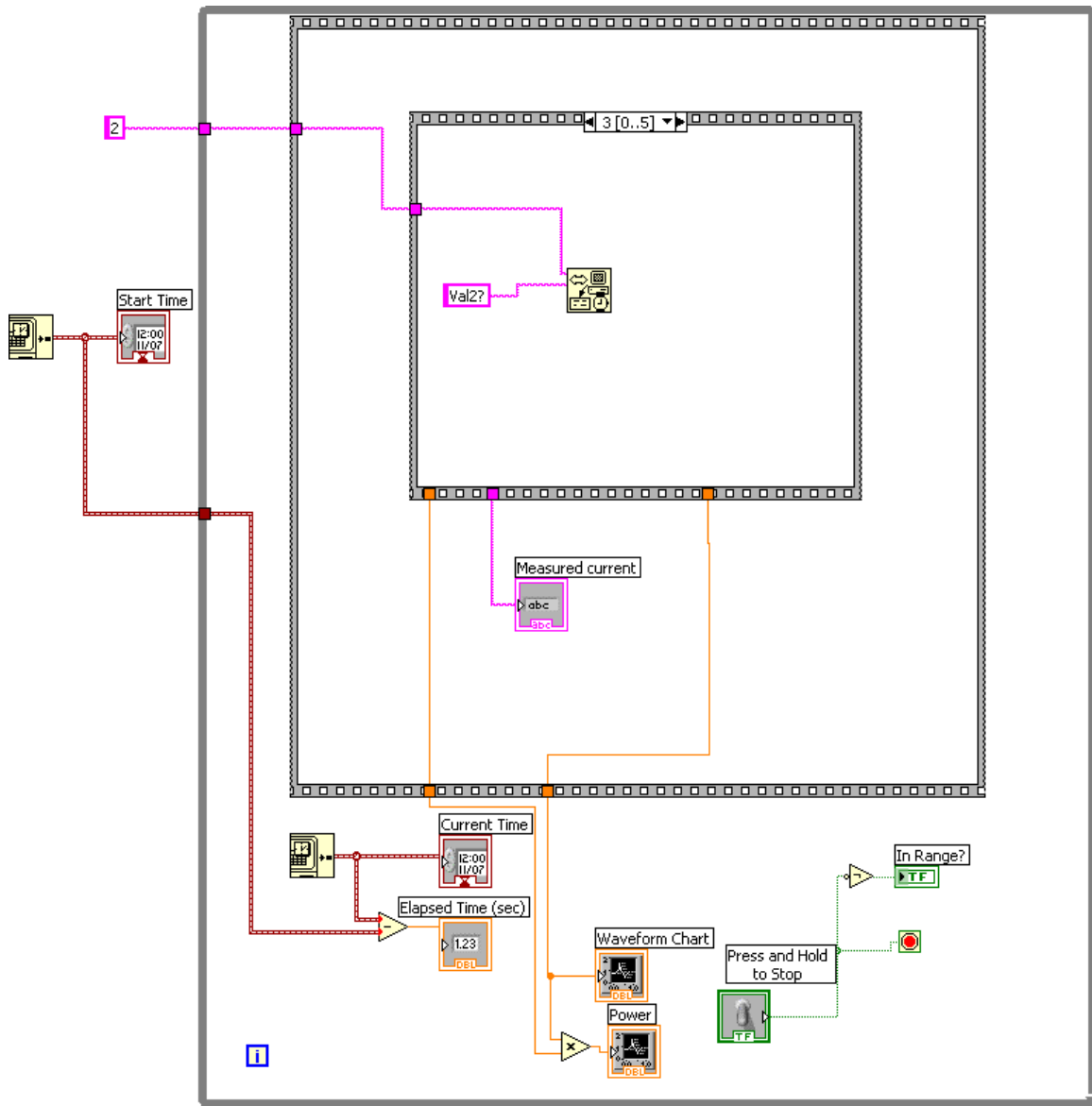
Figure 61.   Block Diagram 3
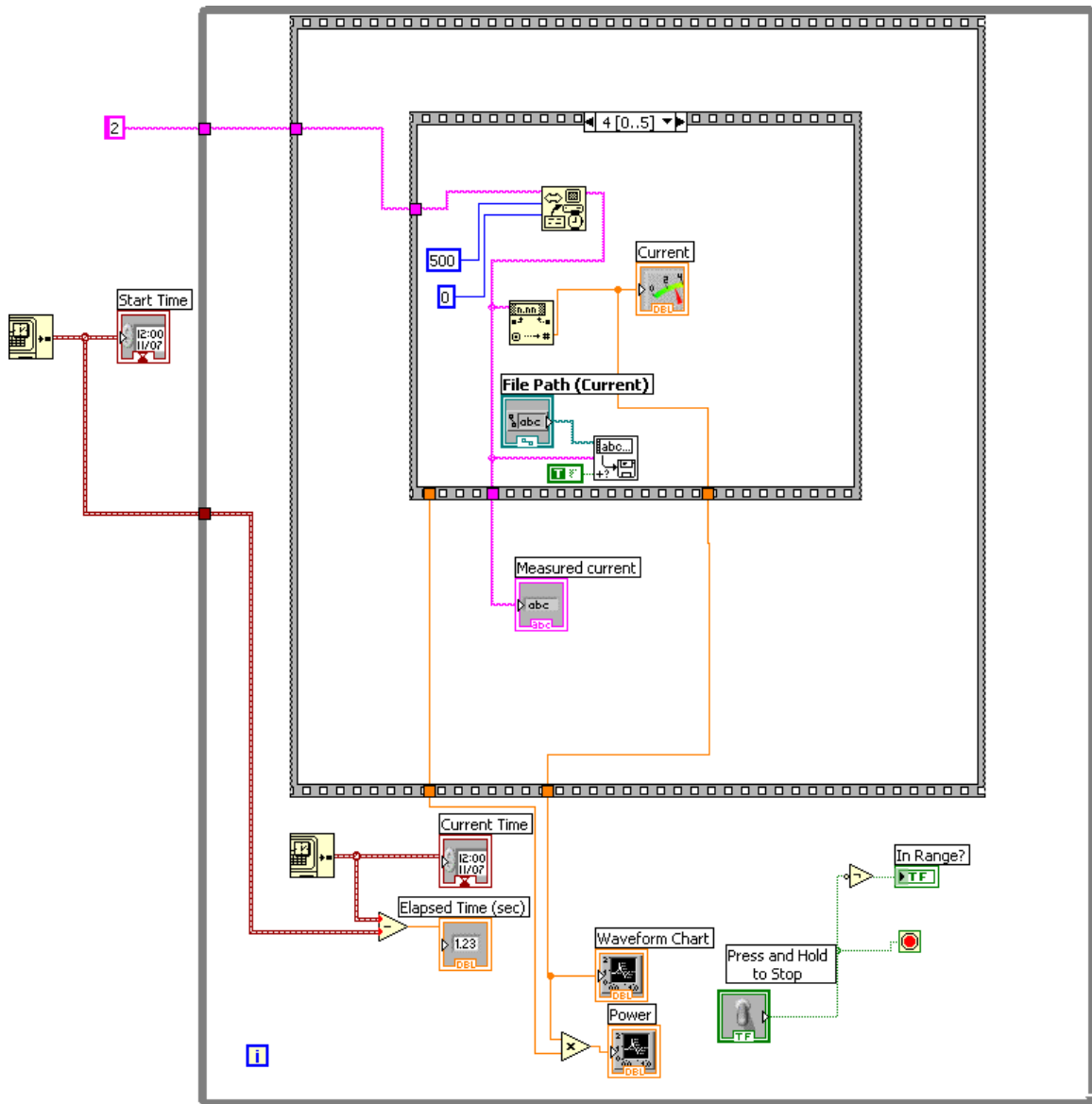
Figure 62.   Block Diagram 4

APPENDIX C.

This appendix provides solar energy potential maps for the locations involved in the ExFOB process.
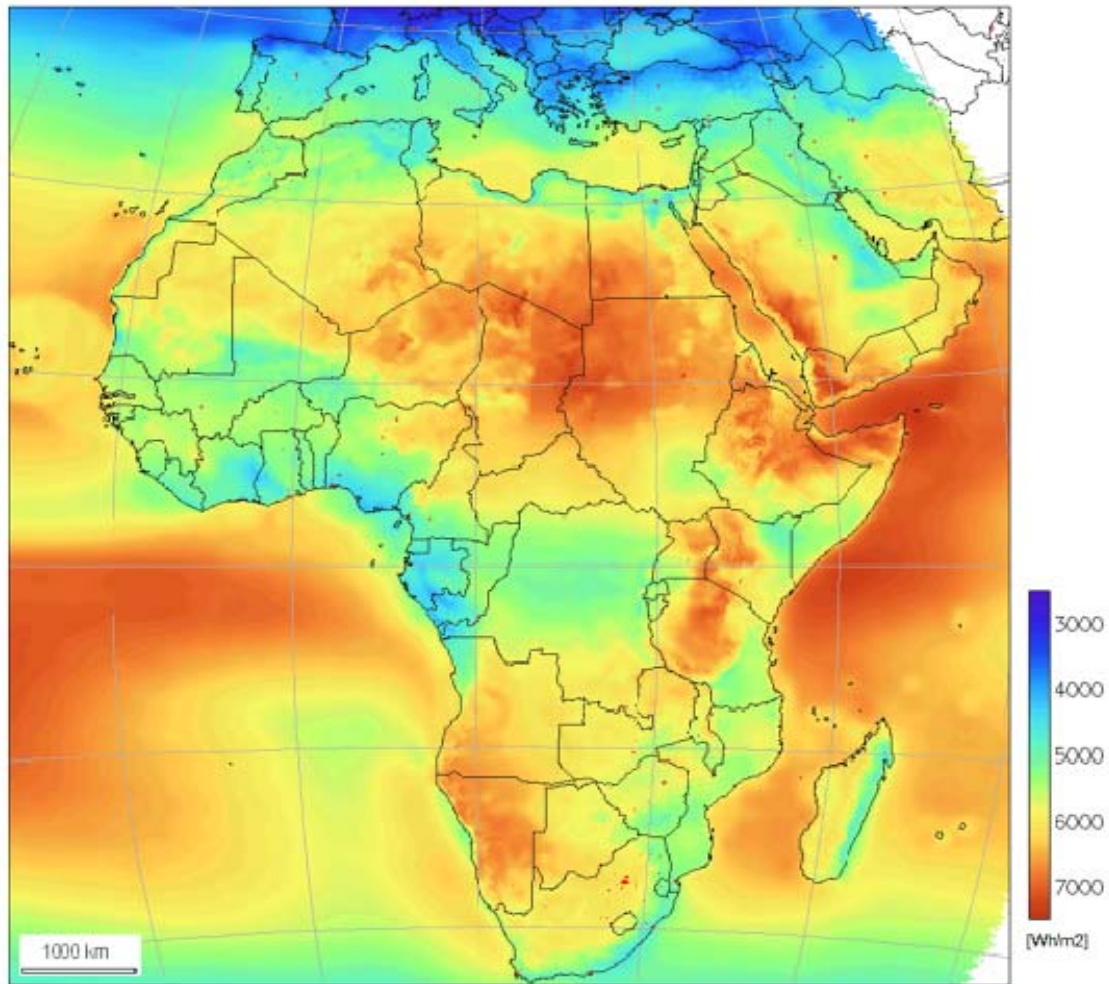

Figure 63. **Photovoltaic Solar Resource in the United States Map produced by the National Renewable Energy Laboratory for the U.S. Department of Energy, From [36]**

Figure 64. Africa, South West Asia and Mediterranean Region (Yearly Average of Daily Sum of Global Horizontal Irradiation), From [37]
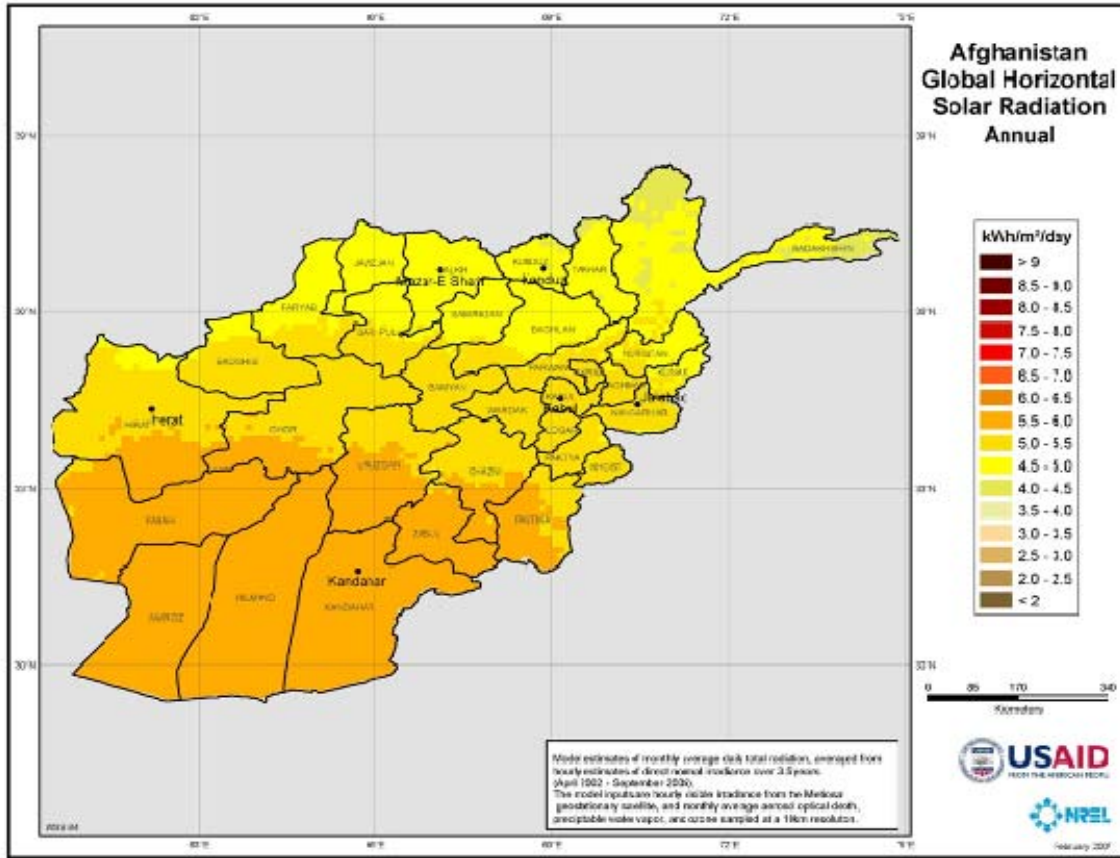
Figure 65.   Afghanistan Global Solar Radiation, From [38]

THIS PAGE INTENTIONALLY LEFT BLANK

LIST OF REFERENCES

[1]   General J. T. Conway, "Opening remarks," presented at USMC Energy Summit, Washington, DC, August 2009.

[2]   Colonel T.C. Moore, "Afghanistan assessment outbrief," presented at USMC Energy Symposium, New Orleans, LA, January 2010.

[3]   Marine Energy Assessment Team, "Draft: Report of the Afghanistan Marine Energy Assessment Team," October 2009.

[4]   USMC, "Memorandum 11/09: Establish the Marine Corps Expeditionary Energy Office," November 2009.

[5]   USMC Expeditionary Energy Office, "Experimental Forward Operating Base Charter," January 2010.

[6]   T. Lambert, P. Gilman, P. Lilienthal, in "Micropower system modeling with HOMER," Integration of Alternative Sources of Energy, F. A. Farret, M.G. Simões, John Wiley & Sons, December 2005, pp. 379–416.

[7]   Navy Region Southwest, Renewable Energy and Distributed Generation Projects, Navy Region Southwest, June 2006.

[8]   HOMER Energy LLC, "History page," June 2010, http://homerenergy.com/history.html [accessed September 2010].

[9]   Master Gunnery Sergeant Rowan Dickson (private communication), September 2009.

[10]   Southwest Windpower, Air X Technical Specifications, Southwest Windpower, 2010, http://www.windenergy.com/documents/spec_sheets/3-CMLT-1339-01_Air_X_Spec.pdf [accessed September 2010].

[11]   Kyocera, Kyocera KD205GX-LP Technical Specifications, Kyocera, 2010, http://ww.kyocerasolar.com/pdf/specsheets/KyoceraSolar_KD205GX_Web.pdf [accessed September 2010].

[12]   SunnyBoy, SunnyBoy 3800U Technical Specifications, SunnyBoy, 2010, http://www.sunwize.com/info_center/pdf/sma_3800U.pdf [accessed September 2010].

[13]   USMC, "ExFOB Initial Planning Team Brief," presented at ExFOB Initial Planning Team Meeting, Quantico, VA, January 2010.

[14]   S. Dootsen, Naval Postgraduate School Renewable Energy Manager, (private communication), May 2010.

[15]   NASA, Surface Solar Energy Data Set, NASA, 2010, http://eosweb.larc.nas.gov/sse/ [accessed September 2010].

[16]   S. Michael (private communication), 2010.

[17]   PowerFilm, Product Brochure, PowerFilm, 2010, http://www.powerfilmsolar.com/downloads/pdf/PowerFilm_ProductLine_2010.pdf [accessed September 2010].

[18]   Engineering.com Inc., "Photovoltaics," August 2010, http://www.engineering.com/SustainableEngineering/RenewableEnergyEngineering/SolarEnergyEngineering/Photovoltaics/tabid/3890/Default.aspx [accessed September 2010].

[19]   R.M. Young, Ultrasonic Anemometer: Voltage and Serial Output, Model 85000, RM Young, 2010, http://www.youngusa.com/products/6/1.html [accessed September 2010].

[20]   Southwest Windpower, "Products," August 2010, http://www.windenergy.com/products/air_x.htm [accessed September 2010].

[21]   MAXIM, MAX4080/4081 Technical Specifications, MAXIM, 2010, http://datasheets.maxim-ic.com/en/ds/MAX4080-MAX4081.pdf [accessed September 2010].

[22]   Kyocera, Kyocera KC 50T Technical Specifications, Kyocera, 2010, http://www.kyocerasolar.com/pdf/specsheets/KC50T.pdf [accessed September 2010].

[23]   Dictionary.com, "Turbulence," 2010, http://dictionary.reference.com/browse/turbulence [accessed September 2010].

[24]   M. Sagrillo, "Back to the Basics: Turbulence," Solar Today, vol. 24, p. 28, March 2010, http://www.solartoday-digital.org/solartoday/201003?pg=28#pg28 [accessed September 2010].

[25]   M. Sagrillo, "Back to the Basics: Ground Drag," Solar Today, vol. 23, p. 40, Jan/Feb 2010, http://www.solartoday-digital.org/solartoday/20100102/#pg40 [accessed September 2010].

[26]   HOMER Energy, HOMER Help Menu: Turbulence, HOMER Energy, 2010.

[27]   Global Energy Concepts, AWS Truewind, LLC, Wind Power Project Site Identification and Land Requirements, New York State Energy Research and Development, 2005,

http://www.powernaturally.org/programs/wind/toolkit/13_windpowerproject.pdf
[accessed September 2010].

[28] Office of Naval Research, "ExFOB Request For Information to Industry," USMC, January 2010.

[29] Expeditionary Energy Office, "ExFOB Update Brief," presented at ExFOB Executive Initial Planning Team Meeting, Quantico, VA, March 2010.

[30] Program Manager Expeditionary Power Systems, GREEN Performance Specifications, Marine Corps Systems Command, 2010.

[31] M. Gallagher, Expeditionary Power Systems Program Manager, (private communication), March 2010.

[32] Expeditionary Energy Office, "Experimental Forward Operating Base Extended User Evaluation Brief," 2010.

[33] Sunmodule, SW 155/165/175 mono Specifications Sheet, Sunmodule, May 2007, http://www.hardysolar.com/solar-panel/dl/solar-world-ws-155-175.pdf [accessed September 2010].

[34] T. Lederly, VP of NEST Energy Systems, (private communication), May 2010.

[35] OutBack Power, OBX Rugged Water Resistant Inverter/Charger, OutBack Power, http://www.outbackpower.com/docman/2503101014415OBXWaterResistantSpec SheetRevB.pdf [accessed September 2010].

[36] National Renewable Energy Laboratory, "United States Solar Photovoltaic Resource," 2010, www.nrel.gov/gis/solar.html [accessed September 2010].

[37] Joint Research Centre European Commission, "Solar radiation and PV maps – Africa," 2010, http://re.jrc.ec.europa.eu/pvgis/cmaps/afr.htm [accessed September 2010].

[38] National Renewable Energy Laboratory, "Afghanistan Resource Maps and Toolkit," 2010, http://www.nrel.gov/international/ra_afghanistan.html [accessed September 2010].

THIS PAGE INTENTIONALLY LEFT BLANK

2003 - 2010 Sponsored Research Topics

Acquisition Management

- Acquiring Combat Capability via Public-Private Partnerships (PPPs)
- BCA: Contractor vs. Organic Growth
- Defense Industry Consolidation
- EU-US Defense Industrial Relationships
- Knowledge Value Added (KVA) + Real Options (RO) Applied to Shipyard Planning Processes
- Managing the Services Supply Chain
- MOSA Contracting Implications
- Portfolio Optimization via KVA + RO
- Private Military Sector
- Software Requirements for OA
- Spiral Development
- Strategy for Defense Acquisition Research
- The Software, Hardware Asset Reuse Enterprise (SHARE) repository

Contract Management

- Commodity Sourcing Strategies
- Contracting Government Procurement Functions
- Contractors in 21st-century Combat Zone
- Joint Contingency Contracting
- Model for Optimizing Contingency Contracting, Planning and Execution
- Navy Contract Writing Guide
- Past Performance in Source Selection
- Strategic Contingency Contracting
- Transforming DoD Contract Closeout
- USAF Energy Savings Performance Contracts
- USAF IT Commodity Council

- USMC Contingency Contracting

Financial Management

- Acquisitions via Leasing: MPS case
- Budget Scoring
- Budgeting for Capabilities-based Planning
- Capital Budgeting for the DoD
- Energy Saving Contracts/DoD Mobile Assets
- Financing DoD Budget via PPPs
- Lessons from Private Sector Capital Budgeting for DoD Acquisition Budgeting Reform
- PPPs and Government Financing
- ROI of Information Warfare Systems
- Special Termination Liability in MDAPs
- Strategic Sourcing
- Transaction Cost Economics (TCE) to Improve Cost Estimates

Human Resources

- Indefinite Reenlistment
- Individual Augmentation
- Learning Management Systems
- Moral Conduct Waivers and First-tem Attrition
- Retention
- The Navy's Selective Reenlistment Bonus (SRB) Management System
- Tuition Assistance

Logistics Management

- Analysis of LAV Depot Maintenance
- Army LOG MOD
- ASDS Product Support Analysis
- Cold-chain Logistics
- Contractors Supporting Military Operations
- Diffusion/Variability on Vendor Performance Evaluation

- Evolutionary Acquisition
- Lean Six Sigma to Reduce Costs and Improve Readiness
- Naval Aviation Maintenance and Process Improvement (2)
- Optimizing CIWS Lifecycle Support (LCS)
- Outsourcing the Pearl Harbor MK-48 Intermediate Maintenance Activity
- Pallet Management System
- PBL (4)
- Privatization-NOSL/NAWCI
- RFID (6)
- Risk Analysis for Performance-based Logistics
- R-TOC AEGIS Microwave Power Tubes
- Sense-and-Respond Logistics Network
- Strategic Sourcing

Program Management

- Building Collaborative Capacity
- Business Process Reengineering (BPR) for LCS Mission Module Acquisition
- Collaborative IT Tools Leveraging Competence
- Contractor vs. Organic Support
- Knowledge, Responsibilities and Decision Rights in MDAPs
- KVA Applied to AEGIS and SSDS
- Managing the Service Supply Chain
- Measuring Uncertainty in Earned Value
- Organizational Modeling and Simulation
- Public-Private Partnership
- Terminating Your Own Program
- Utilizing Collaborative and Three-dimensional Imaging Technology

A complete listing and electronic copies of published research are available on our website: www.acquisitionresearch.org

ACQUISITION RESEARCH PROGRAM
GRADUATE SCHOOL OF BUSINESS & PUBLIC POLICY
NAVAL POSTGRADUATE SCHOOL

THIS PAGE INTENTIONALLY LEFT BLANK